KINETICS AND MECHANISMS OF OXIDATION OF SOME ALKALOIDS (CAFFEINE, IMIDAZOLE, THEOBROMINE AND THEOPHYLLINE) BY PERMANGANATE ION IN AQUEOUS ACIDIC MEDIUM

BY

JONES, FRANK B.Sc (Hons) (UNIMAID 2007)
M.Sc/SCIE/04720/ 09–10

A THESIS SUBMITTED TO THE
POSTGRADUATE SCHOOL,
AHMADU BELLO UNIVERSITY, ZARIA
NIGERIA

IN PARTIAL FULFILMENT OF THE REQUIREMENTS FOR THE AWARD OF MASTER OF SCIENCE IN INORGANIC CHEMISTRY

DEPARTMENT OF CHEMISTRY
AHMADU BELLO UNIVERSITY, ZARIA
NIGERIA

OCTOBER , 2012

DECLARATION

I hereby declare that this thesis entitled "Kinetics and mechanism of oxidation of some alkaloids (caffeine, imidazole, theobromine and theophylline) by permanganate ion in aqueous acidic medium" contains the report of my research work and has not been presented in any previous application for a higher degree. All information from other sources has been acknowledged by means of references.

_____ _____

Frank Jones Date

DEDICATION

This piece of work is dedicated to the entire family of Mr. and Mrs. Jones Joel Adams.

CERTIFICATION

This thesis entitled 'Kinetics and mechanisms of oxidation of some alkaloids (caffeine, imidazole, theobromine and theophylline) by permanganate ion in aqueous acidic medium meets the regulation governing the award of the degree of Master of Science of Ahmadu Bello University and is approved for its contribution to scientific and literary presentation.

……. Date: ……

Prof. J.F. Iyun

Chairman, Supervisory Committee

……. Date: ……

Dr. S.O. Idris

Member, Supervisory Committee

……. Date: ……

Prof. C. E. Gimba

Head of Department

……. Date: ……

Prof. A. A. Joshua

Dean, Postgraduate School

ACKNOWLEDGEMENT

To God be the glory forever and ever, for His help and guidance throughout the course of my research work.

I would like to acknowledge the contributions of my supervisors, Prof. J. F. Iyun and Dr. S. O. Idris. As supervisors they have been both supportive and as scientists they have shown insight and integrity. I would like to particularly thank them for their patience.

I am grateful to Prof. C. E., Gimba (Head of Chemistry Department) , Prof. I.G, Ndukwe (Coordinator Postgraduate Program Department of Chemistry), Dr. Adamu Uzairu, Prof. V.O. Ajibola, P rof. J.J. Bonire and Prof. (Mrs) E.B. Agbaji for professional assistance.

I owe extraordinary special thanks to my many friends, among who are Dr. Innocent Edward, Kolo Yetu, Joel Pagiel, Dlama Joseph, Babatope Meduteni and Japheth Tikikus.Thank you all for being there for me. I am also grateful to my clas mates, especially Adjumi Esther, Idongesit Bassey, Damola Olawepo Franklin and Emmanuel Uwaiya ("Akane").

With love, I wish to express my heartfelt gratitude to Miss Kind Nimfas for her consistent support, love and diligent attention to my special needs, throughout the research period. Thanks for being there and showing that there is more strength in me than meets the eye.

My acknowledgement would not be complete if I did not mention Mr Simon Madanga, Mrs O.R.A Iyun, and Mr Celestine Ochigbo (all of Chemistry Department, A.B.U., Zaria)for their prompt, cheerful and professional assistance.

Finally, to my parents, thank you for your encouragement and prayers, I am forever indebted to you.

ABSTRACT

The kinetics of the redox reactions of caffeine (CAF), imidazole (IDZ), theobromine (TB) and theophylline(TP) have been studied in aqueous acid medium. Stoichiometries of the reactions, determined by the mole ratio method were observed to be 1:1(CAF- MnO_4^- and TP – MnO_4^-) and 1:2 (IDZ- MnO_4^- and TB- MnO_4^-) systems respectively. The rate of the reactions showed two parallel acid pathways, the acid dependent and the acid independent pathway for all the systems studied. The kinetic results showed first order dependence with respect to permanganate ion and reductants (CAF, IDZ, TB, TP) concentrations respectively. The reactions obey second order kinetics with the following general rate laws. $-d[MnO_4^-]/dt = k_2[MnO_4^-][S]$ where (S = CAF, IDZ, TB or TP) with k_2 (CAF) = $4.0 \times 10^{-2} \pm 0.02$ mol dm^{-3}, k_2 (IDZ) = $9.1 \times 10^{-2} \pm 0.1$ mol dm^{-3}, k_2 (TB) = $9.2 \times 10^{-2} \pm 0.02$ mol dm^{-3} and k_2 (TP) = $5.4 \times 10^{-1} \pm 0.2$ mol dm^{-3} Spectroscopic studies and Michaelis-Menten plots showed no evidence of the formation of intermediate complex in all the systems. Free radical were also not observed. Added ions ($HCOO^-$, CO_3^{2-} Mg^{2+} and Ca^{2+}) were observed to catalyze the reactions.The outer-sphere mechanism is proposed for these reactions .

TABLE OF CONTENTS

Title Page -- -- -- -- -- -- -- -- -- --i

Declaration -- -- -- -- -- -- -- -- -- --ii

Certification -- -- -- -- -- -- -- -- -- --iii

Dedication -- -- -- -- -- -- -- -- -- --iv

Acknowledgement -- -- -- -- -- -- -- --v

Abstract -- -- -- -- -- -- -- -- -- --vi

Table of contents -- -- -- -- -- -- -- -- --vii

List of Tables -- -- -- -- -- -- -- -- -- --viii

List of Figures -- -- -- -- -- -- -- -- -- --ix

Abbreviations -- -- -- -- -- -- -- -- -- --x

CHAPTER ONE

1.0 Introduction -- -- -- -- -- -- -- -- --1

1.1 Types of electron transfer reactions -- -- -- -- -- --2

1.1.1 Homonuclear or self exchange electron transfer reactions -- -- --2

1.1.2 Heteronuclear or cross electron transfer reactions -- -- -- --2

1.2 Mechanism of redox reactions -- -- -- -- -- --3

1.2.1 The outer-sphere mechanism -- -- -- -- -- -- --4

1.2.2 The inner-sphere mechanism -- -- -- -- -- -- --5

1.3.0 Diagnosis of redox reaction mechanisms -- -- -- -- --6

1.3.1 Rate of redox process versus rate of substitution -- -- -- --7

1.3.2 Identification of binuclear intermediate -- -- -- -- --7

1.3.3 Products analyses -- -- -- -- -- -- -- --8

1.3.4 Reactivity patterns -- -- -- -- -- -- -- --9

1.3.5 Activation parameters -- -- -- -- -- -- --9

1.3.6 Effect of added ions on the reaction rate -- -- -- -- --10

1.3.7 Use of ambidentate bridging ligand -- -- -- -- -- --11

1.3.8 Marcus theory -- -- -- -- -- -- -- -- --12

1.4.0 Rate-- monitoring techniques -- -- -- -- -- -- --13

1.4.1 Conventional methods -- -- -- -- -- -- --13

1.4.2 Fast reaction techniques -- -- -- -- -- -- --14

1.5.0 Concept of electron transfer -- -- -- -- -- -- --16

1.5.1 Franck - Condon principle -- -- -- -- -- -- --16

1.5.2 Electron tunneling theory -- -- -- -- -- -- --17

CHAPTER TWO

2.0 Literature review -- -- -- -- -- -- -- --19

2.1.0 Caffeine -- -- -- -- -- -- -- -- -- --19

2.2.0 Imidazole -- -- -- -- -- -- -- -- -- --20

2.3.0 Theobromine -- -- -- -- -- -- -- -- --22

2.4.0 Theophylline -- -- -- -- -- -- -- -- --22

2.5.0 Redox reactions of permanganate ion -- -- -- -- -- --23

CHAPTER THREE

3.0 Experimental -- -- -- -- -- -- -- -- --29

3.1 Materials and reagents -- -- -- -- -- -- --29

3.1.1 Preparation of standard solutions of caffeine -- -- -- --29

3.1.2 Preparation of standard solutions of imidazole -- -- -- -- --29

3.1.3 Preparation of standard solutions of theobromine -- -- -- -- --29

3.1.4 Preparation of standard solutions of theophylline. -- -- -- --29

3.1.5 Preparation and standardization of potassium permanganate solution --29

3.1.6 Preparation of standard solutions of sulphuric acid -- -- -- --30

3.1.7 Preparation of standard solutions of sodium carbonate -- -- --30

3.1.8 Preparation of standard solutions of sodium formate - -- --30

3.1.9 Preparation of standard solutions of calcium sulphate solution magnesium sulphate -- -- -- -- -- -- -- -- -- --30

3.2.0 Stoichiometric studies -- -- -- -- -- -- -- --30

.3.3.0 Kinetic measurements -- -- -- -- -- -- --31

3.4.0 Acid dependence -- -- -- -- -- -- -- --32

3.5.0 Effect of ionic strength and dielectric constant on the rate of reaction --33

3.6.0 Tests for the presence of intermediate complex -- -- -- -- --33

3.6.1 Spectrophotometric investigation -- -- -- -- -- -- --33

3.62 Free radical test -- -- -- -- -- -- -- --34

3.7.0 Product analysis -- -- -- -- -- -- --34

CHAPTER FOUR

4.0. Results -- -- -- -- -- -- -- -- --35

4.1 Stoichiometry -- -- -- -- -- -- -- --35

4.2 Product analyses -- -- -- -- -- -- -- --40

4.3 Order of reaction -- -- -- -- -- -- -- --40

4.4 Effect of hydrogen ion on the rate of the reactions -- -- -- --54

4.5 The effect of ionic strength and dielectric constant (D) on the rates -- 59

4.6 Tests for intermediate complex formation -- -- -- - --59

4.6.1 Spectrophotometric test -- -- -- -- -- --59

4.7 Test for free radicals -- -- -- -- -- -- --77

4.8 Kinetic test -- -- -- -- -- -- -- -- --77

4.9 Effect of added anions on the rate of the reaction -- -- -- --82

4.10 Effect of added cation on the rate of the reaction -- -- -- --95

CHAPTER FIVE

5.0 Discussion -- -- -- -- -- -- -- -- --116

5.1 Oxidation of caffeine by permanganate ion -- -- -- -- --108

5.2 Oxidation of imidazole by permanganate ion -- -- -- -- --110

5.3 Oxidation of theobromine by permanganate ion -- -- -- --112

5.4 Oxidation of theophylline by permanganate ion-- -- -- -- --114

5.5 Summary and conclusion -- -- -- -- -- -- --116

References -- -- -- -- -- -- -- -- --118

LIST OF TABLES

Table 4.1: Pseudo –first and second order rate constants for the reaction of caffeine and MnO_4^- -- -- -- -- -- -- --42

Table 4.2: Pseudo – first and second order rate constants for the reaction of imidazole and MnO_4^- -- -- -- -- -- -- --43

Table 4.3: Pseudo–first and second order rate constants for the reaction of theobromine and MnO_4^- -- -- -- -- --44

Table 4.4: Pseudo–first and second order rate constants for the reaction of theophylline and MnO_4^- -- -- -- --45

Table 4.5: Effect of changes in dielectric constants of reaction medium for the oxidation of CAF by MnO_4^---65

Table 4.6: Effect of changes in dielectric constants of reaction medium for the oxidation of IDZ by MnO_4^- --66

Table 4.7: Effect of changes in dielectric constants of reaction medium for the oxidation of TB by MnO_4^- --67

Table 4.8: Effect of changes in dielectric constants of reaction medium for the oxidation of TP by MnO_4^- . --68

Table 4.9: The effect of added anions on the rate of oxidation of CAF by MnO_4^- --83

Table 4.10: The effect of added anions on the rate of oxidation of IDZ by MnO_4^- --84

Table 4.11: The effect of added anions on the rate of oxidation of TB by MnO_4^-, -- -- --85

Table 4.12: The effect of added anions on the rate of the reaction of TP and MnO_4^- , -- --86

Table 4.13: Rate constants for the effect of added cation for the oxidation of caffeine by MnO_4^-96

Table 4.14: Rate constants for the effect of added cation for the oxidation of imidazole by MnO_4^- 97 -- --

Table 4.15: Rate constants for the effect of added cation for the oxidation of theobromine by MnO_4^- . -- -- --98

Table 4.16: Rate constants for the effect of added cation for the oxidation of theophylline by MnO_4^-.-- -- --99

LIST OF FIGURES

Figure. 1.1: Electron transfer by penetration of a potential energy barrier-- -- -- --18

Figure 4.1.: Stoichiometric plot for the oxidation of CAF by MnO_4^- -- -- -- **--36**

Figure 4.2: Stoichiometric plot for the oxidation of IDZ by MnO_4^- -- --- -- **--37**

Figure 4.3: Stoichiometric plot for the oxidation of TB by MnO_4^- -- -- -- **--38**

Figure 4.4: Stoichiometric plot for the oxidation of TP by MnO_4^- -- -- -- **--39**

Figure 4.5: Typical pseudo–first order plot for the oxidation of CAF by MnO_4^- . **---** **--46**

Figure 4.6: Typical pseudo –first order plot for the oxidation of IDZ by MnO_4^- . **---** **--47**

Figure 4.7: Typical pseudo–first order plot for the oxidation of TB by MnO_4^- . **----** **--48**

Figure 4.8: Typical pseudo–first order plot for the oxidation of TP by MnO_4^- . **----** **--49**

Figure 4.9: Log k_{obs} versus log [CAF] plot for the oxidation of CAF by MnO_4^- . **---** **--50**

Figure 4.10 : Log k_{obs} versus log [IDZ] plot for the oxidation of IDZ by MnO_4^- . **---** **--51**

Figure 4.11: Logk_{obs} versus log[TB] plot for the oxidation of TB by MnO_4^- . **------** --52

Figure 4.12: Logk_{obs} versus log[TP] plot for the oxidation of TP by MnO_4^- -- --- --53

Figure 4.13: k_{obs} versus $[H^+]$ plot for the oxidation of CAF by MnO_4^--- -- --- --55

Figure 4.14: k_{obs} versus $[H^+]$ plot for the oxidation of IDZ by MnO_4^- ---- -- --- --56

Figure 4.15: k_{obs} versus $[H^+]$ plot for the oxidation of TB by MnO_4^- -- -- - --57

Figure 4.16: k_{obs} versus $[H^+]$ plot for the oxidation of TP by MnO_4^- -- -- -- --58

Figure 4.17: Log k_2 versus $I^{1/2}$ plot for the oxidation of CAF by MnO_4^- . -- -- --61

Figure 4.18: Log k_2 versus $I^{1/2}$ plot for the oxidation of IDZ by MnO_4^- -- -- -- --62

Figure 4.19: Logk_2 versus $I^{1/2}$ plot for the oxidation of TB by MnO_4^- -- -- -- --63

Figure 4.20: Log k_2 versus $I^{1/2}$ plot for the oxidation of TP by MnO_4^- . -- -- --64

Figure 4.21: Log k_{obs} versus 1/D plot for the oxidation of CAF by MnO_4^- . -- -- --69

Figure 4.22: Log k_{obs} versus 1/D for the oxidation of IDZ by MnO_4^- . -- -- -- --70

Figure 4.23: Log k_{obs} versus 1/D for oxidation of TB by MnO_4^- . -- -- -- --71

Figure 4.24: Log k_{obs} versus 1/D for the oxidation of TP by MnO_4^- . -- -- -- --72

Figure: 4.25: Spectra of MnO_4^- and MnO_4^-+ CAF -- -- -- -- --73

Figure 4.26: MnO_4^- and MnO_4^-+ IDZ -- -- -- -- -- --74

Figure 4.27: MnO_4^- and MnO_4^-+ TB -- -- -- -- -- -- --75

Figure 4.28: MnO_4^- and MnO_4^-+ TP -- -- -- -- -- -- --76

Figure 4.29: Michealis–Mentens plot of 1/ k_1 versus 1/ [CAF] for the oxidation of CAF by MnO_4^- -- -- -- -- --78

Figure 4.30: Michealis–Mentens plot of 1/ k_{obs} versus 1/ [IDZ] for the oxidation of IDZ by MnO_4^- ---79

Figure 4.31: Michealis–Mentens plot of 1/ k_{obs} versus 1/ [TB] for oxidation of TB by MnO_4^- -- --80

Figure 4.32: Michaelis-Mentens plot of 1/ k_{obs} versus 1/ [TP] for the oxidation of TP by MnO_4^- -- - -- -- --81

Figure 4.33: k_2 versus [$HCOO^-$] plot for the oxidation of CAF by MnO_4^- -- -- --87

Figure 4.34: k_2 versus [CO_3^{2-}] for the oxidation of CAF by MnO_4^- -- -- -- --88

Figure 4.35: k_2 versus [CH_3COO^-] plot for the oxidation of IDZ by MnO_4^- -- -- --89

Figure 4.36: k_2 versus [NO_3^-] plot for the oxidation of IDZ by MnO_4^- ---- -- --90

Figure 4.37: k_2 versus [$HCOO^-$] plot for the oxidation of TB by MnO_4^- -- --91

Figure 4.38: k_2 versus [NO_3^-] plot for the oxidation of [TB] by MnO_4^- -- -- -- --92

Figure 4.39: k_2 versus [$HCOO^-$] plot for the oxidation of TP by MnO_4^--- -- -- --93

Figure 4.40: k_2 versus [NO_3^-] plot for the oxidation of TP by MnO_4^- -- -- -- --94

Figure 4.41: k_2 versus [Mg^{2+}] plot for the oxidation of CAF by MnO_4^- ---- -- --100

Figure 4.42: k_2 versus [Ca^{2+}] plot for the oxidation of CAF by MnO_4^- -- -- -- --101

Figure 4.43: k_2 versus [Mg^{2+}] plot for the oxidation of IDZ by MnO_4^--- -- -- --102

Figure 4.44: k_2 versus [Ca^{2+}] plot for the oxidation of IDZ with MnO_4^- -- -- --103

Figure 4.45: k_2 versus [Mg^{2+}] plot for the oxidation of [TB] by MnO_4^- --- -- --104

Figure 4.46: k_2 versus [Ca^{2+}] plot for the oxidation of TB by MnO_4^- -- -- -- --

Figure 4.47: k_2 versus [Mg^{2+}] plot for the oxidation of TP by MnO_4^- -- -- -- --106

Figure 4.48: k_2 versus [Ca^{2+}] plot for the oxidation of TP by MnO_4^- -- -- -- --107

ABBREVIATIONS

Abbreviation	Name
AR	Analar Reagent
aq	Aqueous
BDH	British Drug House
CAF	Caffeine
cal.	Calculated
conc.	Concentrated
D	Dielectric constant
E_a	Activation
E^o	Redox Reaction
EDTA	Ethylenediaminetetraacetate
e.s.r	Electron Spin Resonance
H.n.m.r.	Proton Nuclear Magnetic Resonance
IDZ	Imidazole
K	Equilibrium Constant
k	Rate Constant
k_{cal}	Calculated Rate Constant
k_{obs}	Observe Rate Constant
obs	Observed
ox	Oxidant
red	Reductant
Redox	Oxidation – Reduction
Sub	Substitution
TB	Theobromine

TP	Theophylline
viz	namely

CHAPTER ONE

2.0 Introduction

Electron transfer (ET) reactions are important chemical processes as they play important roles in many biological, physical, and chemical (both organic and inorganic) processes like reactions of metalloproteinase, photo-induced electron transfer processes transfer and the reaction of the hydrated electron (Lippardds, 1973; Finnegan *et al*., 2002;Yoshihara *et al*., 1995). Electron transfer is one of many pathways by which redox reactions can occur (Basolo and Pearson, 1967; Burgess, 1978). Proper understanding of the electron transfer helps in understanding, development, and eventual effective control of a wide area of science and technology (Iyun, 1982).

Redox reactions are those reactions in which there is a change in the formal oxidation state of the species involved (Purcell and Kotz, 1977).The rate at which a redox reaction occurs is qualitatively related to the redox potential. Generally, systems with higher electrode potential (oxidants) are reduced by systems with lower electrode potential (reductants). This is however, assumed that the entropy terms of the redox processes are favorable or negligible. The electron configuration of a metal ion is also an important factor in determining the stability of a particular oxidation state and thus governs the redox potential.

1.1 Types of electron transfer reactions

Electron transfer (ET) reactions can be broadly classified as homonuclear or self exchange electron transfer and heteronuclear electron transfer or cross electron transfer reactions based on thermodynamic parameters.

1.1.1 Homonuclear or self exchange electron transfer reactions

In homonuclear reactions, transfer of electrons occur between two identical metal ion centre existing in different oxidation states, in what is usually referred to as self exchange electron transfer reactions. In this reaction, the reactant and product ion concentrations are the same and hence the overall free energy of the reaction is approximately zero with the possibility of very small differences in the free energies of the reactant and products existing as a result of mixing thus, $K_{eq} = 1$ and $\Delta G = 0$. Isotopic labeling techniques have been employed to monitor the rate of such electron exchange reactions when they are slow. For fast exchange reactions, however, the nuclear magnetic resonance spectroscopic technique is employed (Wilkins, 1974). Some examples of self – exchange reactions are;

$$\text{Fe(phen)}_3^{2+} + \text{Fe(phen)}_3^{3+} \longrightarrow \text{Fe(phen)}_3^{2+} + \text{Fe(phen)}_3^{3+} \quad ..1.1$$

$$PtCl_4^{2-} + {}^*PtCl_6^{2-} \longrightarrow PtCl_6^{2-} + {}^*PtCl_4^{2-} \quad ..1.2$$

1.1.2 Heteronuclear or cross electron transfer reactions

In these types of redox reactions, electron transfer is between different metal ion centers. Products of such reactions are chemically distinct from the reactants and the net change in free energy is less than zero, (AG < 0) and AH≠0. Examples of these types of reactions are given in equations (1.3) and (1.4) below

$$2Fe^{2+} + Tl^{3+} \longrightarrow 2Fe^{3+} + Tl^{+} \quad ...1.3$$

$$Co(NH_3)_5X^{2+} + Cr^{2+}\ 5H^{+} \longrightarrow CrX^{2+} + Co^{2+} + 5NH_4^{+} \quad ..1.4$$

Reactions of the type in which the oxidant and reductant change oxidation state by the same number of electrons are termed complimentary (i.e. 1:1 stoichiometry) and non-complimentary where

the reactants undergo unequal changes in oxidation state (i.e stoichiometry ≠ 1:1). Examples are reaction (equation 1.5 and 1.6) respectively

$$[Co(en)_3]^{3+} + [Ru(NH_3)_6]^{2+} \longrightarrow [Co(en)_3]^{2+} + [Ru(NH_3)]^{3+} \quad \text{....1.5}$$

$$Sn^{2+} + 2Fe^{3+} \longrightarrow Sn^{4+} + 2Fe^{2+} \quad \text{.....1.6}$$

A wide range of experimental techniques have been used to study redox reactions (Sykes, 1966; Rosseinsky, 1972; Wilkins, 1974; Burgess, 1978). The range of those techniques varies from conventional Spectrophotometric methods for slow redox reactions to continuous and stopped-flow methods for fast reactions.

These methods have been exhaustively reviewed (Stranks, 1960; Caldin, 1974; Wilkins, 1974). The transmission coefficient, which always remains less than one, increases as the exchanging partners come closer together.

1.2 Mechanism of redox reactions

When undertaking the study of the mechanism of redox reaction, the following parameters need to be investigated:

1. The stoichiometry and product(s) of the reaction.
2. The driving force of the reaction.
3. The significance of acid-base (pH) catalysis if any.
4. The nature of the intermediate(s) involved (if any).
5. The type of specie transferred (atom or electrons)
6. The number of electron transferred in a single step, for a multiple-step process.

Attempt to rationalize the results from the above points have led Taube and his co-workers to establish two outstanding mechanisms for redox reactions (Taube *et al.,* 1953). The two mechanisms are the outer - sphere and the inner - sphere mechanisms.

1.2.1 The outer-sphere mechanism

An outer-sphere mechanism requires that:

1. A rate law is first order in both species, corresponding to an activated complex containing all the ligands in the coordinated spheres of both ions.

2. The rate of electron transfer is faster than the rate of substitution into the coordination sphere of either of the metal ions. In essence, outer-sphere mechanism occurs when the metal ion is surrounded by easily polarisable ligands such as phenanthroline and diphridyl in which ET is relatively more rapid and therefore, the coordination shell remain essentially the same after the act of ET (Larsen and Wahl, 1965). Examples are illustrated in equations (1.7), (1.8) and (1.9) respectively.

$$*Fe(phen)_3^{2+} + Fe(phen)_3^{3+} \longrightarrow *Fe(phen)_3^{3+} + Fe(phen)_3^{2+} \quad ..1.7$$

$$W^{IV}(CN)_8^{4-} + Fe^{III}(CN)_6^{3-} \longrightarrow W^{V}(CN)_8^{3-} + Fe^{II}(CN)_6^{4-} \quad ..1.8$$

$$(Os^{II}(dipy)_3)]^{2+}\ [Mo^{v}(CN)_8]^{3-} \rightleftharpoons [O_s^{III}(dipy)_3]^{3+} + [MO^{IV}(CN)_8]^{4-} \quad ..1.9$$

In equation (1.7), the phenanthroline could not be detached from the inert Fe(II) and Fe(III) centres during the course of the rapid redox process. Therefore, the coordination shells of the two reactants essentially remain intact before and after the electron transfer process.

A typical example of a reaction occurring by the outer - sphere mechanism is given below:

$W^{IV}(CN)_8^{4-} + Fe^{III}(CN)_6^{3+} \rightarrow W^{V}(CN)_8^{3-} + Fe^{II}(CN)_6^{4-}$ ..1.10

The mechanism is thought to occur in four stages as shown below:

Stage 1: Formation of precursor complex

$W^{IV}(CN)_8^{4-} + Fe(CN)_6^{3-} \rightarrow [(CN)_7\, W^{IV}CN//CNFe^{III}(CN)_5]^{7-}$ ..1.11

Stage 2: Activation of the Precursor complex

$[(CN)_7W^{IV}CN//CNFe^{III}(CN_5)]^{7-} \rightarrow [(CN)_7W^{IV}CN//CNFe^{III}(CN)_5]^{7-\neq}$ ..1.12

Stage 3: Electron transfer and formation of successor complex (Rate determining step)

$[(CN)_7W^{IV}CN//CNFe^{III}(CN)_5]^{7-\neq} \rightarrow [(CN)_7W^{V}CN//CN\,Fe^{II}(CN)_5]^{7-}$ ..1.13

Stage 4: Decomposition of successor complex to give final products.

$[(CN)_7W^{V}CNCN\,Fe^{II}(CN)_5]^{7-} \rightarrow W(CN)_8^{3-} + Fe(CN)_6^{4-}$ …..1.14

1.2.2 The inner-sphere mechanism

In this type of mechanism, electron transfer is preceded by substitution into the coordination shell of one of the reactants, with formation of a bridged intermediate in which two metal ions are linked by a common ligand. The two reactants are therefore linked by at least one bridging ligand common to their coordination shells. Electron transfer then occurs through the bridging ligand, which is usually (but not always) transferred from one metal centre to the other. This can be seen by the typical inner-sphere reaction between chromium (II) and cobalt(III) (Candlin and Halpern, 1965).

The following steps have been identified to operate in most inner-sphere electron transfer process:

(a) Formation of collision complex

$$L_5M^{III}WX^{2+} + N^{II}(H_2O)_6^{2+} \rightleftharpoons [L_5M^{III}X//N^{II}(H_2O)_6]^{4+} \quad .....1.15$$

(b) Formation of bridged precursor complex

$$[L_5M^{III}X//N^{II}(H_2O)_6]^{4+} \rightleftharpoons [L_5M^{III} - X - N^{III}(H_2O)_5]^{4+} + H_2O \quad .....1.16$$

(c) Activation of precursor complex, electron transfer and formation of successor complex

$$[L_5M^{III} - X - N^{II}(H_2O)_5^{4+}] \rightleftharpoons [L_5M^{II} - X - N^{III}(H_2O)_5^{4+}]^{\neq} \quad .....1.17$$

(d). Deactivation of successor complex and formation of products, through decomposition of the successor complex

$$[L_5M^{II} - X - N^{III}(H_2O)_5^{4+}]^{\neq} \rightleftharpoons [L_5M^{II} - X - N^{III}(H_2O)_5]^{4+} \quad .....1.18$$

$$[L_5M^{II} - X - N^{III}(H_2O)_5]^{4+} \rightleftharpoons L_5M^{II}H_2O^{2+} + XN^{III}(H_2O)_5^{2+} \quad .....1.19$$

The rate determining step could be any of the steps in this reaction; depending on which one is the slowest step. If the rate of formation of the precursor complex or the rate of dissociation of successor complex is slow, then the reaction is said to be a substitution-controlled reaction. Alternatively, if the rate of electron transfer is slow, then we are dealing with an electron transfer controlled system (Haim, 1983).

A typical example of this scheme is the inner-sphere reduction of trans - $Co(en)_2H_2OCl^{2+}$ by Fe^{2+}, where substitution takes place first on the labile Fe^{2+} ion, followed by electron transfer and subsequent rupture of Co—Cl bond to yield $FeCl^{2+}$ and Co^{2+} as initial products (Haim and Sutin, 1966).

1.3.0 Diagnosis of redox reaction mechanisms

The experimentally determined rate equation is generally the most important evidence in the diagnosis of a reaction mechanism. However, the importance of acquiring all possible information cannot be overemphasized. The assignment of a mechanism to a reaction under investigation could be simple (when two inert complexes are involved and the obvious mechanism is the outer-sphere), but most often complex if not impossible. The confirmation of a mechanism suggested on the basis of rate equation may be obtained from the following factors:

1.3.1 Rate of redox process versus rate of substitution

In the inner-sphere mechanism, substitution into the coordination shell occurs before electron transfer, hence if $k_{redox} >> k_{subs}$ such a reaction is likely to occur by the outer-sphere path (Rosseinheim *et al*., 1974). For example, electron exchange reaction between $Fe(CN)_6^{4-}$ and $Fe(CN)_6^{3-}$ (Campion *et al.,* 1967; Deck and Wahl, 1954). Also electron exchange reaction between $Fe(phen)_3^{2+}$ and $Fe(phen)_3^{3+}$ (Larsen and Wahl, 1965), occurs by the outer-sphere pathway. The rate constants values for the substitution of phenanthroline are 7.5×10^{-5} s^{-1} for

*$Fe(phen)_3^{3+}$ and 5.01×10^{-5} s^{-1} for $Fe(phen)_3^{2+}$ while k exchange is 10^5 dm^3 mol^{-1} s^{-1}. Since $k_{red} >> k_{sub}$, in this example, the outer-sphere mechanism is operative. However for a reaction in which $k_{sub} >> k_{red}$ and in the presence of a suitable bridging ligand, the inner-sphere mechanism may operate.

1.3.2 Identification of binuclear intermediate

One of the evidences in support of the inner-sphere mechanism is the presence of binuclear intermediate. The binuclear intermediate can either be a stable product or a transient intermediate along the pathway between reactants and products. This represents experimental information that is taken to be very persuasive evidence in favor of the inner–sphere mechanism (Haim, 1983).

These intermediates are formed between two reactants and must of necessity be formed before electron exchange can occur (Basolo and Pearson, 1967; Al-Jallal and Sulfab, 1983). Some of these intermediates are kinetically stable and have appreciable life-time that their detection through spectrophotometry or stopped flow techniques is possible.

In the reaction between VO^{2+} and Cr^{2+}, an intermediate, $VOCr^{4+}$ was characterized (Espenson, 1965).The rate of decomposition of the intermediate showed hydrogen ion dependence. In the inner-sphere mechanism, the identification of binuclear intermediate is possible if the reduced oxidant and the oxidized reductant are relatively inert and the rate of decomposition of the intermediate is slower than the rate of electron transfer.

In some cases where the binuclear intermediate has 'transient' nature, their presence can be inferred indirectly from empirical rate law or kinetic data. An example of such indirectly identified binuclear intermediate is $CrOHV^{5+}$ (Espenson, 1965) and $(OHTiXCo(NH_3)_5^{5+}$ (Orhanovic and Earley, 1975) However, the detection of binuclear intermediate is not a sufficient condition for the diagnosis of the inner-sphere mechanisms since the presence of an intermediate does not automatically mean that it lays on one path of the product.

1.3.3 Products analyses

In the inner-sphere mechanism, electron transfer takes place through a bridging ligand. After the act of electron transfer, if the bridging ligand is transferred from one metal centre to another, it provides an empirical evidence for the operation of the inner-sphere mechanism. For example, in the reaction between Cr^{II} and Co^{III} (Taube *et al*., 1953) $CrCl^{2+}$ was formed as one of the products which resulted from the formation of the binuclear intermediate, $[(NH_3)_5 — Co — ClCr]^{4+}$, showing an evidence in favour of the inner-sphere mechanism for the reaction. The criteria must be applied with caution because:

i. Atom transfer does not occur in all reactions that proceed via the inner–sphere mechanism. For example.

$$[Co(EDTA)]^{2-} + [Fe(CN)_6]^{3-} \longrightarrow [Co(EDTA)]^{-} + [Fe(CN)_6]^{4-} \quad \text{.....1.20}$$

(Huchital and Wilkins. 1976)

ii. The product of some reactions involving reductants such as Fe^{2+}, V^{2+} and Eu^{2+} undergo rapid hydrolysis making the detection difficult, except in few cases, for example $Co(NH_3)_5SCN^{2+}$ / V^{2+} system, where a stopped - flow technique has been used. (Davies and Espenson, 1969; Sykes and Green, 1970; Green *et al*., 1971).

1.3.4 Reactivity patterns

Reactivity patterns that can be used to assign mechanisms to redox reactions are discussed below.

1.3.4.1 Reactivity pattern with a wide range of reactants

When similar complexes, for example (Co $(NH_3)_5X^{2+}$ (X = Cl^-, F^-, Br^- or NO_3^-) are reacted with a particular reductant a comparison of the rate of reaction gives possible insight into the mechanism that is operating. If the rates of the reactions are similar, then the outer -sphere mechanism is operating. While for the inner–sphere mechanism, the rate would be expected to be sensitive to the nature of X, since it is the bridging ligand (Sykes, 1967; Shea and Haim, 1973).

1.3.4.2 Relative rate of reaction of hydroxyl and aquo complexes

The hydroxyl group is a better bridging ligand than water. So it is expected that the hydroxo complexes should react faster via the inner-sphere mechanism. For example the reaction of $Co(NH_3)_5OH^{2+}XCr(H_2O)_6^{2+}$ goes through the activated binuclear complex, $[(NH_3)_5CoOHCr(OH_2)_5^{4+}]$.Therefore when $k_{OH^-} << k_{H_2O}$ the outer-sphere mechanism is said to be operating while the converse is true when $k_{OH^-} >> k_{H_2O}$.

1.3.5 Activation parameters

There is no strong correlation between the types of mechanism operating in a particular redox process and the activation parameters such as ΔH, ΔS and ΔG, e.t.c. However, their signs and magnitude can be used in support of or against a particular mechanism. Negative values of ΔH for example, indicate the formation of precursor complex as in the inner-sphere mechanism (Wilkins, 1974).

Measurement of the volume of activation (ΔV) for the reduction of various complexes has been applied as diagnostic tool in reaction kinetics. Similarly; the volume of activation, ΔV for the inner-

sphere mechanism is expected to increase since the effective volume of free water is more than that of a coordinated water molecule (Hubbard *et al.,* 1991).

1.3.6 Effect of added ions on the reaction rate

Added ions have been reported to catalyse a variety of reactions known to occur by the outer-sphere mechanism. For the outer-sphere reaction, the reactants must be sufficiently in close proximity to create an electronic interaction which provides a basis for the delocalization of the exchanging electron. This implies that reactions operating by the outer-sphere mechanism can be catalyzed in the presence of added ions which can increase the proximity between the oxidant and reductant, thereby shortening the distance through which the electron can be transferred by forming a bridge (Mayer and Taube, 1987). However, effects of added ions on known inner-sphere redox reactions are much less.

For a particular reaction, involving reactants having positive charges, any added anion, can catalyse the reaction by coordinating to one of the reactants (reductants) thereby reducing the degree of repulsion between the reactants, in that way, the act of electron transfer becomes faster.

Also, for reactants carrying negative charges, any added cation can catalyse the reaction by coordinating to one of the reactants (oxidant) thereby reducing the degree of repulsion between the redox partners. This also enhances the rate of electron transfer, since the reactants are now brought into close proximity to each other. However, for redox reductants having opposite charges, added ions could retard the reaction rate since coordination to any of the reactants could reduce the degree of attraction between the reactants. This will increase the distance between redox partners and slow down the rate of electron transfer.

For a reaction between $(H_3N)_5Co(III)X$ and Cr(II), an activated complex of the form $[(H_3N)_5Co.X.Cr(OH_2)_4Y]^*$ has been suggested where Y (catalyst) is the added anion. This shows that the anion affect largely the activity of the reducing agent and usually appear in the Cr(III) product for both the inner–sphere and the outer–sphere reactions (Hunt and Earley, 1960; Diebler and Taube, 1965).

Generally, catalysed reactions have been rationalised on the basis of the outer–sphere mechanism (Pennington and Haim, 1967; Przystas and Sutin, 1973; Adegite e*t al*., 1977) and the effectiveness of the catalytic behaviour of added ions shown to be in the order $Br^- < Cl^- < F^-$(Candling *et al.,*1965).

1.3.7 Use of ambidentate bridging ligand

The inner-sphere mechanism can be distinguished from outer-sphere mechanism on the basis of the difference in rate of electron transfer observed with symmetrical bridging ligand. For example, thiocyanate, isothiocyanate and azide complexes.

If the rate constants for the reaction of azide and thiocyanate complexes are the same or similar, then the outer–sphere mechanism should be operating, while the converse is true for reactions of the inner–sphere mechanism (Candin *et al*., 1964; Espenson, 1965; Fay Sutin, 1970; Wang and Espenson, 1971).

1.3.8 Marcus theory

In the outer–sphere mechanism, the weak interaction between the reactants has permitted its theoretical treatment and correlation between kinetic and thermodynamic parameters (Sutin, 1966;

Diebler and Sutin, 1968). Probably, the most widely used of these treatments is the Marcus theory (Marcus, 1956).

Marcus theory was initially used for the calculation of absolute rate constants for homonuclear exchange reaction. It was later extended to cross-reactions. The theory predict that when work terms are small, little reorganization is involved prior to electron transfer, for the cross reaction

$$Ox_1 + Red \overset{K_{12}}{\rightleftharpoons} Red_1 + Ox_2 \qquad \text{....1.21}$$

And relative isotropic exchange reaction equations (1.23) and (1.24)

$$Ox_1 + {}^*Red_1 \overset{k_{11}}{\rightleftharpoons} Red_1 + {}^*Ox_1 \qquad \text{....1.22}$$

$$Ox_2 + {}^*Red_2 \overset{k_{22}}{\rightleftharpoons} Red_2 + {}^*Ox_2 \qquad \text{....1.23}$$

The Marcus equation for the cross reaction is

$$\log k_{12} = 1/2 \log k_{11} + 1/2 \log k_{22} + 1/2 \log k_{12} + \tfrac{1}{2} \log f \qquad \text{....1.24}$$

The value of f is evaluated from equation (1.25)

$$\log f = \frac{(\log K_{12})^2}{(4 \log k_{11} Z^{-2})} \qquad \text{....1.25}$$

where k_{11} and k_{22} are the homonuclear electron exchange rate constants and K_{12} are the rate constants for cross reaction and the equilibrium constant for the cross reaction respectively,

Z = frequency of collision = 10^{11} dm^3 mol^{-1} s^{-1} for homogeneous reactions and

f = Transmission coefficient usually assumed to be 1.

Thus, from the Marcus equation, the theoretical rate constant for the electron transfer reaction can be calculated from equation (1.26).

$$K = Ze - \frac{\Delta G^*}{RT} \qquad \text{....1.26}$$

ΔG* = Gibbs free energy for the cross reaction. A reasonable agreement between k_{cal} and k_{obs} is usually taken as evidence in support of outer-sphere mechanism.

Marcus theory can be applied in various forms. For example in a linear energy relationship it is given by the equation (1.27)

$$\Delta G_{12}^* = 0.5\Delta G_{11}^* + 0.5\Delta G_{22}^* + 0.5\Delta G_{12}^0 \qquad \text{....1.27}$$

Thus, for a series of reactions, a plot of ΔG_{12}^* versus ΔG_{12}^0 gives a slope of 0.50 if the reaction is of the outer-sphere mechanism.

1.4.0 Rate monitoring techniques

A wide range of techniques for monitoring the rate of electron transfer have been developed as evidence from the large number of reviews (Wilkins, 1974, 1991; Burgess, 1978). A particular technique is chosen depending on whether the reaction to be monitored is slow or fast.

1.4.1 Conventional methods

Conventional methods include photometric, spectrophotometric, radiometric and polarometric. These methods are applicable to slow redox reactions. The methods involve measuring the concentration or any physical property of one or more of the reactants or products as a function of time.

For instance, in some reactions, absorbance of any of the reactants or products could be measured and related directly to its concentration (Wilkins, 1974).

1.4.2 Fast reaction techniques

Special techniques are employed for fast reactions with half-life of about a millisecond. Fast reaction techniques can be broadly classified into, flow, relaxation and resonance methods.

1.4.2.1 Flow methods

Flow techniques are frequently employed for rapid reactions. Different flow techniques exist, depending on the treatment given to the reaction after mixing (Caldin, 1974). Flow methods that are common are discussed below:

(a) Quenched - flow method

In this method, the reaction solution is quenched after a predetermined time and the quenched solution is analyzed by any conventional method.

(b) Continuous - flow method

The application of this method involves allowing the reaction solution to flow continuously along an observation tube, with the flow maintained at constant rate or at a fixed point on the tube with varied flow rate. The changes in the reaction mixture are monitored at different points along the tube or at a fixed point on the tube. In either case, a series of values for the extent of reaction is obtained at different times. These values constitute the kinetic data required.

(c) Stopped - flow method

In this method, the reactants (in solution) are forced together through a mixing devise and allowed to flow along a tube. As the mixed solution flows, along the tube, it is abruptly stopped so that the solution comes to rest within a few milliseconds. The rate of the flow along the observation tube is such that when the solution is stopped, a segment within 1cm of mixing device has been mixed for only 1 - 2 milliseconds. Monitoring any reaction taking place in this segment can be done and the signal relayed to an oscilloscope.

1.4.2.2. Relaxation method

Very fast reversible reactions with half – lives ($t_{1/2}$) as short as 10^{-9} s, are measured using the relaxation methods (Eigen and De Meyer, 1963). Any equilibrium attained during the reaction is perturbed by sudden variation of a physical parameter such as temperature, pressure, or electric field intensity and the time taken to readjust to a new equilibrium is monitored, which is then related to the rate constants of the forward and reverse reactions. The dependence of a particular equilibrium on a chosen external physical parameter largely determines the method of perturbation used for such equilibrium and hence these methods are referred to as 'temperature–jump', 'pressure–jump' or 'electric field–jump' (Wilkinson, 1980). Rates of electron transfer reaction has been monitored using the 'temperature jump' method between tris-(4, 7 – dimethyl – 1, 10 phenanthroline) iron (III) and $IrC1_6^{2-}$ (Halpern *et al.,* 1963).

1.4.2.3 Resonance method

Rate of reactions could be measured using both nuclear magnetic resonance (n.m.r) and electron spin resonance (e.s.r) techniques. These techniques have been used to study complex formation (Pearson and Buch, 1962) and aquation of metal ions (Connick and Poulson, 1959) in solution. In cases where n.m.r and e.s.r techniques are the methods of choice, the resonance absorption lines are related to the life time of the nucleus in a given spin state and life - time of paramagnetic species in a given energy state, respectively. If the life time of these states is reduced by a chemical interaction, it results in line broadening. On addition of increasing amount of a reagent, measurement of the corresponding increase in width of the line due to the second reagent can be made. For instance, H.n.m.r line broadening has been used to measure the rate of exchange of several mono and bidentate nitrogen and oxygen donor ligands coordinated to Mn^{II}, Fe^{II}, Co^{II}, Ni^{II} and Cu^{II} (Caldin, 1974; Burgess, 1978).

1.5.0 Concept of electron transfer

1.5.1 Franck – Condon principle

The actual electron transfer process involving bond breaking and formation is subject to the restrictions of “Franck Condon Principle”. The principle states that the motion of the nuclei is slow (10^{-13}s) compared to that of the electron (10^{-15}s) and that electron transfer occurs without an appreciable movement of the nuclei (Platzman and Franck, 1954 Sutin, 1966). This implies that electron transitions are rapid compared with nuclear motions and electron transfer occurs without significant movement of the atom (the nuclei virtually remain stationary). The operation of this principle for electron transfer requires that:

(a) Both reactants (oxidant and reductant) must undergo re-organization before electron transfer, such that their energies in the transition states become identical, thus minimizing the energy changes on electron transfer. The total change in free energy (ΔG) involved in the process can be represented by equation (1.28)

$$\Delta G = \Delta G_t^{\neq} + \Delta G_i^{\neq} + \Delta Go^{\neq} \quad \text{..... 1.28}$$

where $\Delta G_t^{\neq}$ = Association free energy, $\Delta G_i^{\neq}$ = Inner-sphere re-organization energy and $\Delta G_o^{\neq}$ = Outer-sphere re-organization energy.

(b) No angular momentum can be transferred to or from the transition state during the act of electron transfer and a restriction is also imposed on the change in spin angular momentum.

1.5.2 Electron tunneling theory

This theory states that solvent and ligands produce an electronic energy barrier that the transferring electron must penetrate (Weiss, 1954; Marcus, 1956).Electron tunneling occurs when a potential barrier exist for electron motion in space between donor-acceptor pair.The rate of electron tunneling depends on the magnitude of the electron coupling strength, between donor and acceptor. The electron coupling strength is the effective electronic Hamiltonian matrix element that couples the reactant and product state for the electron transfer. For weakly coupled (nonadiabatic) electron transfer reactions, the transition state must be formed many times before an electron is transferred to form product. The implication is that the electron will be able to travel distances much greater than would correspond to the actual collision of reactants (Basolo and Pearson, 1967). Reorganization of the solvent molecules had to occur prior to electron transfer (Marcus, 1957). In terms of the transition state theory, their results may be written in the form

$$k = \frac{KTk^1}{h} \exp\left(\frac{-\Delta G_r^{\neq} - \Delta G_e^{\neq}}{RT}\right) \quad \text{...1.29}$$

where k^1 = electron transmission coefficient,

k = rate constant,

K = Boltzman constant,

T = absolute temperature,

$\Delta G_r^{\neq}$ = activation free energy for rearrangement of the hydration and coordination shell,

$\Delta G_e^{\neq}$ = Activation free energy for overcoming electron repulsion between the ions and

R = Gas constant

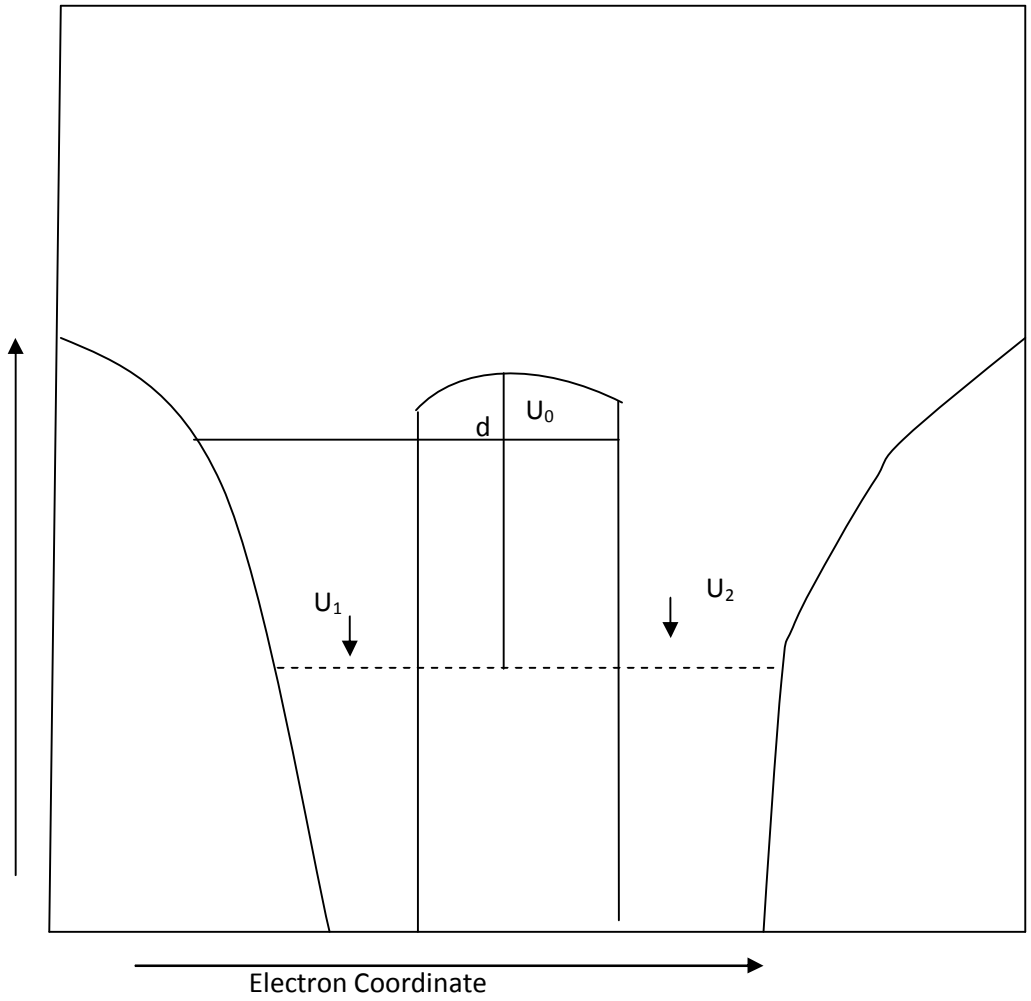


Figure.1.1: Electron transfer by penetration of a potential energy barrier.

where U_1 and U_2 are the ground states of the electrons in cation 1 and 2 respectively, D = width of barrier at height of penetration, W = kinetic energy of the electron and U_o = height of the barrier.

1.6 Objective of the study

Caffeine is a common ingredient in many medications such as Anacin and Vivanius (Maram and Mundra, 2000). It has been reported to have ability to scavenge free radicals and excited state of oxygen thus protects crucial biological molecules from these species (Kasavana and Sarma, 1995). Imidazole is found in many important biological molecules like histidine and it plays important role in structure and binding function of haemoglobin. It has been used extensively as corrosion inhibitor on metals (Antonijevic and Petrovic, 2008).Theophylline is used in the therapy of respiratory diseases such as bronchial asthma (Nunes, *et al.,* 2009). In modern medicine, theobromine is used as a vasodilator and as a diuretic (William, 1945).

However, in spite of these and other numerous uses, research focus has been mostly on their physiological effects. (Maram and Mundra, 2000), only few mechanistic investigations have been carried out on the oxidation of these compounds. It is believed that most biochemical reactions in the biological systems involve electron transfer at some point or another during the course of the reaction. Understanding the kinetics and mechanism of *in vitro* redox reactions of these reactants can serve as a model to providing deeper insights into the nature of these biochemical reactions. Therefore, there is need for sufficient kinetic data which will assist in the better understanding and more efficient utilization of these reactions. This aim will be achieved through the following objectives:

Determination of the stoichiometry of the reaction,

Determination of the order of the reaction,

Effect of changes in acid concentration on the reaction rate,

Effect of added cations and anions on the reaction rate,

Effect of changes in ionic strength on reaction rate,

Test for intermediate complex formation and for free radicals in the course of the reactions and analyses of the product.

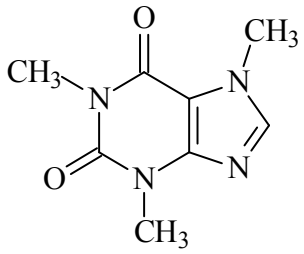
CHAPTER TWO

2.0 Literature review

2.1.0 Caffeine

Caffeine (hereafter referred to as CAF) is an alkaloid found naturally in, tea, kolanuts, yerba mate, guava and (in small amounts) cacao beans. It is added to some drinks such as Mountain dew, Red bull, Horse power etc. (Gurdeep, 2005; Stephen, 2010). The compound has pharmacological properties such as stimulating action on the central nervous system and a stimulation of respiration, heart rate and a mild diuretic effect (Trease and Evans, 2005). It has been reported to have significant abilities to scavenge highly reactive free radicals and excited states of oxygen and thus protects crucial biological molecules against these species (Davasagayam *et al.,* 1996; Telo and Viera, 1997). The antioxidant ability of caffeine is reported to be similar to that of biological antioxidant glutathione and significantly much higher than that of ascorbic acid (Kesavana and Sarma, 1995).

A common ingredient in many prescription and over-the-counter medications, caffeine is present in drugs such as Anacin tablets and caplets, Vivanius and Excedrin migraine. Thus, because of the vast consumption of caffeine-containing beverages, researches have focused on its physiological effect (Maram and Mundra, 2000). The structure of caffeine is as shown below.



Caffeine

Kinetic study on the oxidation of caffeine by sodium m-chlorobenzene sulphanamide (CAB) in hydrochloric acid solution (0.02–0.10 $moldm^{-3}$) has been shown to have first order dependence on (CAB) fractional order in $[H^+]$ and is independent of substrate concentration and ionic strength (Jayaram and Mayanna, 1983). On decreasing the dielectric constant of the medium by adding butanol, the rate decreases slightly. The kinetic data suggest a complex formation between RNC^- and HCl.

Maram and Mundra (2000), studied the electron transfer reaction of caffeine by phosphate radical anion in aqueous solution. The rate of the reactions increased with increase in peroxydiphosphate (PDP), while they are independent of caffeine. The order of reaction with respect to [PDP] has been found to be one. The oxidation product was determined to be 1, 3, 7− trimethyluric acid identified by HPLC analyses.

2.2.0 Imidazole

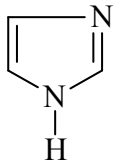
Imidazole (1,3–diazo–2–4–cyclopentadienyle) hereafter referred to as IDZ, is a heterocyclic organic compound with the molecular formula $C_3H_4N_2$. It exists in two equivalent tautomeric forms because the hydrogen atom can be located on either of the two nitrogen atoms. The compound is amphoteric in nature, as an acid its pKa is 14.5, making it less acidic than carboxylic acid, phenols and imides. The acid proton is located on N– 1.While as a base; the pKa of the conjugated acid is approximately 7, thus making it more basic than pyridine (Bhatnagar *et al.,* 2011).

Imidazole is incorporated into many important biological molecules and plays a vital role in structure and binding functions of hemoglobin. The most pervasive is the amino acid (“histidine”) which has an imidazole side chain. Another application of this compound is in the purification of His-tagged proteins in immobilized metal affinity chromatography (IMAC). IDZ has become an important part of

many pharmaceuticals synthetic imidazoles and antifungal, antiprotozoal and antihypertensive medications.

It has also been used extensively as a corrosion inhibitor on certain metals, such as copper (Antonijevic and Petrovic, 2008). Preventing copper corrosion is important especially in aqueous systems, where the conductivity of the copper decreases due to corrosion. Substituted imidazole derivatives are used in the treatment of many systematic fungal infections (Shargel, 1998). Examples include ketoconazole, miconazole and dotimazole.

Many compounds of industrial and technological importance contain imidazole derivatives. The thermostable polybenzimidazole (PBI) contain imidazole fused to benzene ring and act as a fire retardant. Salts of imidazole where the imidazole ring is in the cation are known as imidazolium salts example includes imidazolium chloride. The structure of imidazole is as shown below.



Imidazole

Kinetics study on the oxidation of some thioacids by imidazolium fluorochromate has been reported (Gilla *et al*., 2011). The oxidation of thioglycolic, thiolactic and thiomalic acid by imidazolium fluorochromate (IFC) in dimethylsulphoxide (DMSO) leads to the formation of disulphate dimmers. The reactions are thus, of first order with respect to IFC. Michaelis-Menten's type of kinetics is observed with respect to the thioacids. The reaction exhibited a 1:2 stoichiometry as represented in equation 1.1.

$2R – S – H + O_2CrFOImH \rightarrow R – S – S – R + H_2O + OcrFoImH$ …1.1

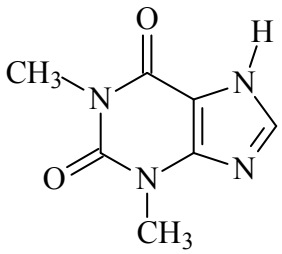
The reaction is catalysed by hydrogen ion. Dependence on acid has taken the form.

$k_{obs} = a + b [H^+]$ …1.2

2.3.0 Theophylline

Theophlline (1,3–dimethylxanthine) also known as dimethylxanthine (hereafter referred to as TP) is an alkaloid of the xanthine family, naturally found in tea, cocoa beans and in number of different salts, the most common of which are aminophylline (the ethylenediamine) and choline theophyllinate.

The compound is used in the therapy of respiratory diseases such as bronchial asthma and reversible bronchopasm acts by inhibiting cyclic nucleotide phosphodiesterase (Rajayashree *et al*., 2011). Its oxidation reactions were investigated as tool for spectrophotometric determination of theophylline concentration in pure or pharmaceutical formulations. On oxidation with sodium metaperiodate in the presence of acetic acid, a blue-coloured product with a λ_{max} of 630nm has been reported. (Singh and Sah, 2006). The structure of theophylline is as shown below.



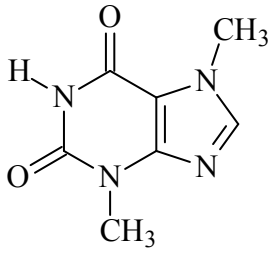
Theophylline

In vitro kinetic release of theophylline from acyclic polymer matrix tablets has been studied (Apu *et al*, 2009). The release kinetics was investigated by using correlation coefficient value of zero order

release plot (cumulative amount of drug released versus time) and Higuchi plot cumulative percentage of drug release versus square root of time). It was observed that in all cases the release of theophylline followed mixed release kinetics where zero order release kinetics was predominant. This was also reported by Chernysleva *et al.*, (2000), the coulometric determination of theophlline in acid solution, was rapidly and quantitatively oxidized with electrogenerated chlorine in a stoichiometry of 2:5.

2.4.0 Theobromine

Theobromine (3,7-dimethylxanthine) also known as xantheose is an alkaloid with chemical formula, $C_7H_8N_4O_2$. It is found in chocolate, kolanuts, tea and other food substances. Even without dietary intake, it may occur in the body as it is a product of human metabolism of caffeine which is metabolized in the liver into 10% theobromine, 4% theophylline, and 80% paraxanthine (Davasagayam and Kesavan, 1966). In modern medicine, it is used as a vasodilator, a diuretic and as a heart stimulant (William, 1945) possible future uses of theorbomine in fields such as cancer prevention have been patented (Sulkalyn *et al.,* 2009). The structure of theobromine is as shown below.



Theobromine

Zbaida *et al*., (1987) reported the oxidation of theobromine by Fenton's reagent. The compound undergoes N-demethylation and hydroxylation to give uric acid derivatives. It is also known to exhibit

antioxidant and prooxidant. Colometric method for the determination of theobromine has been studied in acid solution. The compound was quantitatively oxidized with electrogenerated chlorine in a stoichiometric ratio of 2:5 to give alloxan and urea (Chernysleva *et al.,* 2000).

2.5.0 Redox reactions of permanganate ion

Potassium permanganate ($KMnO_4$) is used primarily to control taste and odors, remove color, control biological growth in treatment plants, and remove iron and manganese. In a secondary role, it may be useful in controlling the formation of trihalomethanes (THMs) and other disinfectant by-products (DBPs) by oxidizing precursors and reducing the demand for other disinfectants (Hazen and Sawyer, 1992). It is widely used as oxidizing agent in synthetic and analytical chemistry (Hiremath, *et al*., 1996). The ion, as an important oxidant in many organic and inorganic redox reactions, involves the Mn(VII) entity which is known for its versatility (Stewart,1965). The oxidizing ability of Mn(VII) is a function of the pH of the medium (Iyun *et al*., 1992). In acidic medium, Mn(VII) is reduced to Mn(II), Mn(IV) and Mn(VI).Under acidic conditions the oxidation half-reactions are:

$$MnO_4^- + 4H^+ + 3e^- \longrightarrow MnO_2 + 2H_2O \quad \ldots 2.1$$

$$MnO_4^- + 8H^+ + 5e^- \longrightarrow Mn^{2+} + 4H_2O \quad \ldots 2.2$$

Under alkaline conditions, the half-reaction is:

$$MnO_4^- + 2H_2O + 3e^- \longrightarrow MnO_2 + 4OH^- \quad \ldots 2.3$$

The appearance of these intermediate oxidation states depends upon various reaction conditions, type of compound and there stability (Sukalyn *et al*., 2009). Been a versatile oxidant, variety of mechanism are possible depending on the nature of the medium and the reactive species. The oxidant has been assigned both inner-sphere and outer-sphere mechanisms in their redox reactions (Hassan, 1991; Azafarany, 2010). Reports have been made on the kinetic studies of the oxidation of

permanganate on specific functional groups of organic compounds. Phenols are considered to be highly reactive by permanganate oxidation (He *et al.,* 2009; Jiang *et al.,* 2009) while benzene ring and their derivatives (xylene and toluene) are considered to oxidize slowly by permanganate (Walder and Tratnyek 2005).

Mohammed *et al.,* (2009) reported the redox reaction of malachite green (MG^+) and permanganate ion (MnO_4^-) in aqueous acidic medium. The stoichiometry of the reaction is

$$MG^+ + MnO_4^- \longrightarrow \text{Product} \quad \ldots 2.4$$

The rate law of the reaction can be expressed as

$$-d[MG^+]/dt = k_2 [MG^+][MnO_4^-] \quad \ldots 2.5$$

First order reaction with respect to $[MG^+]$ and $[MnO_4^-]$ was reported. The rate of the reaction was shown to depend on the acid concentration. The acid dependence study showed two pathways, one which is acid independent and the other which is acid dependent. The overall rate of the reaction conforms to the equation below.

$$-d[MG^+]/dt = (a + b [H^+][MG^+][MnO_4^-] \quad \ldots . 2.6$$

Kinetic study on nicotine oxidation by permanganate in aqueous perchloric solution has been studied (Ishaq, 2010). The stoichiometry of the reaction is:

$$5C_{10}H_{14}N_2 + 4MnO_4^- + 17H^+ \longrightarrow 5C_6H_5NO_2 + 5C_4H_8O + 5NH_4^+ + Mn^{2+} + H_2O \quad \ldots . 2.7$$

The reaction was inhibited by $[H^+]$. The order with respect to $[H^+]$ was found to be of inverse non-integral value. Inverse order dependence in $[H^+]$ may be explained by the release of proton from

nicotine prior to the rate determining step. The oxidation product of nicotine was identified as nicotinic acid.

Babatunde, (2008) reported the kinetics of the oxidation of L-ascorbic acid by permanganate ion in acidic medium. The stoichiometry of the reaction can be expressed as

$$2MnO_4^- + 5H_2A + 6H^+ \xrightarrow{2Mn^{2+}} 5A + 8H_2O \quad \text{...2.8}$$

The reaction shows dependence on acid concentrations and first order in both oxidant and reductant. The proposed rate law is:

$$-d[MnO_4^-]/dt=(a + b[H^+])[MnO_4^-][H_2A] \quad \text{…2.9}$$

Scheme constant with the observed data proposed for the reaction is as shown below:

$$H_2A + H^+ \overset{K}{\rightleftharpoons} H_3A^+ \quad \text{.....2.10}$$

$$MnO_4^- + H_2A \xrightarrow{k_1} A + MnO_3^- + H_2O \quad \text{.....2.11}$$

$$MnO_4^- + H_3A^+ \xrightarrow{k_2} HMnO_3 + A + H_2O \quad \text{...2.12}$$

$$MnO_3^- + H^+ \longrightarrow HMnO_3 \quad \text{…2.13}$$

$$2HMnO_3 + 3H_2A + 4H^+ \xrightarrow{2Mn^{2+}} + 3A + 6H_2O \quad \text{…2.14}$$

$$Rate=k_1[MnO_4^-][H_2A] + k_2[MnO_4^-][H_3A^+] \quad \text{….2.15}$$

$$But\ [H_3A^+] = K[H_2A][H^+] \quad \text{...2.16}$$

Therefore,

$$Rate = k_1 + k_2[H^+][MnO_4^-][H_2A] \quad \text{…2.17}$$

Kinetics of oxidation of glycine by permanganate ion has been reported by Sarathi *et al.*, (2011). The investigation was carried out using spectrophotometric technique in alkaline medium at 525nm. The reaction exhibited first order dependence on permanganate concentration and less than one order (0.34) on glycine concentration and alkaline concentration respectively. The products of the reaction were found to be formaldehyde, ammonia and carbon dioxide. A plausible mechanism is proposed;

$gly_z + OH^- \rightleftharpoons gly^- + H_2O$ ….2.18

$gly^- + Mn(VII) \rightleftharpoons$ Complex (C) ….2.19

Complex (c) $\xrightarrow{k}$ gly° + Mn(VI) …2.20

$gly^{\circ} + Mn(VII) \longrightarrow HCHO + CO_2 + NH_3 + Mn(VI)$ ….2.21

Rate = k[C] ….2.22

$= kK_2[gly^-][Mn(VII)]$ ….2.23

Since $[Mn(VII)]_t = [Mn(VII)]_e + [C]$

But $[gly]_t = [Mn(VII)]_e + [gly^-]$ and

$$K_1 = \frac{[gly^-]}{[gly_z][OH^-]}$$ ….2.24

$$[gly^-]_e = \frac{K_1[gly_z]_t[OH^-]}{1 + K_1[OH^-]}$$ ...2.25

$$\text{Rate} = \frac{k_1K_1K_2[gly]_t[Mn(VII)][OH^-]}{1 + K_1K_2[gly^-]_t[OH]}$$ …..2.26

Refat *et al.,* (2011) reported the kinetics of oxidation of iota-and lamda carageenan by permanganate ion in aqueous per chlorate solution at constant ionic strength of 2.0 dm^3mol^{-1} s^1. The investigation was carried out spectrophotometrically, under pseudo first conditions. The experimental observation showed first order dependence in permanganate ion concentration and fractional order with respect to concentration of carageenan. H^+ dependence study showed that the oxidation process is acid catalyzed. The added ions enhanced the rate of the reaction. Kinetic evidence for intermediate complex formation was observed.

Bahrami and Zahedi, (2004) reported the reaction kinetics of L– ά –amino–n–butyric acid oxidation by permanganate in acidic medium using spectrophotometric technique. The stoichiometry was observed as shown below

$$MnO_4^- + 5CH_3–CH_2– CH_2–CH(NH_3) + COO^- + 11H^+ \longrightarrow 5CH_3–CH_2– CHO + 5NH_4^+ + 5CO_2 + Mn^{+2} + 3H_2O \quad \text{..... 2.27}$$

The reaction is first order with respect to permanganate ion and the amino acid. Therefore, the overall rate equation for reaction is

$$-d[MnO_4^-]/dt = k_1[MnO_4^-] + k2[MnO_4^-][Mn^{2+}]. \quad \text{.... 2.28}$$

CHAPTER THREE

3.0 Experimental

3.1 Materials and reagents

All solutions were prepared with distilled water.

3.1.1 Preparation of standard solution of caffeine

Analar grade (BDH) of caffeine obtained was used without further purification. About 4.855g of caffeine was dissolved in 250cm^3 of distilled water to give 1.0 x10^{-1} mol dm^{-3} of caffeine solution.

3.1.2 Preparation of standard solution of imidazole

Analar grade of 1.7019g (BDH) of imidazole was dissolved in 250 cm^3 of distilled water to give 1.0 x10^{-1}mol dm^{-3} of imidazole solution.

3.1.3 Preparation of standard solution of theobromine

About 3.60g (BDH) of theobromine was dissolved in 200 cm^3 of distilled water to give 1.0 x10^{-1} mol dm^{-3} of theobromine solution.

3.1.4 Preparation of standard solution of theophylline

About 3.60g (BDH) of theophylline was dissolved in 200 cm^3 of distilled water to give 1.0x10^{-1} mol dm^{-3} of theophylline solution.

3.1.5 Preparation and standardization of potassium permanganate solution

The permanganate solution was prepared by dissolving accurately weighed quantity of the $KMnO_4$ in distilled water and standardized by titrimetric method (Vogel, 1978). Accurately weighed 0.3g of dry sodium oxalate was dissolved in 240cm^3 of distilled water and 12.5cm^3 of concentration sulphuric acid was added from a burette until faint pink coloration persist for 30 seconds. The concentration of permanganate was then determined.

3.1.6 Preparation of standard solution of sulphuric acid

A stock solution of sulphuric acid, 2.0 mol dm^{-3} was made by the diluting 98% of concentrated solution of H_2SO_4 (B.D.H, Analar) of specific gravity 1.84.

3.1.7 Preparation of standard solution of sodium formate

This was prepared by dissolving an accurate weight of the salt (BDH) in appropriate volume of distilled water.

3.1.8 Preparation of standard solution of calcium sulphate solution magnesium sulphate solutions

Standard solution of $MgSO_4$ and $CaSO_4$ were prepared by dissolving 1.36g of $MgSO_4$ and 1.2g of $CaSO_4$ each, in 10cm^3 of distilled water to give 0.1 mol dm^{-3} solutions.

3.1.9 Stoichiometric studies

The stoichiometries of the reactions were determined by spectrophotometric titration using the mole ratio method. In each case, the concentration of the permanganate ion was kept constant at 2.0 $x10^{-4}$ mol dm^{-3} while, those of the reductants were varied in the range CAF = (1.0 − 6.0) x 10^{-4} mol dm^{-3}, IDZ = (3.0 − 3.8) x 10^{-2} mol dm^{-3}, TB = (1.0 − 3.8) × 10^{-2} mol dm^{-3} and TP = (1.0–3.8) $x10^{-2}$ mol dm^{-3}. The reactions were allowed to go to completion. This was ascertained by taking the absorbances of the reaction mixture at intervals. The reactions were taken to complete when the absorbances of the solutions remained constant.

Absorbances of the solutions were measured at 530 nm, the wavelength of maximum absorption of potassium permanganate, having certified that none of the reactants or the product absorbed at the wavelength. The reductant – MnO_4^- products were colourless and therefore do not absorb in the visible region (400 –700nm). The stoichiometries indicated by the point of inflexion, were evaluated from the plots of absorbances versus mole ratio.

3.2.0 Kinetic measurements

The rates of the reactions were monitored on a Corning Colorimeter 252. The rate studied (in each case) by monitoring decrease in absorbance ($\log A_t - A_\infty$) of the permanganate at 530nm.The kinetic measurements were carried out under pseudo-first order conditions with respect to the concentrations of caffeine (2.0 – 5.2) $x10^{-2}$ mol dm^{-3}); Imidazole (2.0 – 7.0) x 10^{-2} mol dm^{-3}) theobromine (4.0 $x10^{-3}$ – 2.8 $x10^{-2}$ mol dm^{-3}) and theophylline (4.0 $x10^{-3}$ – 2.8 $x10^{-2}$ mol dm^{-3}) in at least 10–fold excess over the permanganate ion concentration. The hydrogen ion concentration, ionic strength and temperature of each of the reaction system were kept constant. The pseudo-first order plots of the $\log(A_t - A_\infty)$ versus time were made (where A_t and A_∞ are the absorbance at the end of the reaction and at time t) and from

the slope of the plots, the pseudo- first order rate constant (k_{obs}) were determined. The second order rate constants (k_2) were obtained from $k_{obs}/[R]$ where R = CAF, IDZ, TB or TP.

3.3.0 Acid dependence

The effects of $[H^+]$ on the rates of the reactions were determined by keeping the concentrations of the other reactants constant while varying the concentration of the hydrogen ion, under the following conditions: Caffeine–permanganate system: $[H^+]$ = (2.0-34.0) $x10^{-2}$ mol dm^{-3}, [CAF] =3.2 x 10^{-2} mol dm^{-3}, I = 0.5 mol dm^{-3} (Na_2SO_4), $[MnO_4^-]$ = 2.0 $x10^{-4}$ mol dm^{-3} and λ_{max} = 530nm, imidazole–permanganate system: $[H^+]$ = (1.0-4.8) $x10^{-2}$ mol dm^{-3}, [IDZ] = 7.0 $x10^{-2}$ mol dm^{-3}, I = 1.0 mol dm^{-3} (Na_2SO_4), $[MnO_4^-]$ = 2.0 $x10^{-4}$ mol dm^{-3} and λ_{max} = 530nm, theobromine–permanganate system: $[H^+]$ = 0.24 – 0.0.64 mol dm^{-3}, [TB] = 2.0 x 10^{-2} mol dm^{-3}, I = 1.0 mol dm^{-3} (Na_2SO_4), $[MnO_4^-]$ = 2.0 $x10^{-4}$ mol dm^{-3} and λ_{max} = 530nm and theophylline–permanganate system: $[H^+]$ = (1.0 – 4.8) $x10^{-2}$ mol dm^{-3}, [TP] 1.0 $x10^{-2}$ mol dm^{-3}, I = 0.5 mol dm^{-3} (Na_2SO_4), $[MnO_4^-]$ = 2.0 $x10^{-4}$ mol dm^{-3} and λ_{max} = 530nm. The orders of the reactions with respect to hydrogen ion concentration were obtained as the slope of the plot of $logk_{obs}$ versus $log[H^+]$. Variation of acid dependent second order rate constants with $[H^+]$ were obtained by plotting k_2 against $[H^+]$.

3.5.0 E**ffect of ionic strength and dielectric constant on the rate of reaction**

The effects of ionic strength of the reaction medium on the rate constants of the reactions were determined by varying the concentration of the inert electrolyte (Na_2SO_4).The ionic strength was adjusted based on the relationship (equation 3.1).

$$I = \tfrac{1}{2} \sum C_i Z_i^2 \qquad ...3.1$$

where Z_i is the charge number of an ion (positive for cations and negative for anions)

C_i is the concentration of the ion in solution. The effects of medium dielectric constant on the reaction rates were observed by carrying out the reaction in medium of varying dielectric constant. The medium dielectric constant was varied by mixing water and acetone in different ratio and the dielectric constant calculated using equation (3.2).

$$D = \frac{D_{water} x V_{water} + D_{Ace} x V_{Ace}}{V_{Total}} \quad \text{....3.2}$$

where V_{water} and $V_{acetone}$ are the volumes of water and acetone respectively. D_{water} and D_{Ace} are the dielectric constants of water and acetone respectively and V_{Total} is the total volume .The effect of dielectric constant (D) on the rates of the reactions was investigated by varying acetone – water mixture, while other conditions were kept constant. A plot of $\log k_2$ against 1/ D gives the relationship between the second order rate constant and the dielectric constant, D.

3.6.0 Tests for the presence of intermediate complex

3.6.1 Spectrophotometric investigation

This was carried out in order to find out whether spectroscopically determinable intermediate complex were formed during the course of the reactions. The spectra of the reacting mixtures at certain time intervals after the start of the reaction, depending on the speed of the reaction, were taken over the range of 400 – 700 nm for each of the system studied. Similar runs were made for the permanganate alone as control.

3.62 Free radical test

About $5cm^3$ of acrylamide was added to partially oxidized reaction mixture of containing various concentrations of reductant, oxidant and hydrogen ion. This was followed by a large excess of methanol. The acrylamide was also added to the solution of reductant and permanganate separately, serving as control.

3.7.0 Product analyses

Analyses of various products of the redox reaction were carried out where possible. At the completion of the reactions, the products were tested qualitatively and the presence of Mn^{2+} ion was analyzed. Potassium perchlorate oxidizes Mn(II) to purple Mn(VII) as can be represented by the equation below.

$$2Mn^{2+} + 5KClO_4 + 3H_2O \rightarrow 2MnO_4^- + 5KClO_3 + 6H^+ \quad \cdots\cdots 3.3$$

Colourless Purple

CHAPTER FOUR

4.0. Results

4.1 Stoichiometry

The stoichiometric results for the reactions of caffeine – permanganate and theobromine – permanganate systems showed that one mole of each of the reductant (caffeine, theophylline) was consumed by one mole of permanganate ion (1:1). For the reactions of imidazole –permanganate and theobromine – permanganate systems, the stoichiometry showed that for two moles of each of the reductant (imidazole, theobromine), one mole of permanganate was consumed. The titration curves from which the stoichiometries were determined are presented in Figures (4.1) – (4.4). On the basis of these results, the overall equation for the reactions can be presented as equations (4.1) – (4.4).

$C_8H_{10}N_4O_2 + MnO_4^- + H^+ \longrightarrow Mn^{2+} + H_2O$ + Other products ….4.1

$C_4H_8N_4O_2 + MnO_4^- + H^+ \longrightarrow Mn^{2+} + H_2O$ + Other products …4.2

$2C_3H_4N_2 + MnO_4^- + H^+ \longrightarrow Mn^{2+} + H_2O$ + Other products ….4.3

$2C_4H_8N_4O_2 + MnO_4^- + H^+ \longrightarrow Mn^{2+} + H_2O$ + Other products …4.4

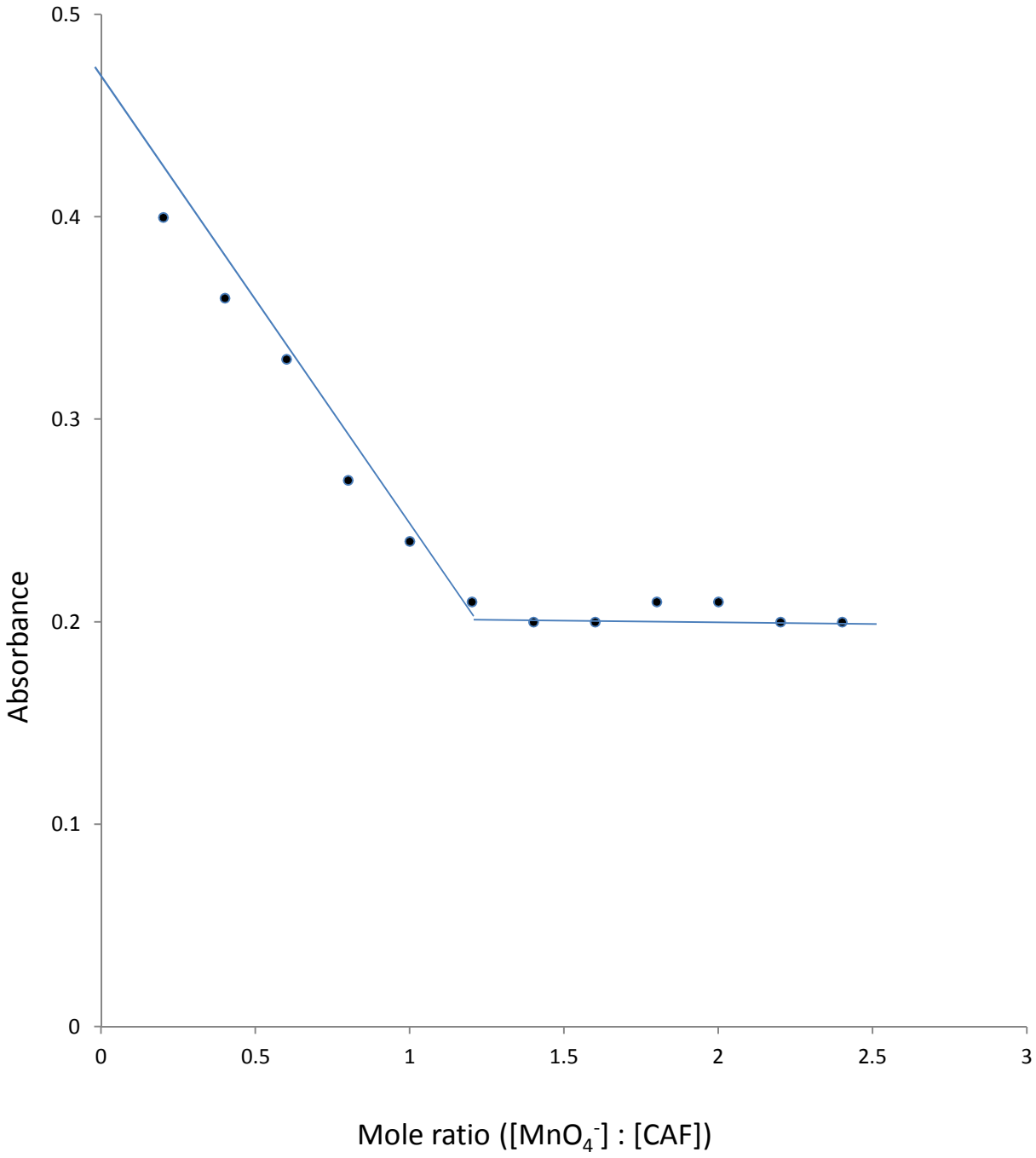

0.5
0.4
0.3
0.2
0.1
0
Absorbance
0
0.5
1
1.5
2
2.5
3
Mole ratio ([MnO4-] : [CAF])

Figure 4.1: Stoichiometric plot for the oxidation of CAF by MnO_4^- at [CAF] = (0.4 – 4.8) × 10^{-4} mol dm^{-3}, [MnO_4^-] = 2.0 × 10^{-4} mol dm^{-3}, [H^+] = 1.0 × 10^{-1} mol dm^{-3}, I = 0.5 mol dm^{-3} (Na_2SO_4), λ_{max} = 530nm and T = 23 ± 0.1℃

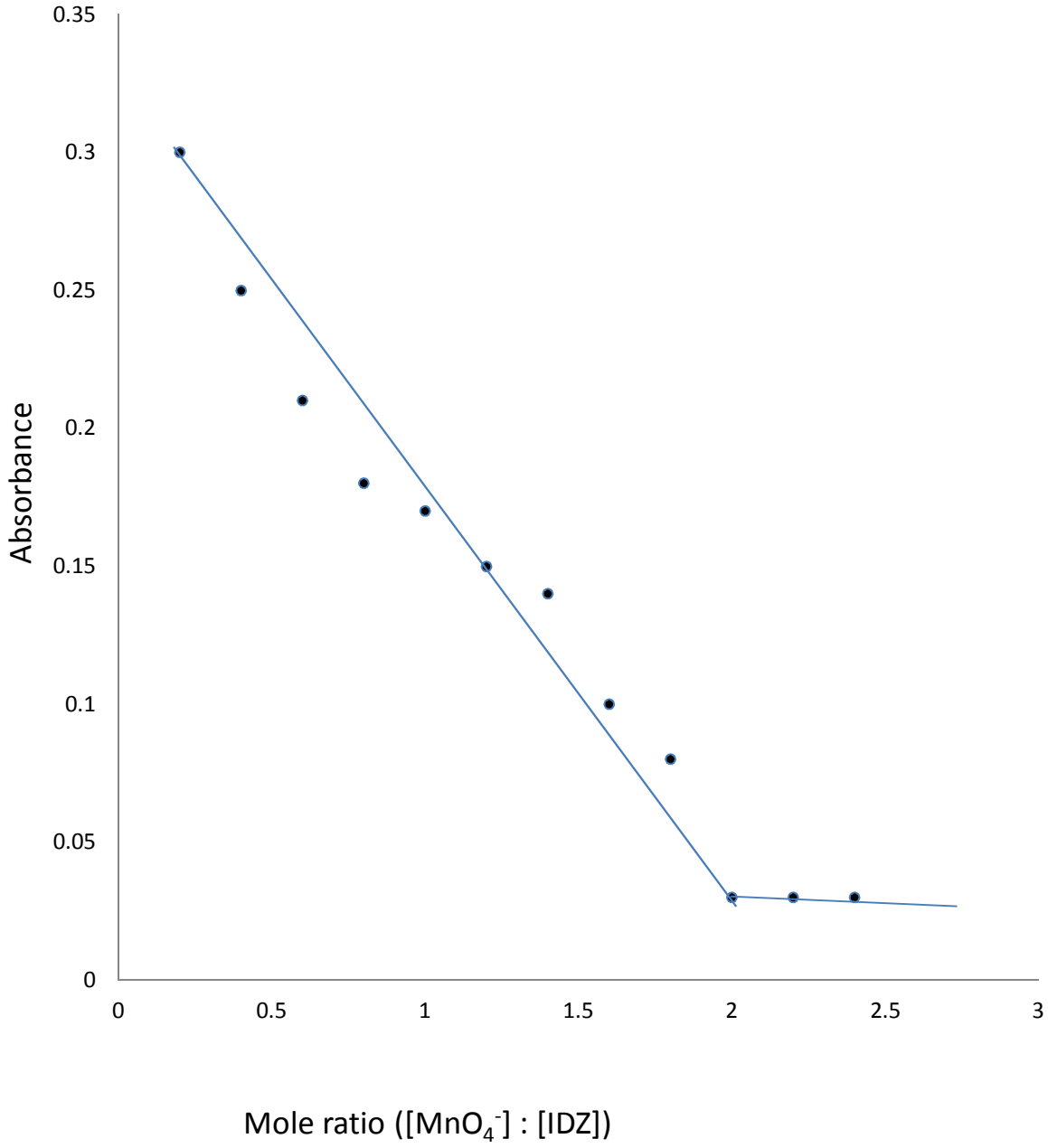


Figure 4.2: Stoichiometric plot for the oxidation of IDZ by MnO_4^- at [IDZ] = (0.4 – 4.8) × 10^{-4} mol dm^{-3}, [MnO_4^-] = 2.0 × 10^{-4} mol dm^{-3}, [H^+] = 1.0 × 10^{-2} mol dm^{-3}, I = 0.5 mol dm^{-3} (Na_2SO_4), λ_{max} = 530 nm and T = 25 ± 0.1°C

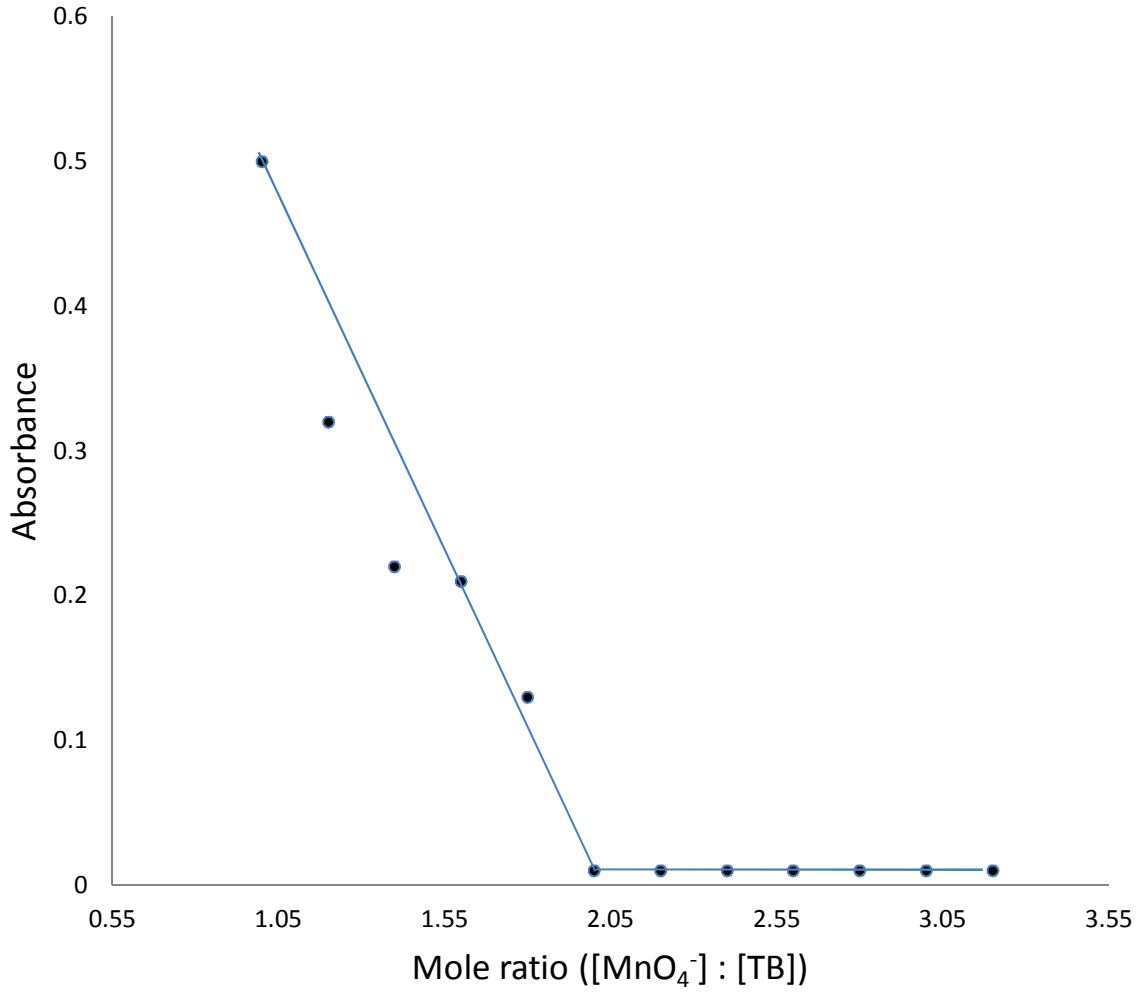


Figure 4.3: Stoichiometric plot for the oxidation of TB by MnO_4^- [TB] = (0.4 – 4.8) × 10^{-4} mol dm^{-3}, [MnO_4^-] = 2.0 × 10^{-4} mol dm^{-3}, [H^+] = 3.2 × 10^{-1} mol dm^{-3}, I = 0.1 mol dm^{-3} (Na_2SO_4) , λ_{max} = 530 nm and T = 23 $\pm$ 0.1^{0}C

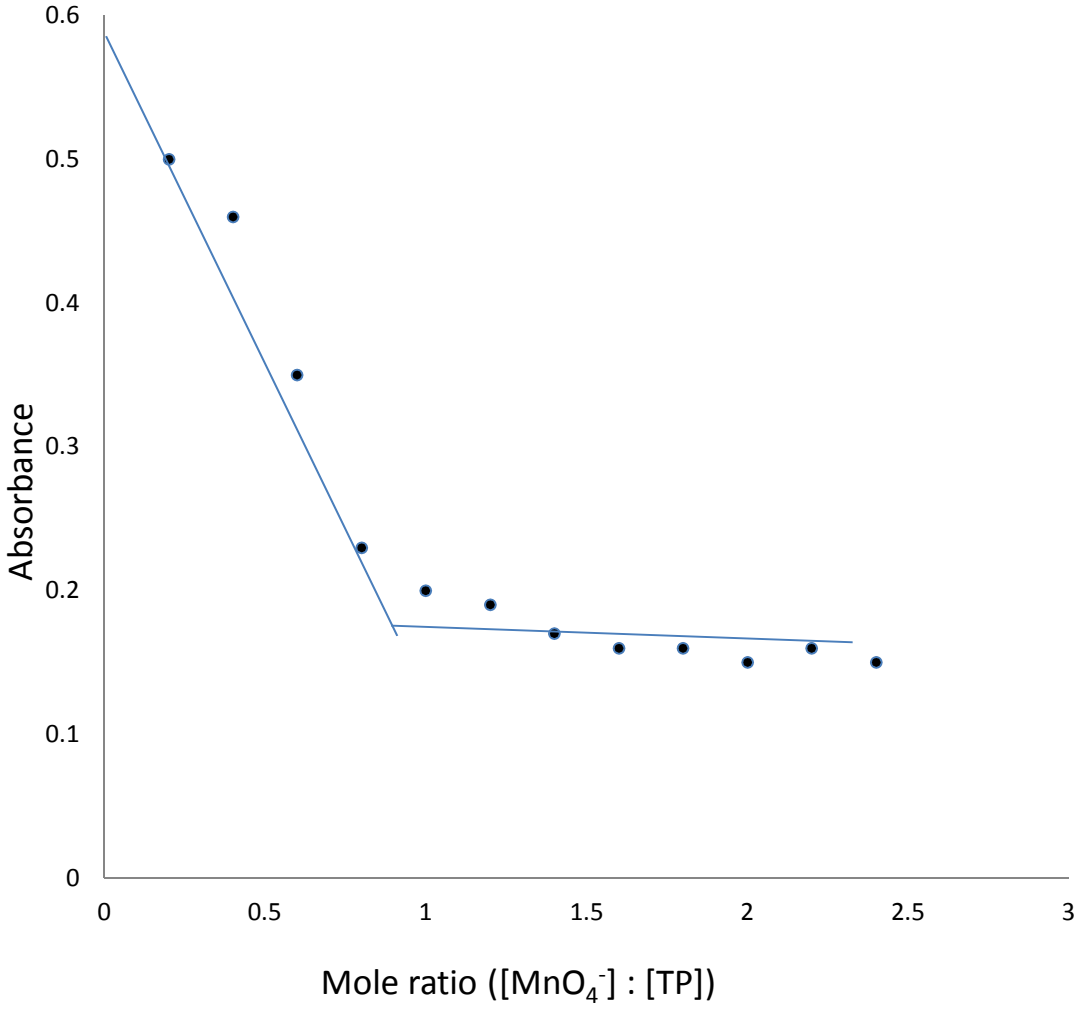


Figure 4.4: Stoichiometric plot for the oxidation of TP by MnO_4^- at [TP] = (0.4 – 4.8) $\times 10^{-4}$ mol dm^{-3}, [MnO_4^-] = 2.0 $\times$ 10^{-4} mol dm^{-3}, [H^+] = 1.0 $\times$ 10^{-2} mol dm^{-3}, I = 0.5 mol dm^{-3} (Na_2SO_4), λ_{max} = 530nm and T = 24.0 ± 0.1.

4.2 Product analyses

At the completion of the reactions, the products were tested qualitatively. The presence of Mn (II) ion was analyzed. The reaction of the colourless product with potassium perchlorate produced a purple coloured product, suggesting presence of Mn(II) ion. Potassium perchlorate oxidizes Mn(II) to purple Mn(VII) as can be represented by the equation 4.5.

$2Mn^{2+} + 5KClO_4 + 3H_2O \rightarrow 2MnO_4^- + 5KClO_3 + 6H^+$ 4.5

Colourless Purple

4.3 Order of the reaction

The pseudo-first order plots of $\log(A_t-A_\infty)$ versus time for these reactions were linear to more than 75% of the reactions (Figures 4.5-4.8). The linearity of these plots indicates that these reactions are first order with respect to the $[MnO_4^-]$. Plot of $\log k_{obs}$ versus log[Reductant] gave a slopes of 0.91, 0.92, 1.02 and 1.04 for CAF– MnO_4^-, IDZ– MnO_4^-, TB – $MnO_4^-$and TP– MnO_4^- systems respectively suggesting that the reactions are also first order in [Reductant] (Figures 4.9 - 4.12). Furthermore, the values of the second order rate constants k_2, obtained from ratio of k_{obs} and [Reductant], were found to be fairly constant (Tables 4.1- 4.4). These confirm that the reactions are first order in reductants respectively. The rate equations for the reactions can be represented as in equations 4.6–4.9, at I = 0.5 $moldm^{-3}$ (Na_2SO_4) and $[H^+] = 1.0 \times 10^{-1}$ mol dm^{-3}.The rate equation for the reaction of CAF with MnO_4^- is;

$-d[MnO_4^-]/dt = k_2[MnO_4^-][CAF]$ …4.6

For the reaction of IDZ with MnO_4^- at $[H^+] = 3.2 \times 10^{-2}$ mol dm^{-3} and I = 0.1 mol dm^{-3} (Na_2SO_4), the rate equation for the reaction is;

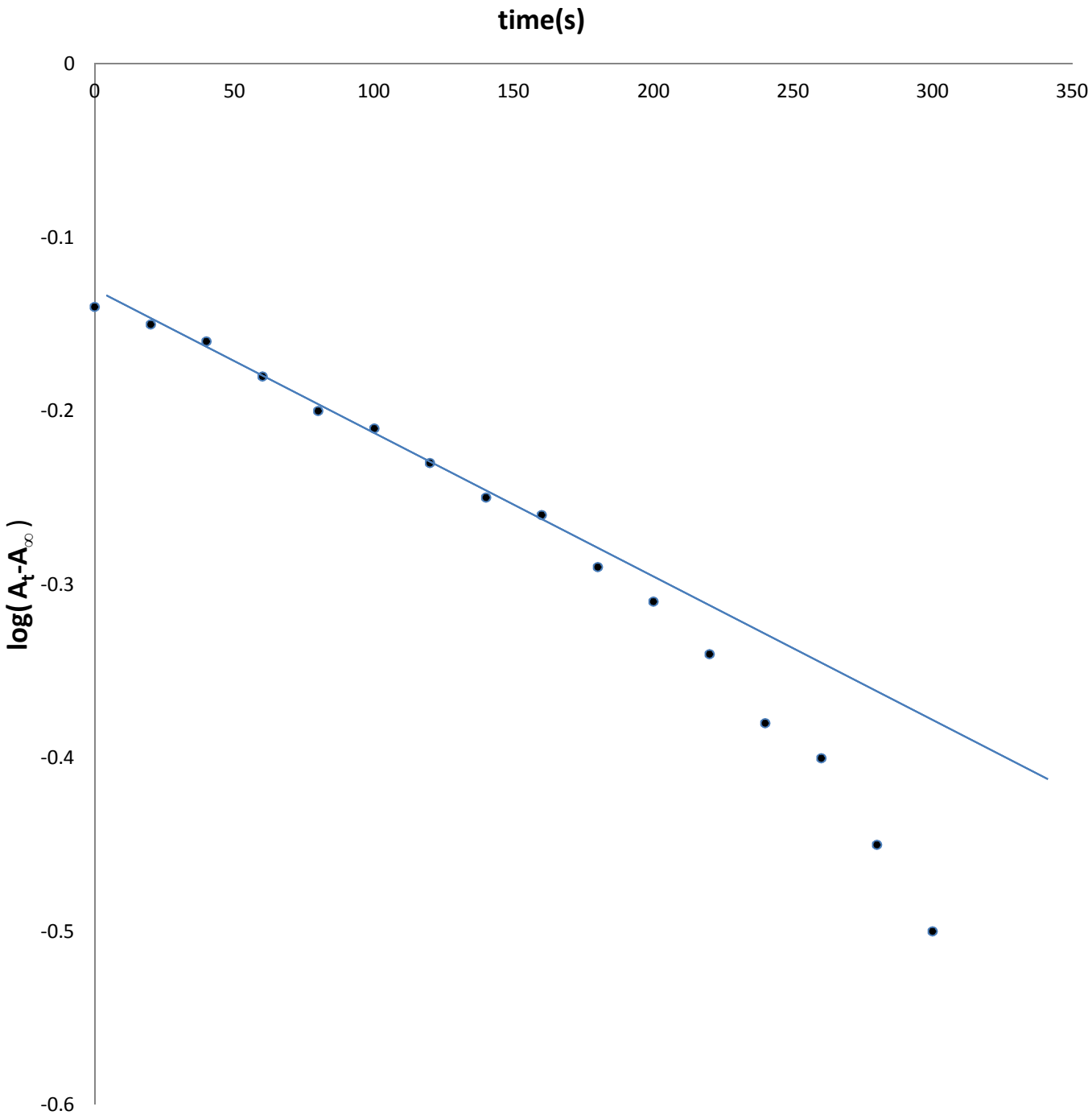


Figure 4.5: Typical pseudo–first order plot for the oxidation of CAF by MnO_4^- at [CAF] = 4.4×10^{-2} mol dm^{-3}, [MnO_4^-] = 2.0×10^{-4} mol dm^{-3}, [H^+] = 1.0×10^{-1} mol dm^{-3}, I = 0.5mol dm^{-3}, λ_{max} = 530nm and T = 24 ± 0.1°C

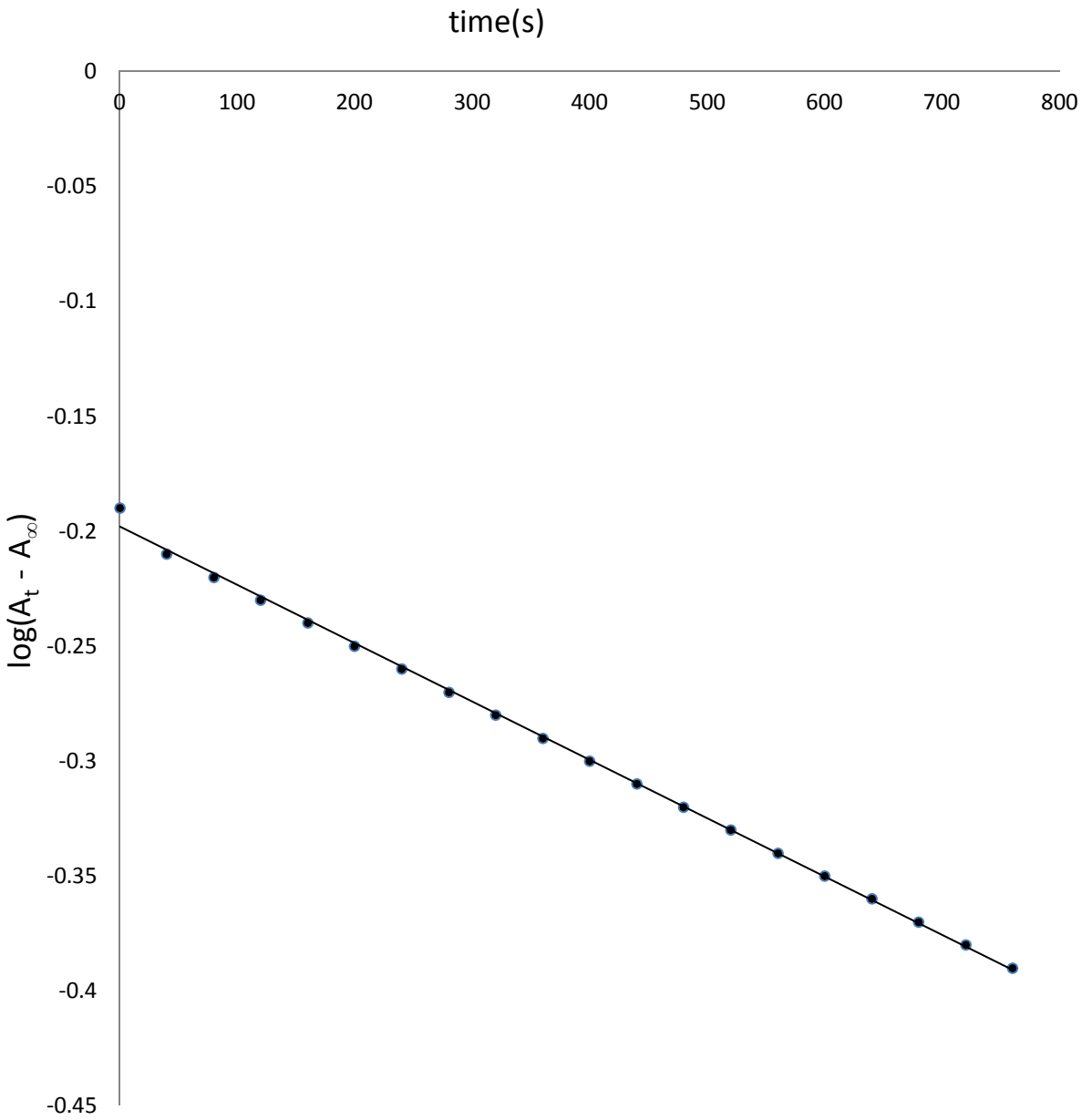


Figure 4.6: Typical pseudo –first order plot for the oxidation of IDZ by MnO_4^- at [IDZ] = 7.0×10^{-2} mol dm^{-3}, [MnO_4^-] = 2.0×10^{-4} mol dm^{-3}, [H^+] = 3.2×10^{-2} mol dm^{-3}, I = 1.0 mol dm^{-3}, λ_{max} = 530nm and T = 25.0 ± 0.1℃

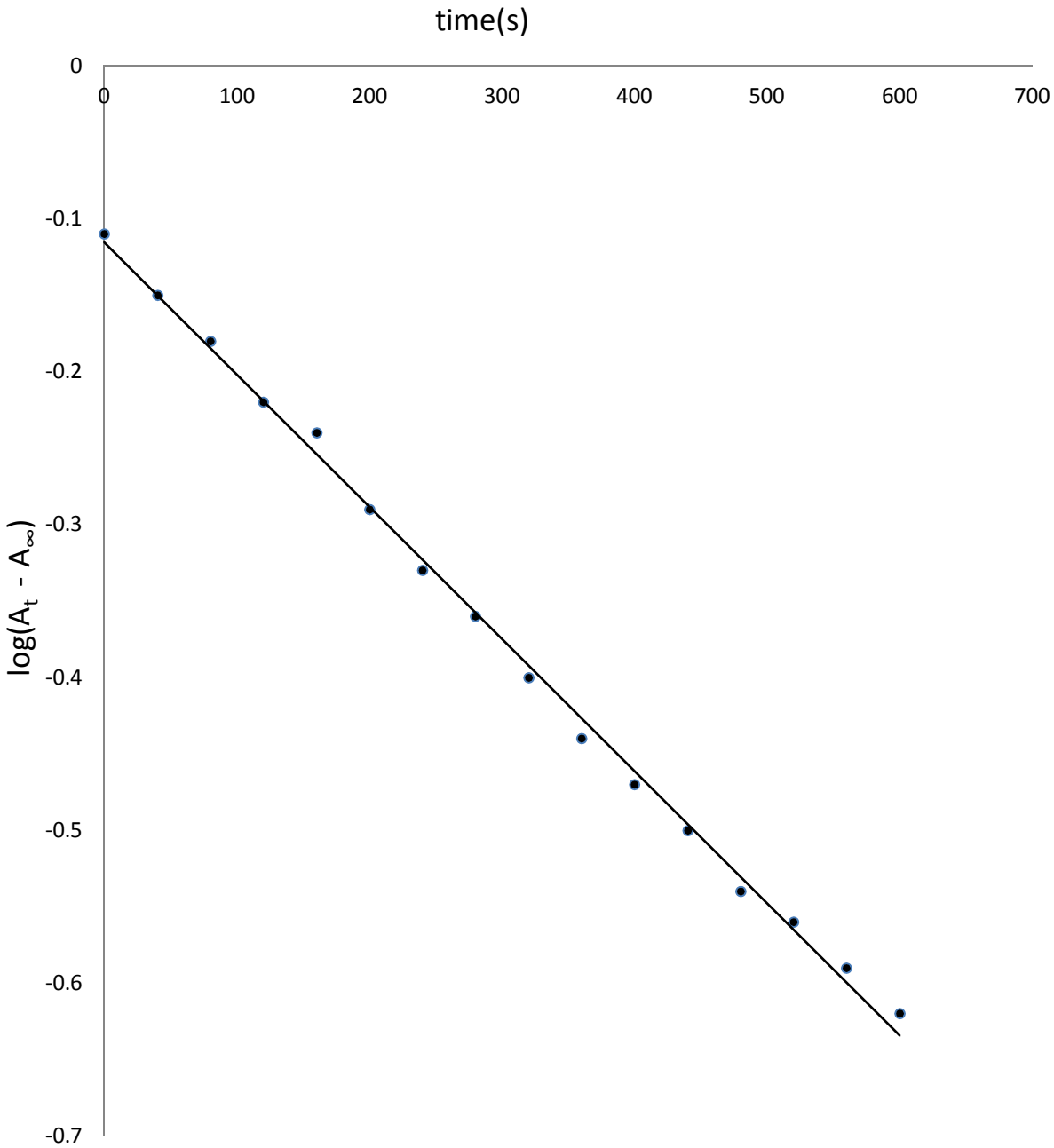
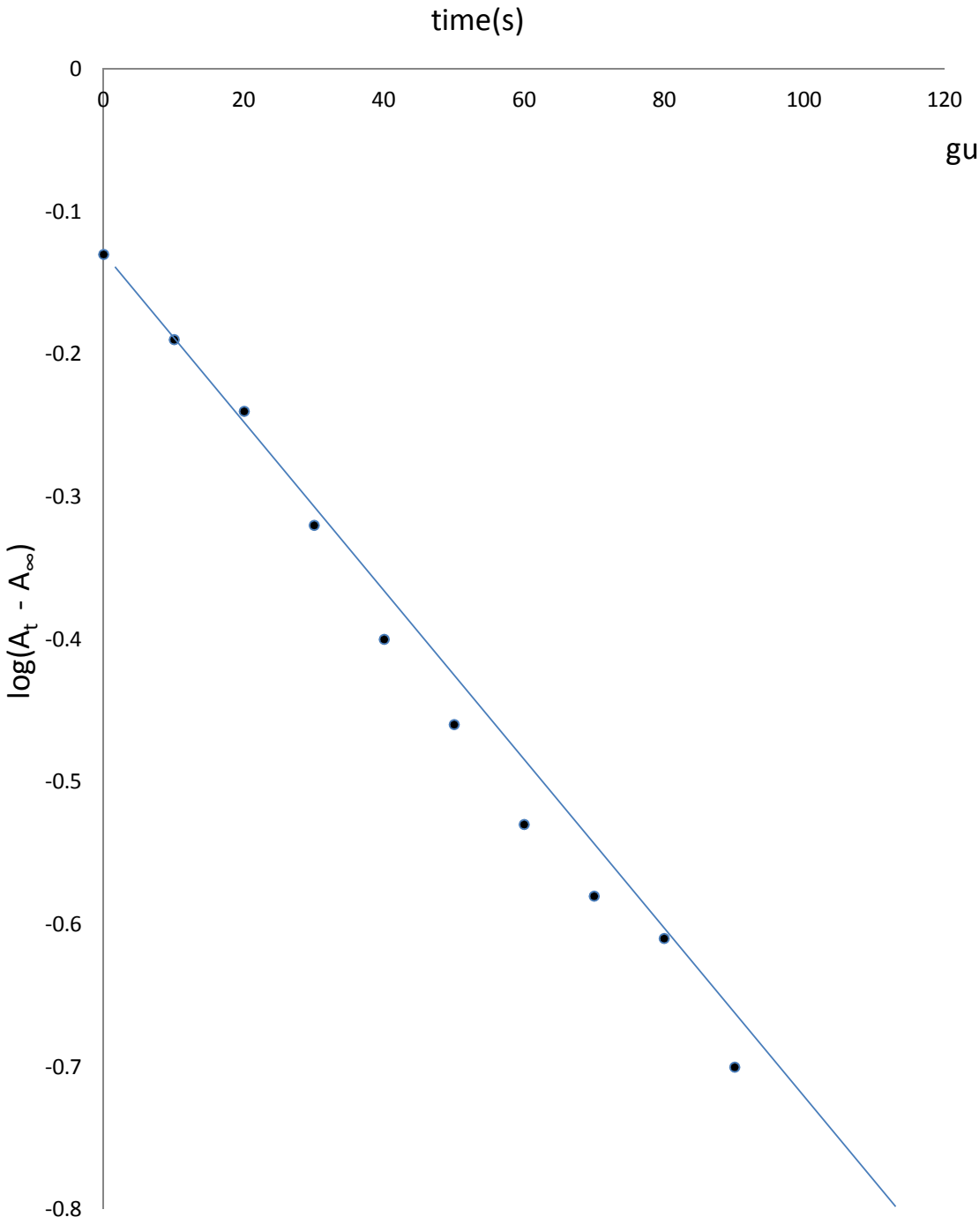


Figure 4.7: Typical pseudo–first order plot for the oxidation of TB by MnO_4^- at [TB] = 1.0×10^{-2} mol dm^{-3}, [MnO_4^-] = 2.0×10^{-4} mol dm^{-3}, [H^+] = 1.0×10^{-2} mol dm^{-3}, I = 1.0 mol dm^{-3}, λ_{max} = 530nm and T =23.0 ± 0.1°C



gure 4.8: Typical pseudo – first order plot for the oxidation of TP by MnO_4^- at [TP] =1.0 × 10^{-2} mol dm^{-3}, [MnO_4^-] = 2.0 × 10^{-4} mol dm^{-3}, [H^+] = 1.0 ×10^{-2} mol dm^{-3}, I = 0.5 mol dm^{-3}, λ_{max} = 530nm and T = 24.0 ± 0.1℃

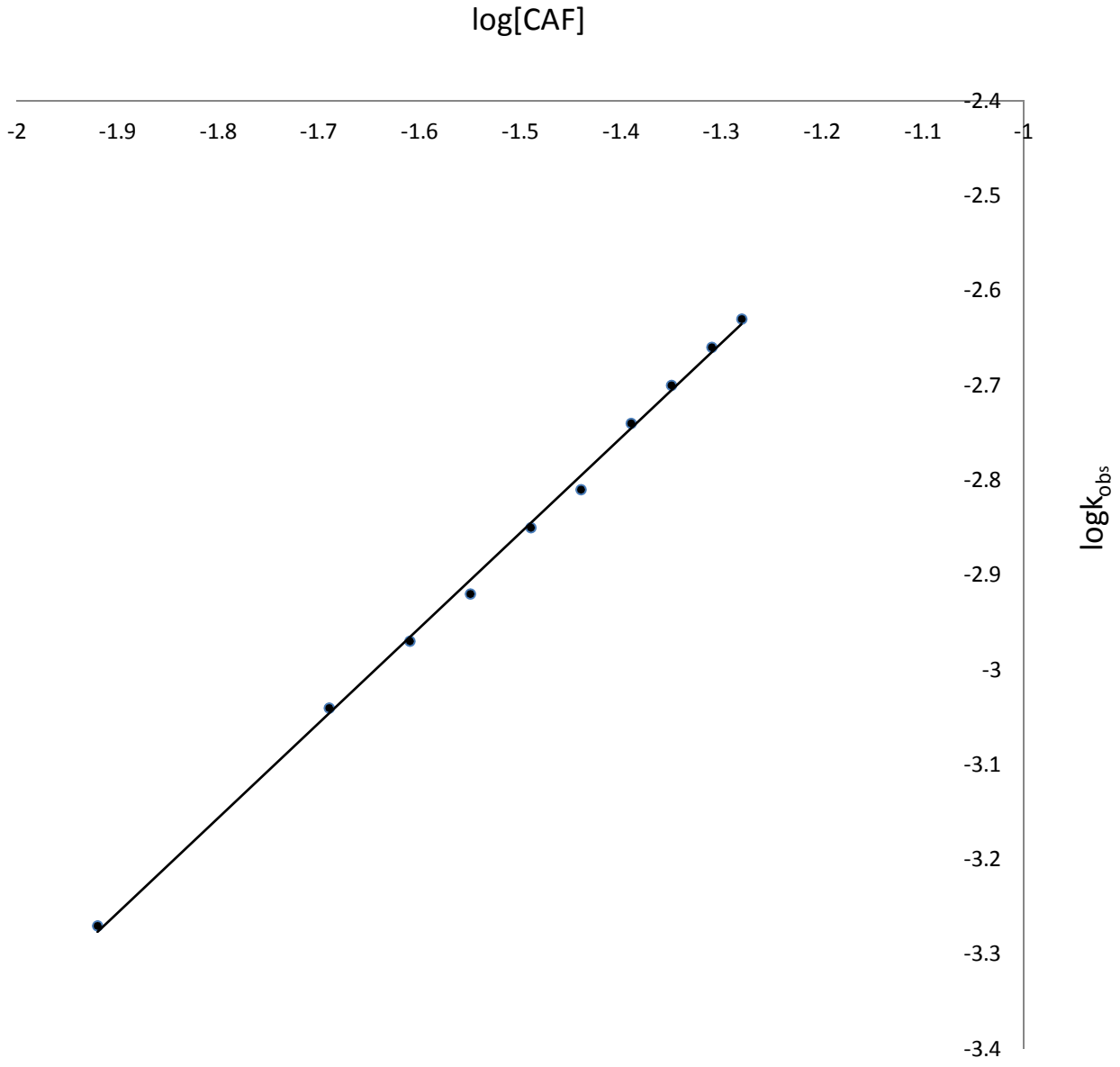

log[CAF]
-2
-1.9
-1.8
-1.7
-1.6
-1.5
-1.4
-1.3
-1.2
-1.1
-1
-2.4
-2.5
-2.6
-2.7
-2.8
-2.9
-3
-3.1
-3.2
-3.3
-3.4
logk$_{obs}$

Figure 4.9: $\log k_{obs}$ versus log [CAF] plot for the oxidation of CAF by MnO_4^- at $[MnO_4^-] = 2.0 \times 10^{-4}$ mol dm^{-3}, [CAF] = $1.2 \times 10^{-2} - 5.2 \times 10^{-2}$ mol dm^{-3}, I = 0.5 mol dm^{-3} (Na_2SO_4), λ_{max} =530nm and T = 24 ± 0.1℃

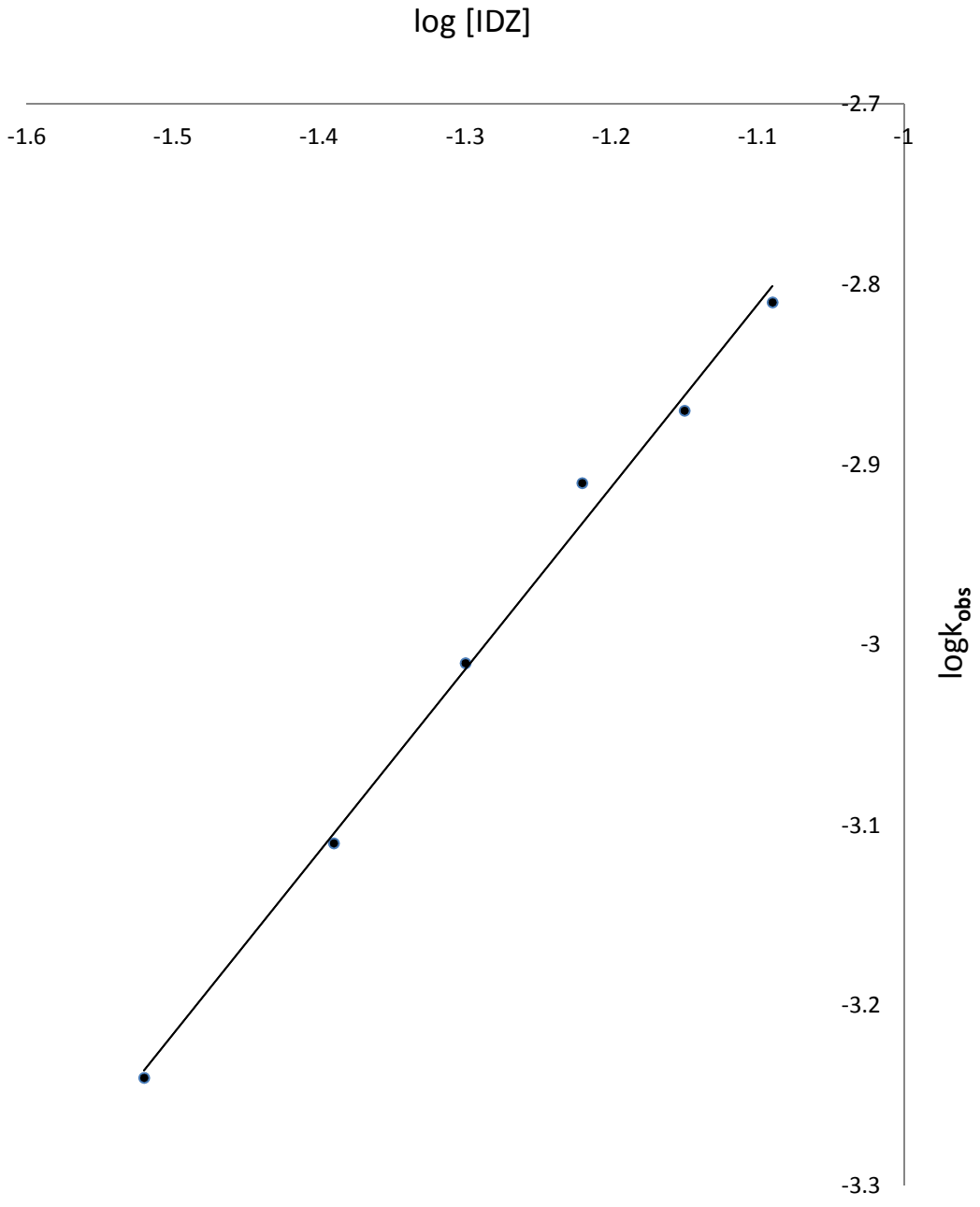


Figure 4.10: $\log k_{obs}$ versus log[IDZ] plot for the oxidation of IDZ by MnO_4^- at $[MnO_4^-]$ = 2.0 × 10^{-4} mol dm^{-3}, [IDZ] = (3.0 – 8.0) × 10^{-2} mol dm^{-3}, I = 1.0 mol dm^{-3} (Na_2SO_4), λ_{max} = 530nm and T =24.0 ± 0.1°C .

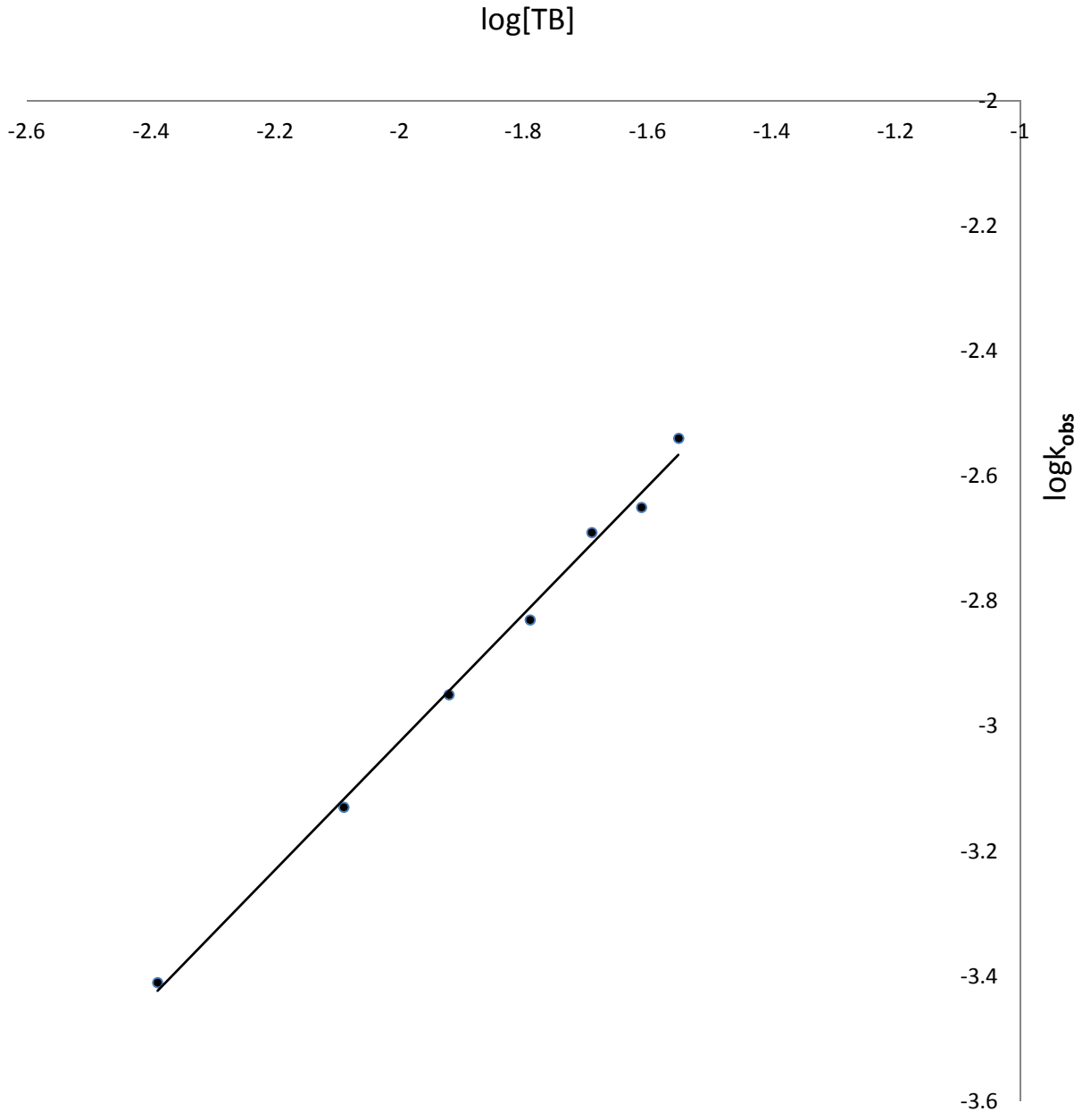


Figure 4.11: $\log k_{obs}$ versus log[TB] plot for the oxidation of TB by MnO_4^- at

$[MnO_4^-] = 2.0 \times 10^{-4}$ mol dm^{-3}, [TB] = (2.0 – 3.8) $\times 10^{-2}$ mol dm^{-3}, I = 1.0 mol dm^{-3} (Na_2SO_4), λ_{max} = 530nm and T = 24 ± 0.1°C

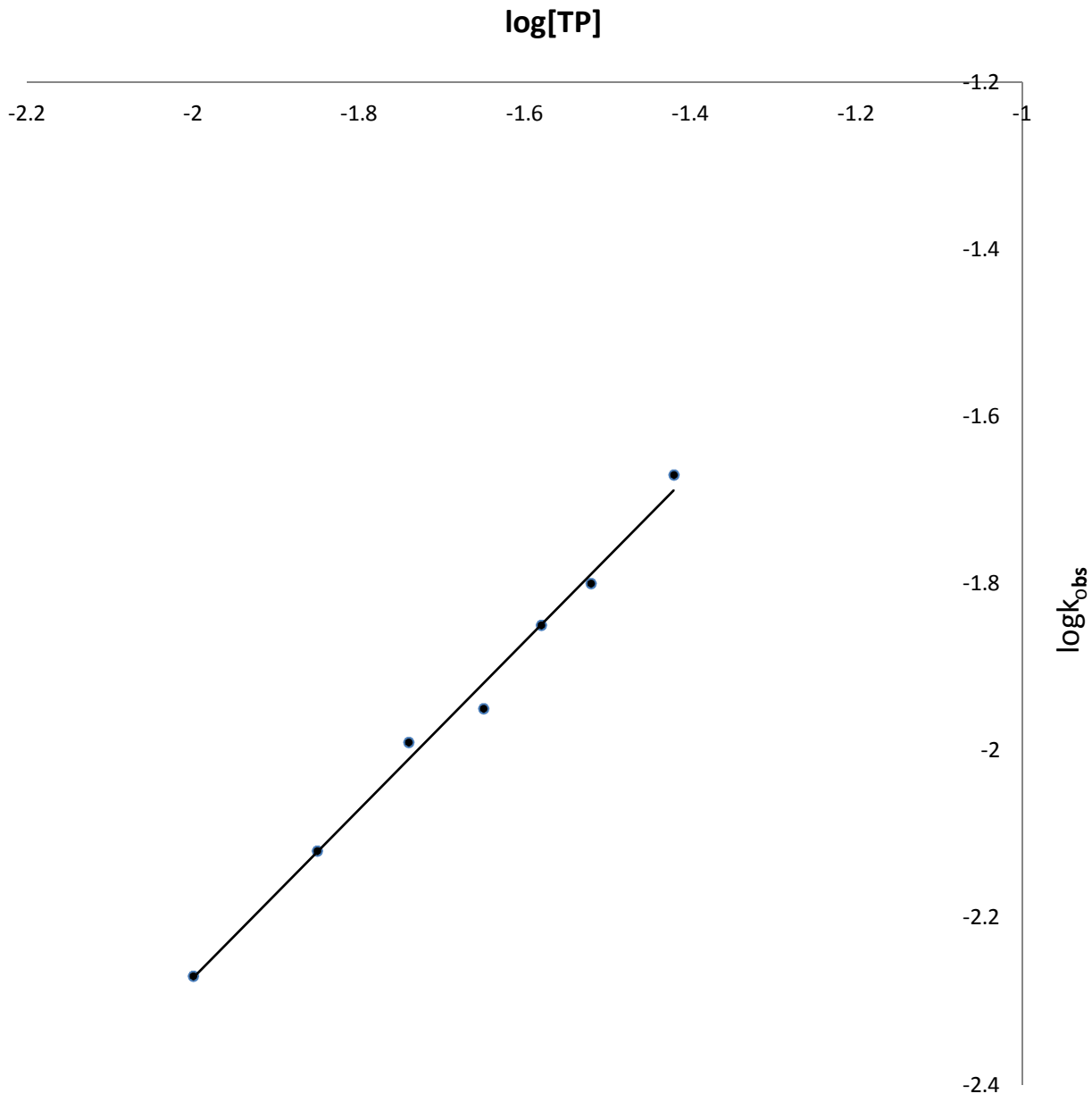


Figure 4.12: $\log k_{obs}$ versus log[TP] plot for the oxidation of TP by MnO_4^- at $[MnO_4^-] = 2.0 \times 10^{-4}$ mol dm^{-3}, [TP] = (1.0 – 3.8) × 10^{-2} mol dm^{-3}, I = 0.5 mol dm^{-3} (Na_2SO_4), λ_{max} = 530nm and T = 24 ± 0.1℃

Table 4.1: Pseudo –first and second order rate constants for the reaction of caffeine and MnO_4^- at $[MnO_4^-] = 2.0 \times 10^{-4}$ mol dm^{-3}, T = 23 ± 0.1℃, I = 0.5mol dm^{-3} and λ_{max} = 530 nm

10^2 [CAF], mol dm^{-3}	10^1 [H^+], mol dm^{-3}	10 [I], mol dm^{-3}	10^3 k_{obs}, s^{-1}	10^2 k_2, dm^3 mol^{-1}s^{-1}
1.2	1.0	5.0	5.26	4.3
1.6	1.0	5.0	7.04	4.0
2.0	1.0	5.0	9.07	4.5
2.4	1.0	5.0	1.07	4.9
2.8	1.0	5.0	1.20	4.3
3.2	1.0	5.0	1.41	4.4
3.6	1.0	5.0	1.53	4.2
4.0	1.0	5.0	1.78	4.4
4.4	1.0	5.0	1.97	4.4
4.8	1.0	5.0	2.16	4.5
5.2	1.0	5.0	2.30	4.4
3.2	0.2	5.0	0.96	3.0
3.2	0.6	5.0	1.18	3.7
3.2	1.0	5.0	1.38	4.3
3.2	1.4	5.0	1.57	4.9
3.2	1.8	5.0	1.76	5.5
3.2	2.2	5.0	2.10	6.5
3.2	2.6	5.0	2.42	7.3
3.2	3.4	5.0	2.70	8.3
3.2	1.0	1.0	1.98	6.2
3.2	1.0	2.0	1.87	5.8

3.2	1.0	3.0	1.71	5.3
3.2	1.0	4.0	1.48	4.6
3.2	1.0	5.0	1.36	4.4
3.2	1.0	6.0	1.22	3.8

Table 4.2: Pseudo – first and second order rate constants for the reaction of IDZ and MnO_4^- at [IDZ] = 1.0×10^{-2} mol dm^{-3} [MnO_4^-] = 2.0×10^{-4} mol dm^{-3}, T = 24.0 ± 0.1℃, I = 1.0 mol dm^{-3} and λ_{max} = 530 nm

10^2 [IDZ], mol dm^{-3}	10^2 [H^+], mol dm^{-3}	[I], mol dm^{-3}	10^3 k_{obs}, s^{-1}	10^2 k_2, dm^3 $mol^{-1}s^{-1}$
3.0	3.2	1.0	5.75	1.91
4.0	3.2	1.0	7.70	1.91
5.0	3.2	1.0	9.60	1.92
6.0	3.2	1.0	12.2	2.03
7.0	3.2	1.0	13.4	1.91
8.0	3.2	1.0	15.3	1.91
7.0	1.6	1.0	8.3	1.10
7.0	2.4	1.0	11.0	1.50
7.0	3.2	1.0	13.3	1.91
7.0	4.0	1.0	14.7	2.10
7.0	4.4	1.0	16.1	2.30
7.0	4.8	1.0	17.9	2.50
7.0	3.2	0.2	8.80	1.25
7.0	3.2	0.4	10.1	1.44
7.0	3.2	0.6	10.5	1.50
7.0	3.2	0.65	11.5	1.64

7.0	3.2	0.8	12.8	1.82
7.0	3.2	1.0	13.3	1.90

Table 4.3: Pseudo–first and second order rate constants for the reaction of theobromine and MnO_4^- at [TB] = 2.0×10^{-2} mol dm^{-3} [MnO_4^-] = 2.0×10^{-4} mol dm^{-3}, T =24. 0 ± 0.1℃ , I = 1.0 mol dm^{-3} and λ_{max} = 530 nm

10^3 [TB], mol dm^{-3}	**10^1 [H^+], mol dm^{-3}**	**[I], mol dm^{-3}**	**10^3 k_1, s^{-1}**	**10^2k_2, dm^3 $mol^{-1}s^{-1}$**
4.00	3.20	1.00	0.380	9.50
8.00	3.20	1.00	0.736	9.20
12.0	3.20	1.00	1.100	9.20
16.0	3.20	1.00	1.470	9.20
20.0	3.20	1.00	2.020	10.1
24.0	3.20	1.00	2.200	9.10
28.0	3.20	1.00	2.820	10.0
20.0	2.40	1.00	1.590	7.90
20.0	3.20	1.00	2.300	11.0
20.0	4.00	1.00	3.070	15.3
20.0	4.80	1.00	3.720	18.6
20.0	5.60	1.00	4.790	23.9
20.0	6.40	1.00	5.860	29.3
20.0	3.20	0.20	1.220	6.00
20.0	3.20	0.60	1.480	7.40
20.0	3.20	0.80	1.660	8.30
20.0	3.20	1.00	2.490	12.0
20.0	3.20	1.40	3.260	16.0

Table 4.4: Pseudo–first and second order rate constants for the reaction of theophylline and MnO_4^- at [TP] = 1.0×10^{-2} mol dm^{-3} [MnO_4^-] = 2.0×10^{-4} mol dm^{-3}, T=24. 0 ± 0.1°C, I= 0.5 mol dm^{-3} and λ_{max} = 530 nm

10^2 [TP], mol dm^{-3}	10^2 [H^+], mol dm^{-3}	10 [I], mol dm^{-3}	10^3 k_{obs}, s^{-1}	$10k_2$, dm^3 mol^{-1}s^{-1}
1.0	1.0	5.0	5.31	5.3
1.4	1.0	5.0	7.53	5.4
1.8	1.0	5.0	1.02	5.7
2.2	1.0	5.0	1.11	5.0
2.6	1.0	5.0	1.42	5.4
3.0	1.0	5.0	1.57	5.2
3.8	1.0	5.0	2.09	5.5
1.0	1.0	5.0	5.37	5.3
1.0	1.6	5.0	6.02	6.0
1.0	2.4	5.0	6.90	6.9
1.0	3.2	5.0	7.53	7.5
1.0	4.0	5.0	8.88	8.8
1.0	4.8	5.0	9.97	9.9
1.0	1.0	1.0	3.78	3.7

1.0	1.0	2.0	3.94	3.9
1.0	1.0	3.0	4.18	4.1
1.0	1.0	4.0	4.60	4.6
1.0	1.0	5.0	5.75	5.7
1.0	1.0	6.0	6.52	6.5

$-d[MnO_4^-]/dt = k_2[MnO_4^-][IDZ]$ …4.7

For the reaction of TB with MnO_4^- at $[H^+] = 3.2\times10^{-1}$ mol dm^{-3}, I = 0.1moldm^{-3} (Na_2SO4,) the rate equation for the reaction is;

$-d[MnO_4^-]/dt = k_2[MnO_4^-][TB]$ …4.8

For the reaction of TP with MnO_4^- at $[H^+]$ = 1.0 x10^{-2} mol dm^{-3}. I = 0.5 mol dm^{-3} (Na_2SO_4), the rate equation for the reaction is;

$-d[MnO_4^-]/dt = k_2[MnO_4^-][TP]$ …4.9

4.4 Effect of hydrogen ion on the rate of the reactions

To examine the influence of $[H^+]$ on the rates of reactions, of some kinetic runs were performed in H_2SO_4 solution. The reaction was investigated by varying the concentration of H_2SO_4 while the concentration of the reductants and that of permanganate ion were kept constant. The rates were

found to be first order acid dependence for all the systems studied. The plots of k_2 versus $[H^+]$ were linear with positive intercept, as represented in Figures (4.13-4.16).The acid dependent rate equations for the reactions can be represented by equation (4.10)

$$-d[MnO_4^-]/dt = (a+b[H^+])[\text{Reductant}][MnO_4^-] \quad \ldots 4.10$$

For reductant = CAF, a = 0.26 $dm^3mol^{-1}s^{-1}$ and b = 1.8 $dm^3mol^{-1}s^{-1}$, for reductant = IDZ, a = 0.412 $dm^3mol^{-1}s^{-1}$ and b = 0.004 $dm^3mol^{-1}s^{-1}$, for reductant = TB, a = 0.041 $dm^3mol^{-1}s^{-1}$ and b = 0.028 $dm^3mol^{-1}s^{-1}$ and for reductant = TP, a = 0.26 $dm^3mol^{-1}s^{-1}$ and b = 1.8 $dm^3mol^{-1}s^{-1}$. **4.5 The effect of ionic strength and dielectric constant (D) on the rates of the reactions**

The effect of ionic strength on the rates of the reactions were investigated by keeping the concentrations of other reactants constant while varying the ionic strength in the range I= 0.1– 0.6 mol dm^{-3} (Na_2SO_4), for CAF– MnO_4^- and TP – MnO_4^- systems; 0.2 – 0.6 mol dm^{-3}

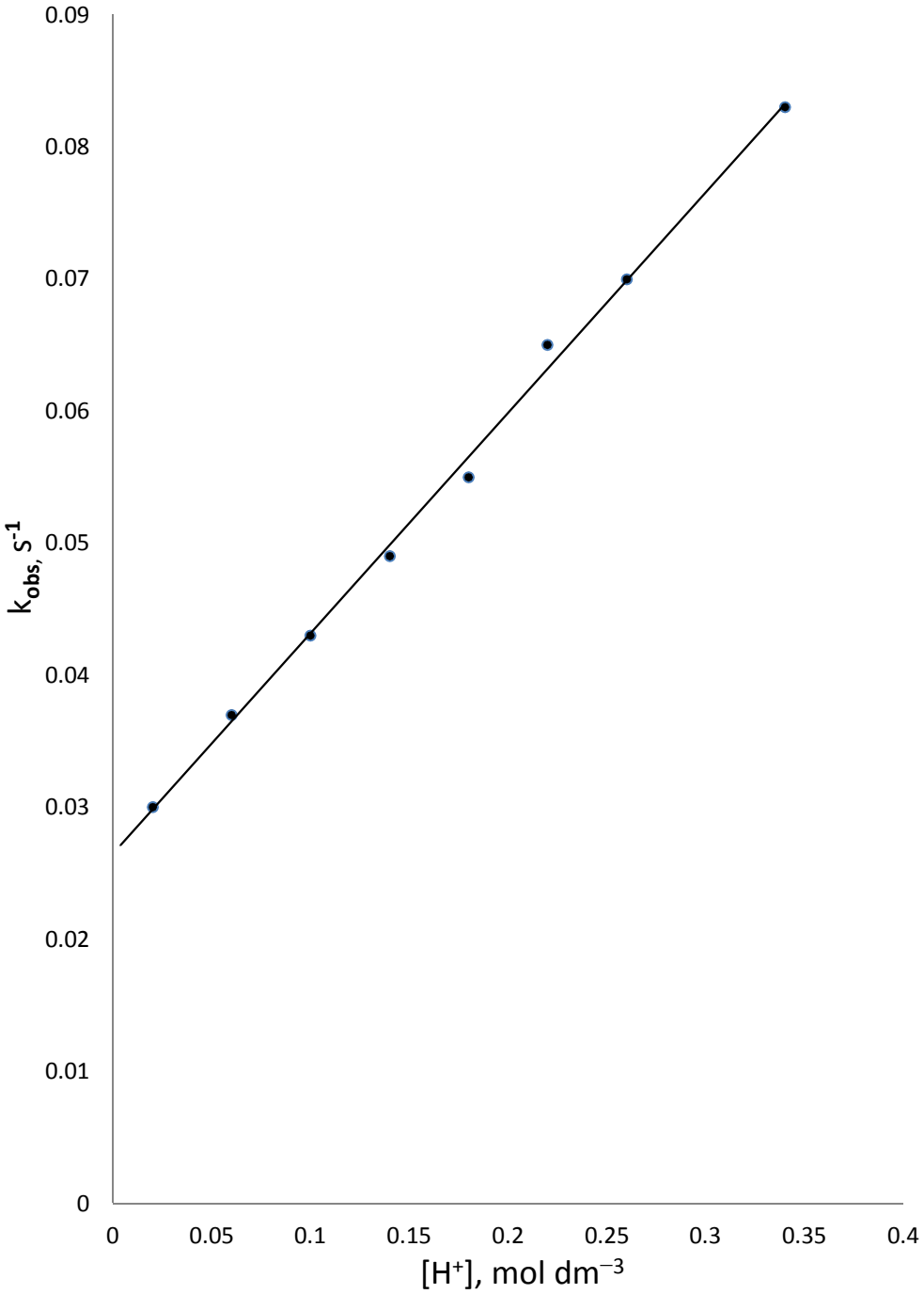


Figure 4.13: k_{obs} versus $[H^+]$ plot for the oxidation of CAF by MnO_4^- , at [CAF] = 3.2×10^{-2} mol dm^{-3}, $[MnO_4^-] = 2.0 \times 10^{-4}$ mol dm^{-3}, $[H^+]$ = (0.2 – 3.4) $\times 10^{-1}$ mol dm^{-3}, λ_{max} = 530nm, I = 0.5mol dm^{-3} and T = 24 ± 0.1°C

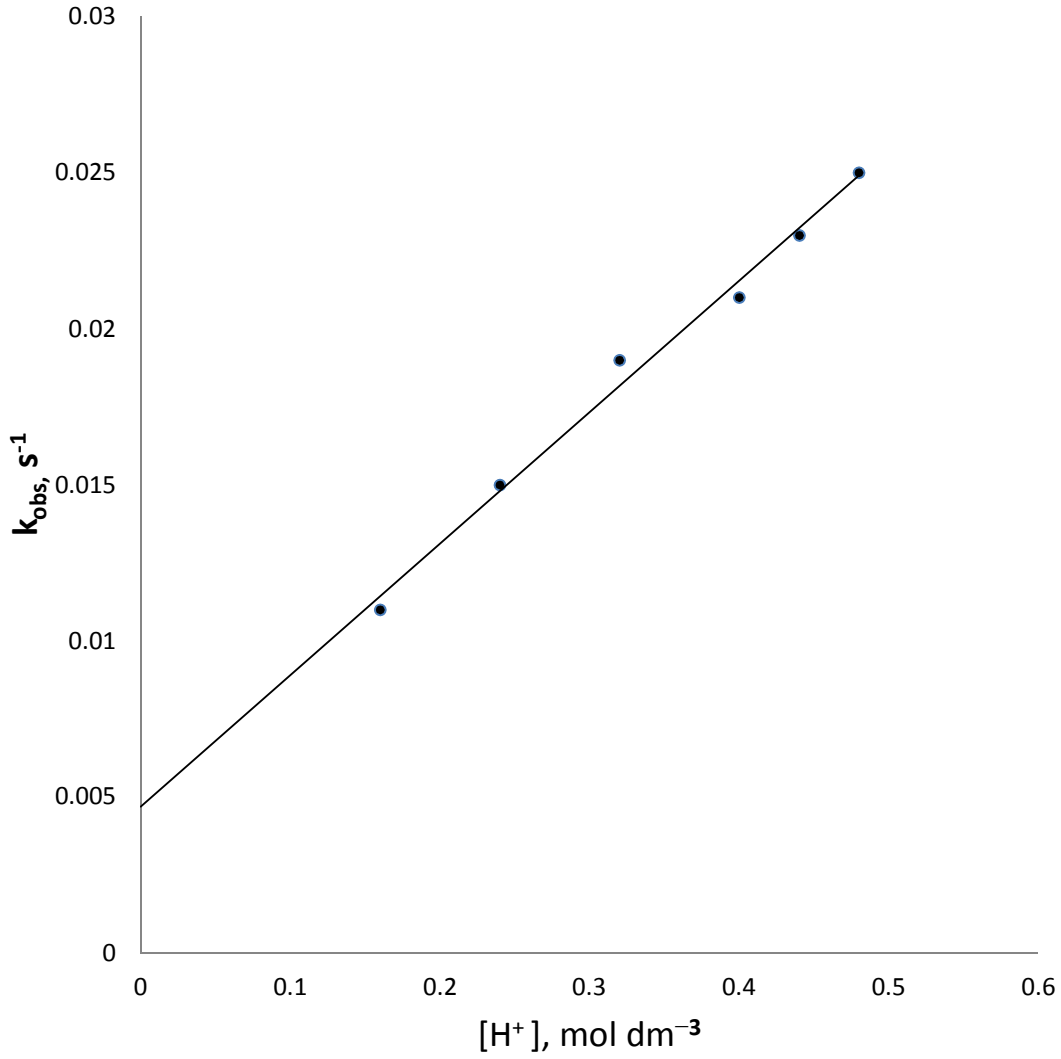


Figure 4.14: k_{obs} versus $[H^+]$ plot for the oxidation of IDZ by MnO_4^-, [IDZ] = 7.0 $\times 10^{-2}$ mol dm^{-3}, $[MnO_4^-]$ = 2.0 × 10^{-4} mol dm^{-3}, $[H^+]$ = (0.2.0 – 3.4) × 10^{-1} mol dm^{-3}, I = 1.0 mol dm^{-3} (Na_2SO_4), λ_{max} = 530nm and T = 24 ± 0.1°C

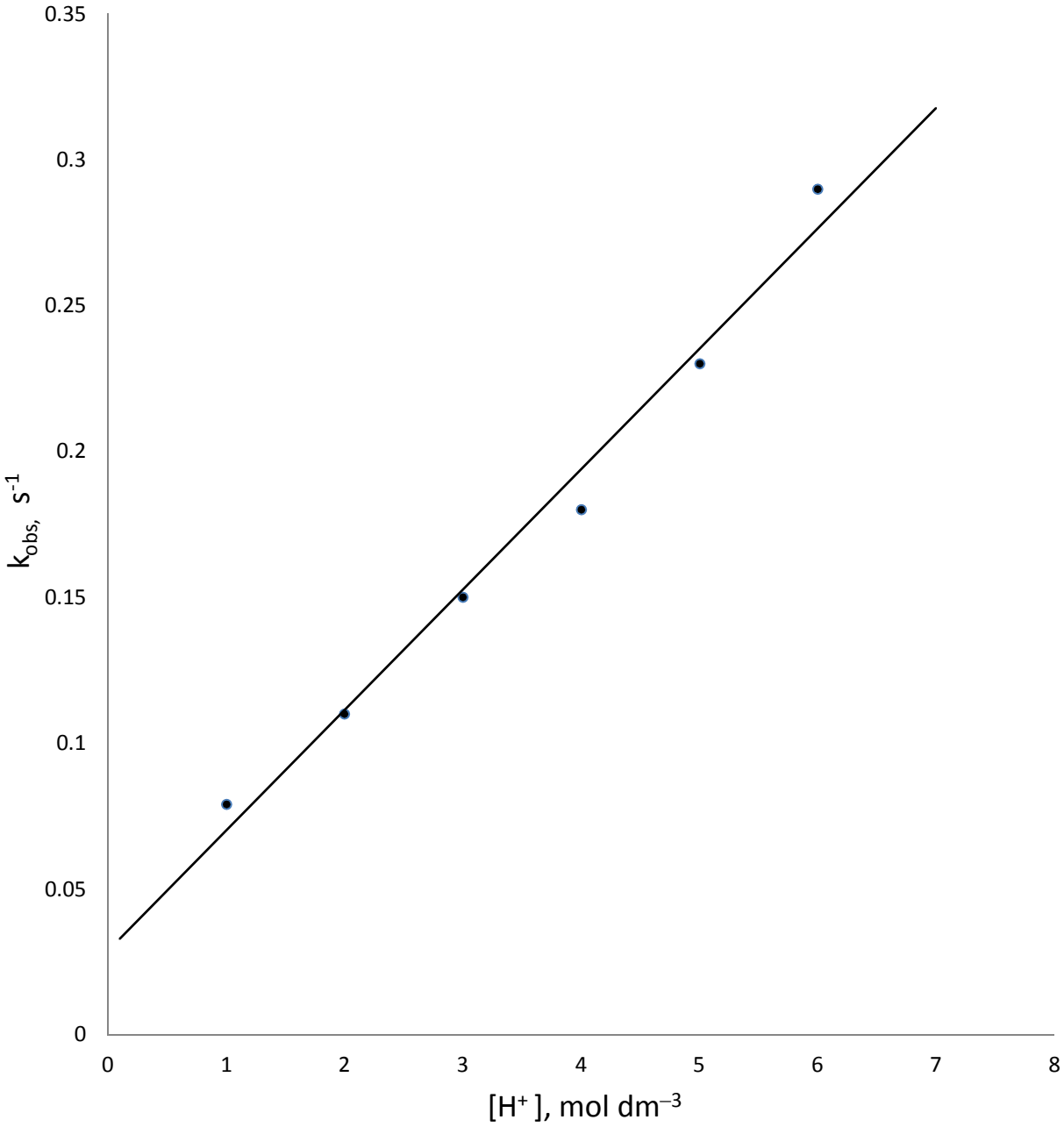


Figure 4.15: k_{obs} versus $[H^+]$ plot for the oxidation of TB by MnO_4^- at [TB] = 1.0×10^{-2} mol dm^{-3}, $[MnO_4^-]$ = 2.0×10^{-4} mol dm^{-3},

$[H^+]$ = (2.4 – 6.4) 10^{-1} mol dm^{-3}, I = 1.0 mol dm^{-3}, (Na_2SO_4) and T = 24 ± 0.1°C

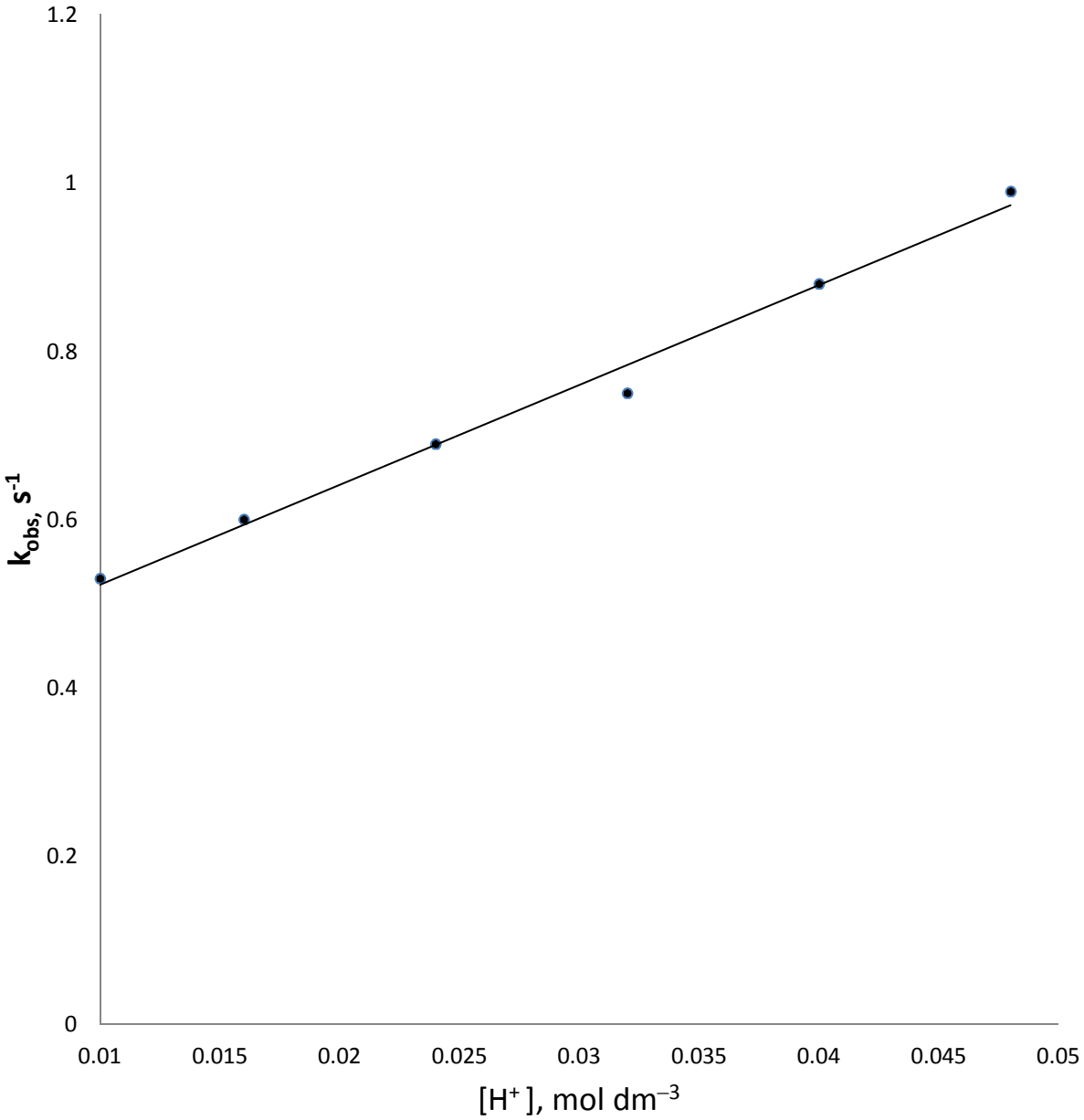


Figure 4.16: k_{obs} versus $[H^+]$ plot for the oxidation of TP by MnO_4^- at [TP] =1.0 × 10^{-2} mol dm^{-3}, $[MnO_4^-]$ = 2.0 × 10^{-4} mol dm^{-3}, $[H^+]$ =

$(20.0 – 3.4) \times 10^{-1}$ mol dm^{-3}, I = 0.5 mol dm^{-3} (Na_2SO_4) and T = 24 ± 0.1°C

(Na_2SO_4), for TB–MnO_4^-system .The rates of the reactions decreased with increase in ionic strength for the reaction of CAF–MnO_4^-suggesting negative Bronsted–Debye (Bronsted, 1922) salt effect. In the reactions of IDZ-MnO_4^-, $TB - MnO_4^-$ and $TP - MnO_4^-$, the rates constants were observed to increase with increase in ionic strength, suggesting positive Bronsted-Debye salt effect. Linear plots were obtained for $logk_2$ versus $I^{1/2}$ (Figures 4.17- 4.20). Results of the ionic strength effects are presented in Tables (4.1)–(4.4).The rate of the reaction of CAF–MnO_4^- decreased with increase in dielectric constant(D) of the reaction medium, while the rates of the reactions of IDZ–MnO_4^-, TB–MnO_4^- and $TP - MnO_4^-$systems, increased with increase in D. The plots of $logk_{obs}$ versus 1/D are presented in Figure (4.21-4.24). The k_2 values for the various systems are presented in Tables (4.51–4.54).

4.6 Tests for intermediate complex

4.6.1 Spectrophotometric test

This test was carried out in order to find out whether any spectroscopically determinable intermediate complex was formed between CAF and MnO_4^-, IDZ and MnO_4^-, TB and MnO_4^-, and TP and MnO_4^-, in the course of the reactions. The spectra of permanganate ion and that of the reaction mixture were taken over the wavelength 400 – 700 nm range, and the spectra were compared. Spectroscopic studies indicate that there was no clear shift from 530nm (Figures 4.25-4.28), the

wavelength of maximum absorption of MnO_4^- studied. This indicates absence of formation of intermediate complex during the course of the reactions.

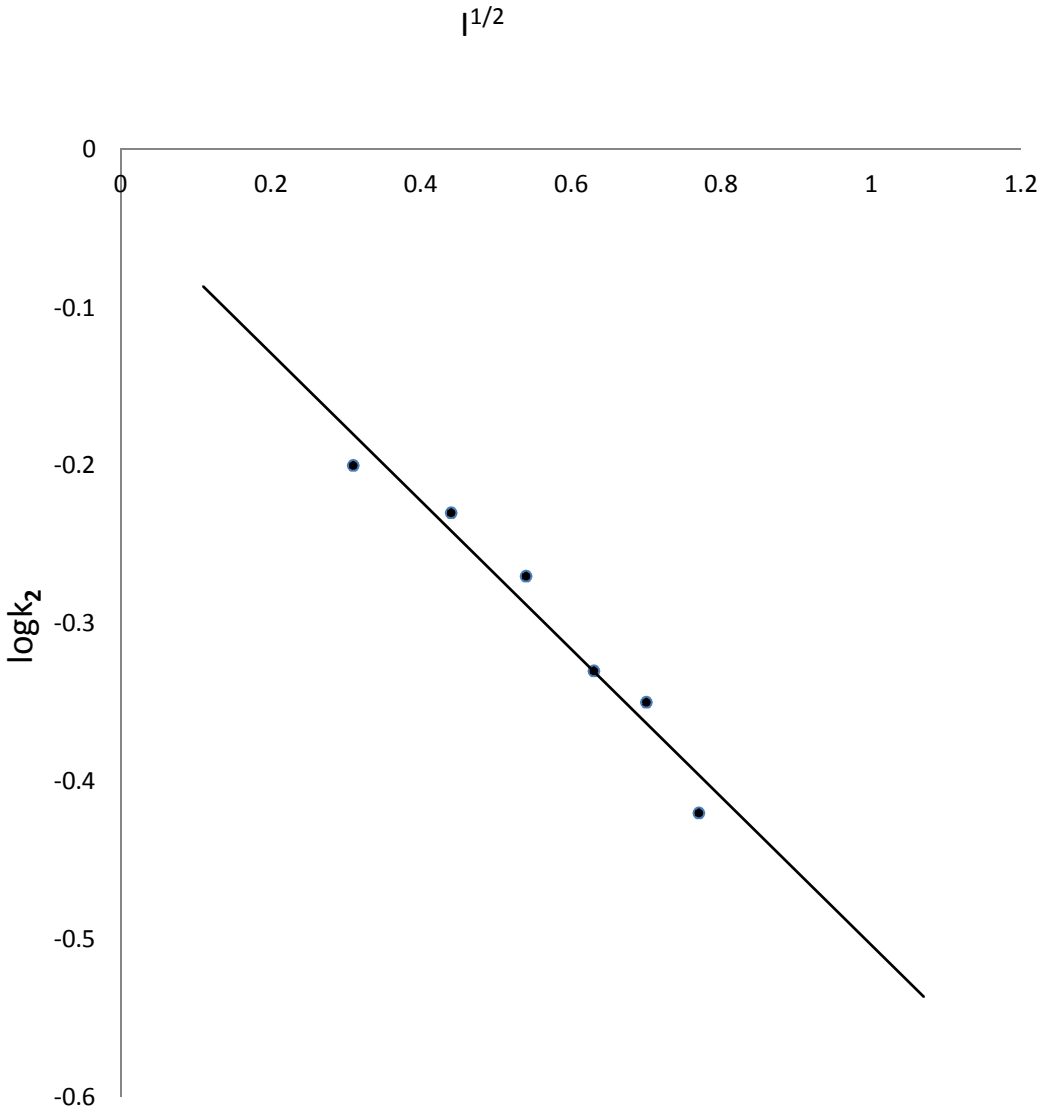


Figure 4.17: $\log k_2$ versus $I^{1/2}$ plot for the oxidation of CAF by MnO_4^- at [CAF] = 3.2×10^{-2} moldm^{-3}, [MnO_4^-] = 2.0×10^{-4} mol dm^{-3}, [H^+] = 1.0×10^{-1} mol dm^{-3}, I = 0.1 – 0.6 mol dm^{-3} (Na_2SO_4) and T = 24 ± 0.1°C

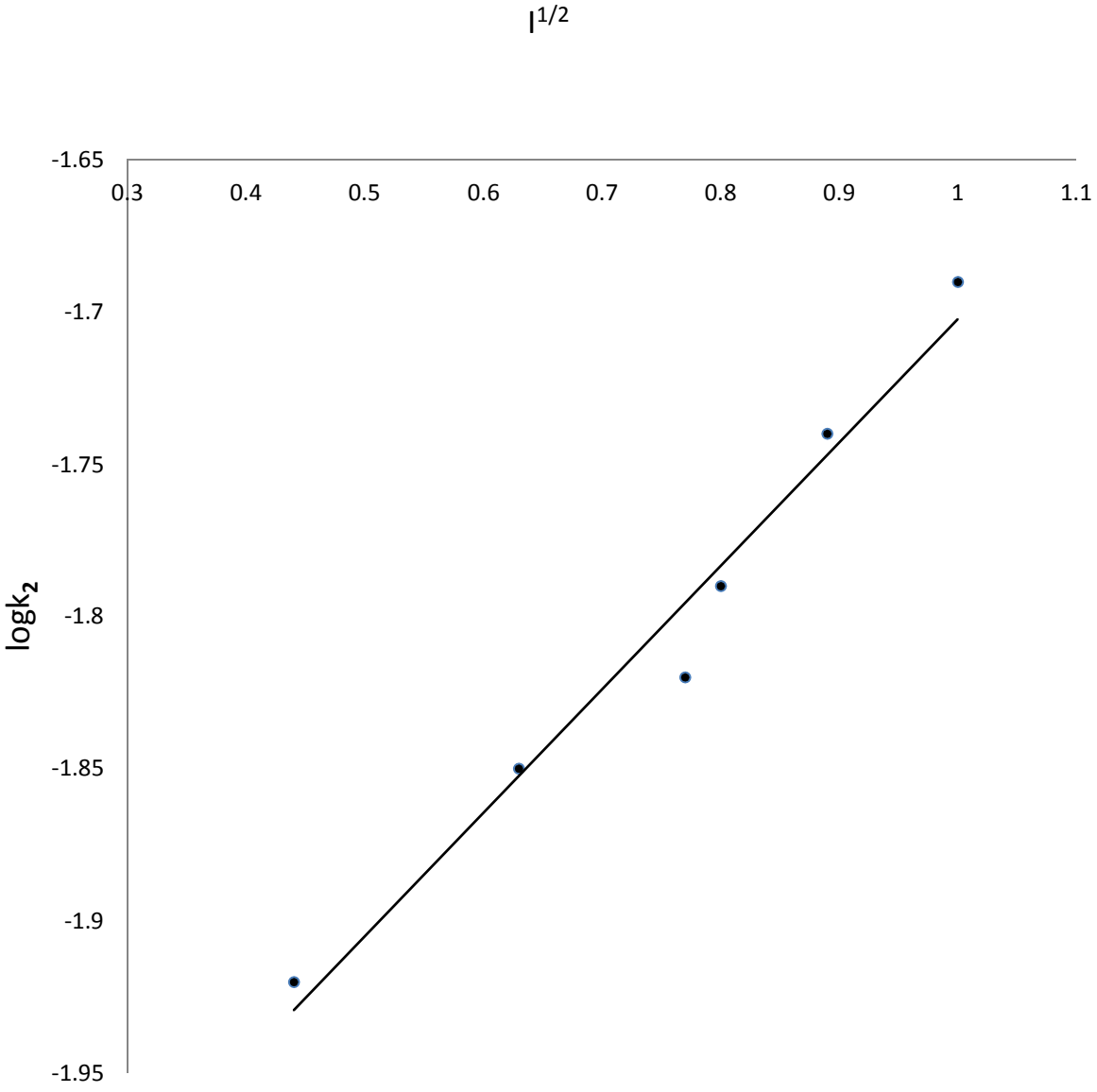


Figure 4.18: $\log k_2$ versus $I^{1/2}$ plot for the oxidation of IDZ by MnO_4^- at [IDZ] = 7.0×10^{-2} mol dm^{-3}, $[MnO_4^-] = 2.0 \times 10^{-4}$ mol dm^{-3}, $[H^+] = 3.2 \times 10^{-2}$ mol dm^{-3}, I = 0.2 – 1.0 mol dm^{-3} (Na_2SO_4) and T = 24 ± 0.1℃

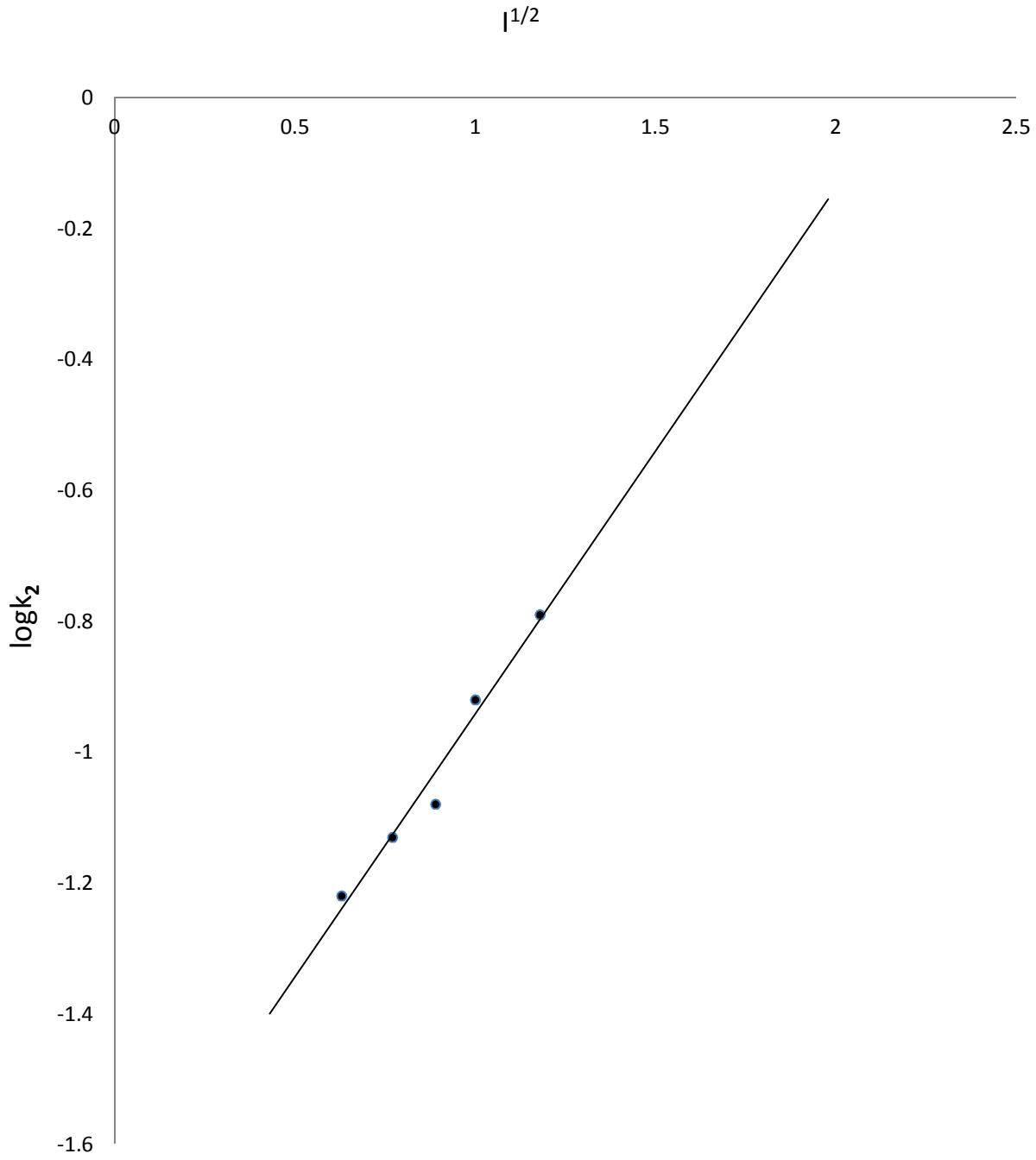


Figure 4.19: $\log k_2$ versus $I^{1/2}$ plot for the oxidation of TB by MnO_4^- at [TB] = 1.0×10^{-2} mol dm^{-3}, $[MnO_4^-] = 2.0 \times 10^{-4}$ mol dm^{-3}, $[H^+] = 3.2 \times 10^{-1}$ mol dm^{-3}, I = 0.2 – 1.4 mol dm^{-3} (Na_2SO_4) and T = 24 ± 0.1°C

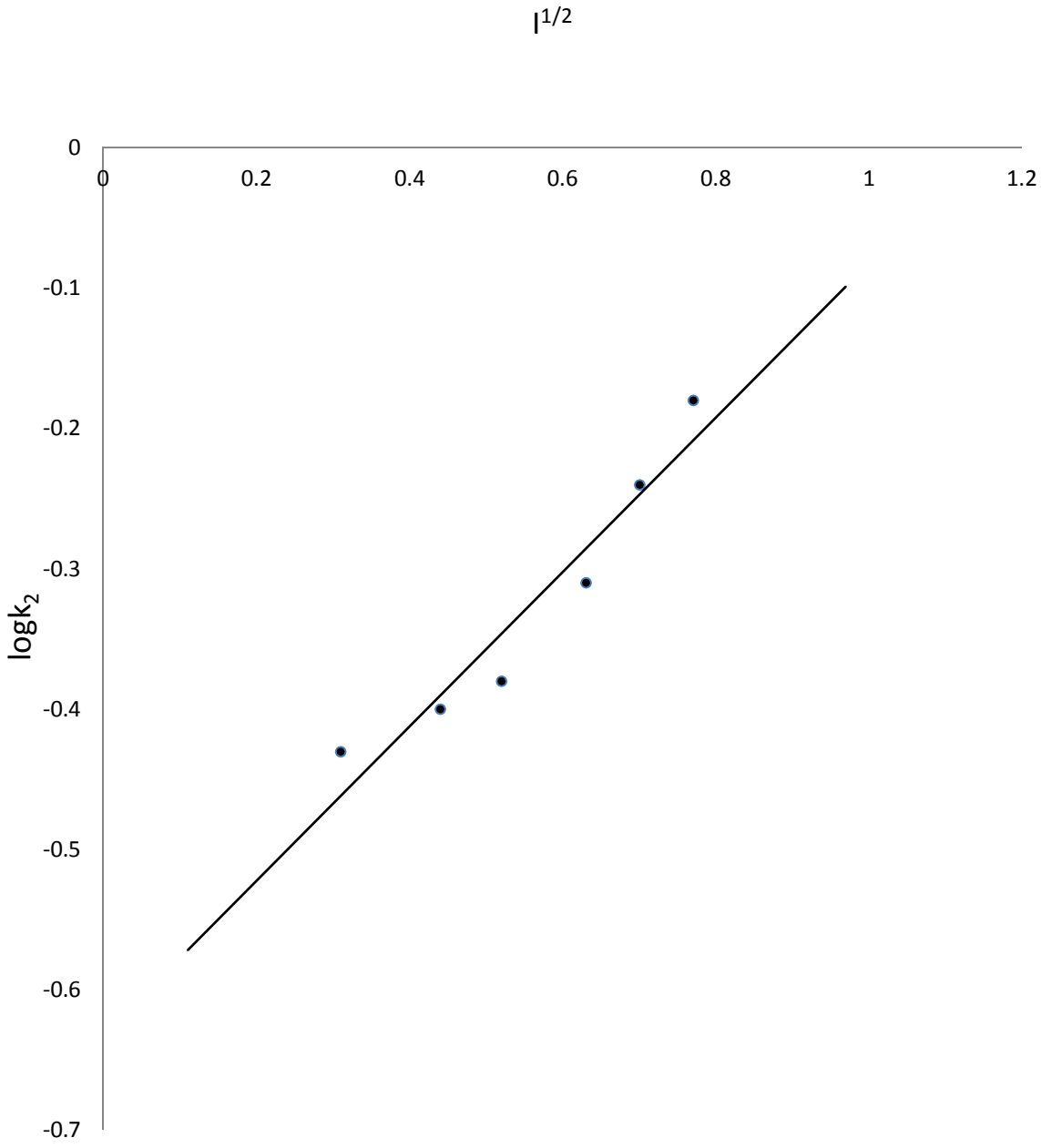


Figure 4.20: log k_2 versus $I^{1/2}$ plot for the oxidation of TP by MnO_4^- at [TP] = 1.0 × 10^{-2} mol dm^{-3}, [MnO_4^-] = 2.0 × 10^{-4} mol dm^{-3}, [H^+] = 1.0 × 10^{-2} mol dm^{-3},I = 0.1 – 0.6 mol dm^{-3} (Na_2SO_4) and T = 24.0 ± 0.1℃

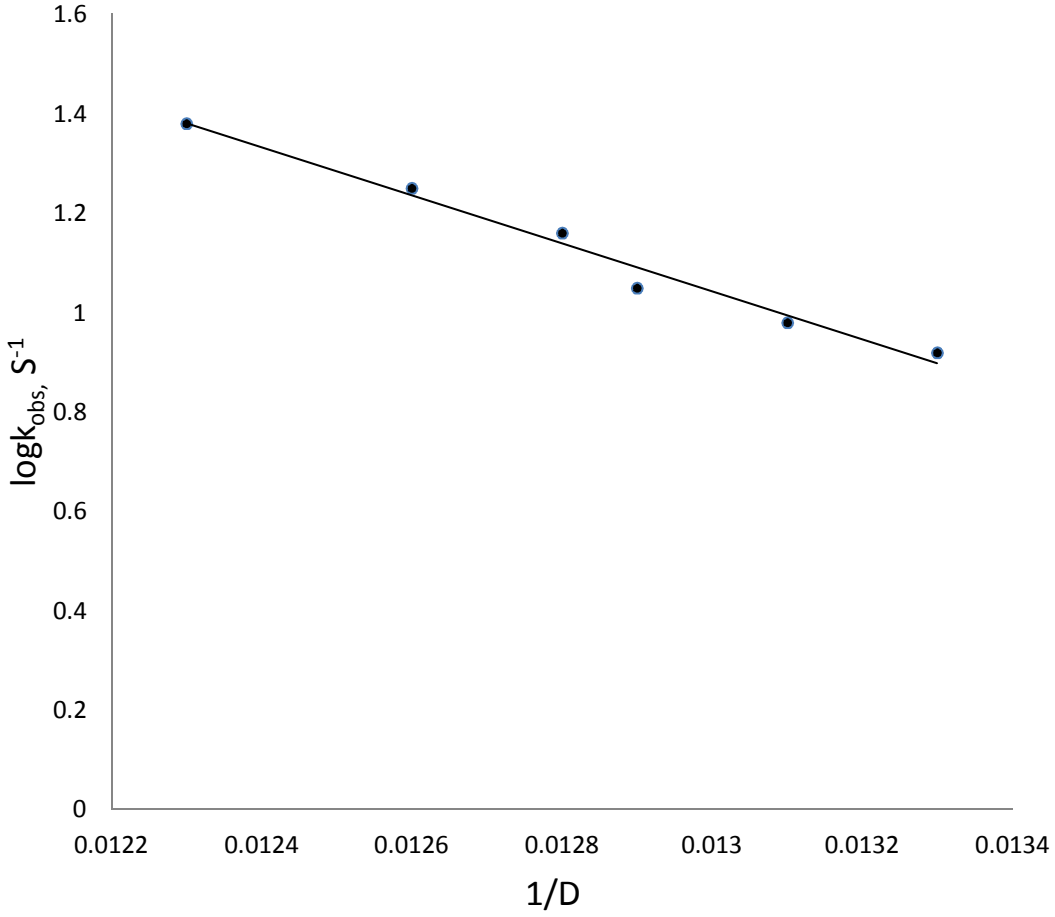

1.6
1.4
1.2
1
0.8
0.6
0.4
0.2
0
logk$_{obs,}$ S^{-1}
0.0122
0.0124
0.0126
0.0128
0.013
0.0132
0.0134
1/D

Figure 4.21: $\log k_{obs}$ versus 1/D plot for the oxidation of CAF by MnO_4^- at [CAF] = 3.2×10^{-2} mol dm^{-3}, $[MnO_4^-] = 2.0 \times 10^{-4}$ mol dm^{-3}, $[H^+] = 1.0 \times 10^{-1}$ mol dm^{-3}, I = 0.5 mol dm^{-3} (Na_2SO_4) and T = 24 ± 0.1°C

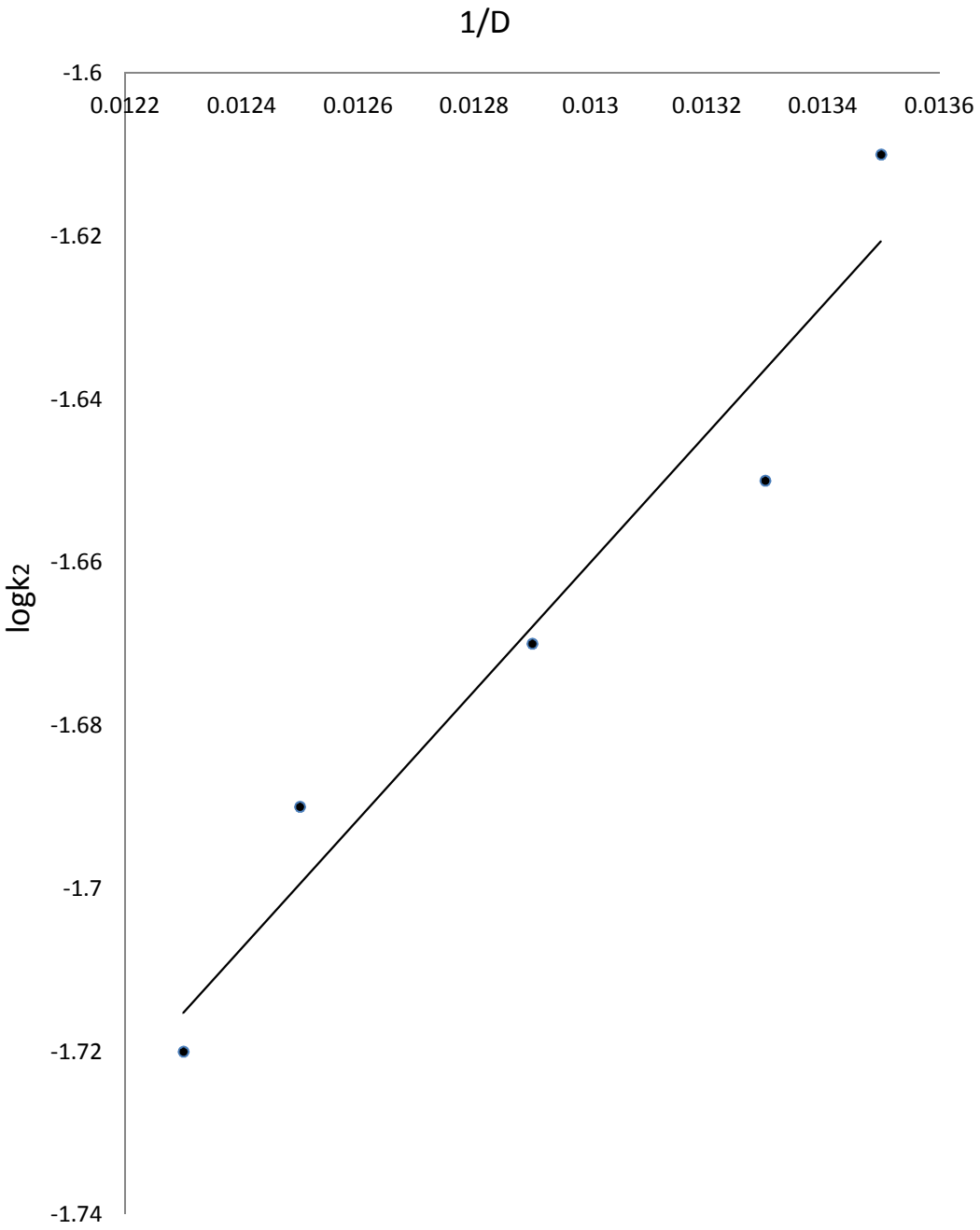


Figure 4.22: $\log k_{obs}$ versus 1/D for the oxidation of IDZ by MnO_4^- at [IDZ] = 1.0×10^{-2} mol dm^{-3} $[MnO_4^-]$ = 2.0×10^{-4} mol dm^{-3}, I = 1.0 mol dm^{-3} (Na_2SO_4) and T =24.0 ± 0.1℃

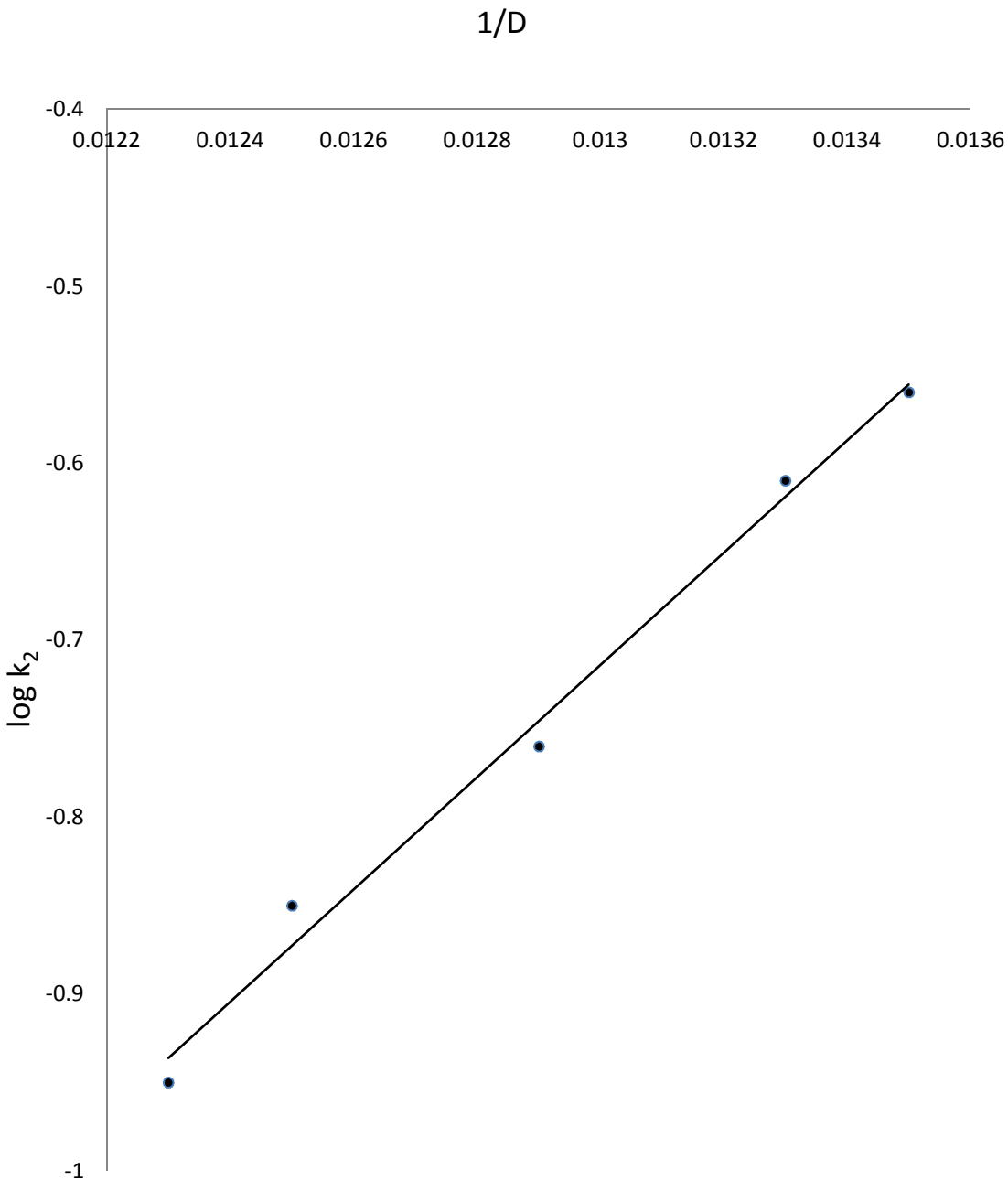


Figure 4.23: $\log k_{obs}$ versus 1/D for oxidation of TB by MnO_4^- at [TB] = 2.0×10^{-2} mol dm^{-3}, [MnO_4^-] = 2.0×10^{-4} mol dm^{-3}, T =24.0 ± 0.1℃ and I = 0.1 mol dm^{-3} (Na_2SO_4)

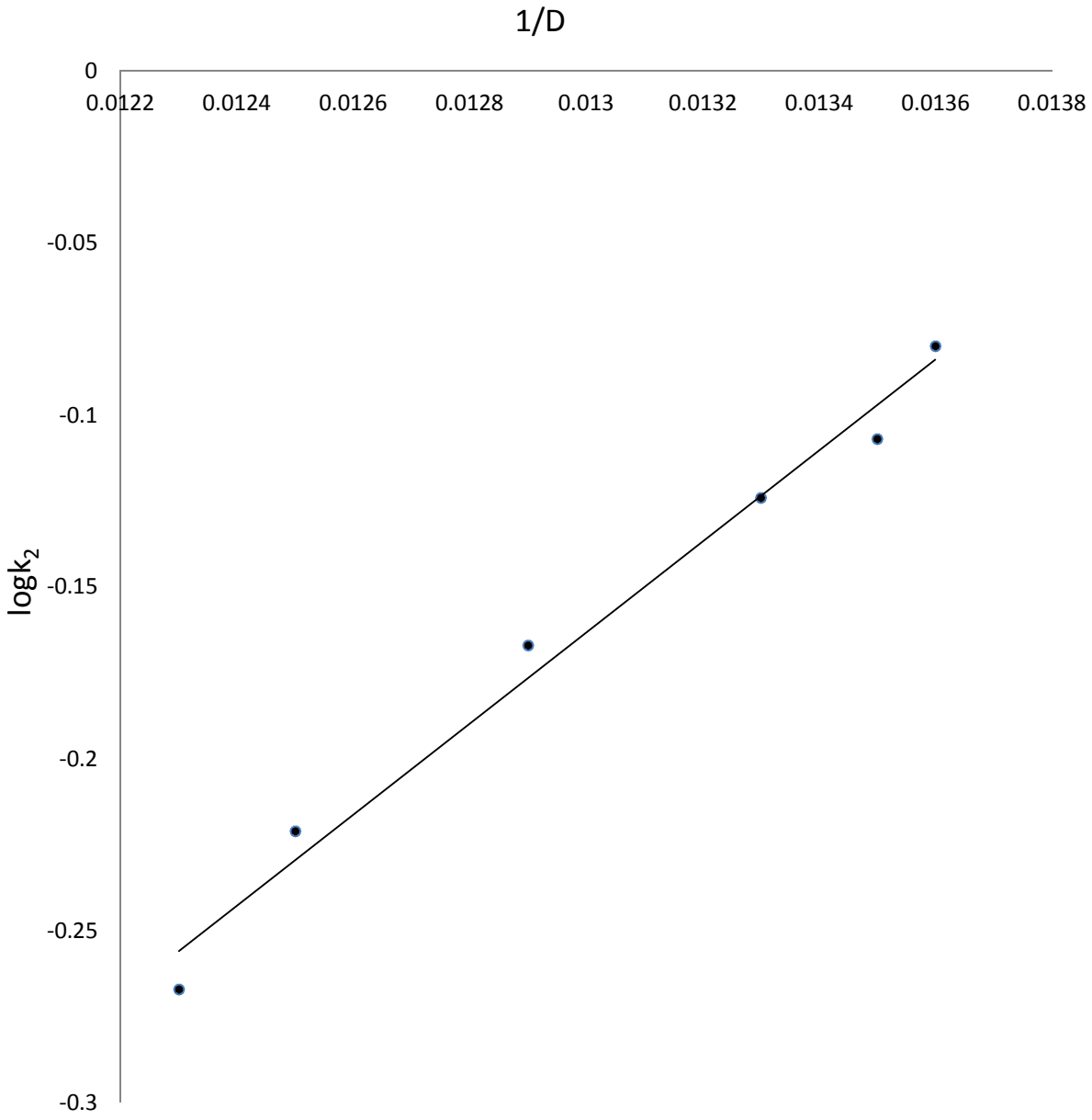


Figure 4.24: $\log k_{obs}$ versus 1/D for the oxidation of TP by MnO_4^- at [TP] = 1.0 × 10^{-2} mol dm^{-3}, [MnO_4^-] = 2.0 × 10^{-4} mol dm^{-3}, T =24. 0 ± 0.1℃ and I = 0.5 mol dm^{-3} (Na_2SO_4)

Table 4.5: Effect of changes in dielectric constants of reaction medium for the oxidation of CAF by MnO_4^-at [CAF] = 3.2 × 10^{-2} mol dm^{-3},[MnO_4^-] = 2.0 × 10^{-4} mol dm^{-3}, T = 23 ± 0.1℃ , [H^+] = 1.0 x 10^{-1} mol dm^{-3}, I = 0.50 mol dm^{-3} (Na_2SO_4) and λ = 530 nm

D	$10^3 k_{obs}$, s^{-1}	$10^2 k_2$, $dm^3\ mol^{-1}, s^{-1}$
81.0	1.38	4.3
80.40	1.25	3.9
79.80	1.16	3.6
78.60	1.05	3.2
77.40	0.98	3.0
76.20	0.92	2.8

Table 4.6: Effect of changes in dielectric constants of reaction medium for the oxidation of IDZ with MnO_4^- at [IDZ] = 1.0×10^{-2} mol dm^{-3},[MnO_4^-] = 2.0×10^{-4} mol dm^{-3}, T = 24. 0 ± 0.1℃ I= 1.0 mol dm^{-3}(Na_2SO_4) and λ = 530 nm

D	**$10^3 k_{obs}$, s^{-1}**	**$10^2 k_2$, $dm^3\ mol^{-1}, s^{-1}$**
81.0	1.36	1.9
79.8	1.47	2.0
77.4	1.53	2.1
75.0	1.58	2.2
74.0	1.68	2.4

Table 4.7: Effect of changes in dielectric constants of reaction medium on the rate of the reaction of TB with MnO_4^- at [TB] = 2.0 × 10^{-2} mol dm^{-3} [MnO_4^-] = 2.0 × 10^{-4} mol dm^{-3}, T =24.0 ± 0.1°C, I = 1.0 mol dm^{-3}, (Na_2SO_4) and λ = 530 nm

D	**$10^3 k_{obs}$, s^{-1}**	**10 k_2, $dm^3\ mol^{-1}, s^{-1}$**

81.0	2.20	1.1
79.8	2.80	1.4
77.4	3.40	1.7
75.0	4.80	2.4
74.0	5.40	2.7

Table 4.8: Effect of changes in dielectric constants of reaction medium on the rate of the reaction of TP with MnO_4^- at [TP] = 1.0×10^{-2} mol dm^{-3} [MnO_4^-] = 2.0×10^{-4} mol dm^{-3}, T =24. 0 ± 0.1℃ , I = 0.50 mol dm^{-3} (Na_2SO_4) and λ = 530 nm

D	$10^3 k_{obs}$,	$10k_2$,

	s^{-1}	$dm^3\ mol^{-1}, s^{-1}$
81.0	5.44	5.4
79.0	6.52	6.5
77.4	7.29	7.2
75.0	7.53	7.5
74.0	7.83	7.8
73.0	8.37	8.3

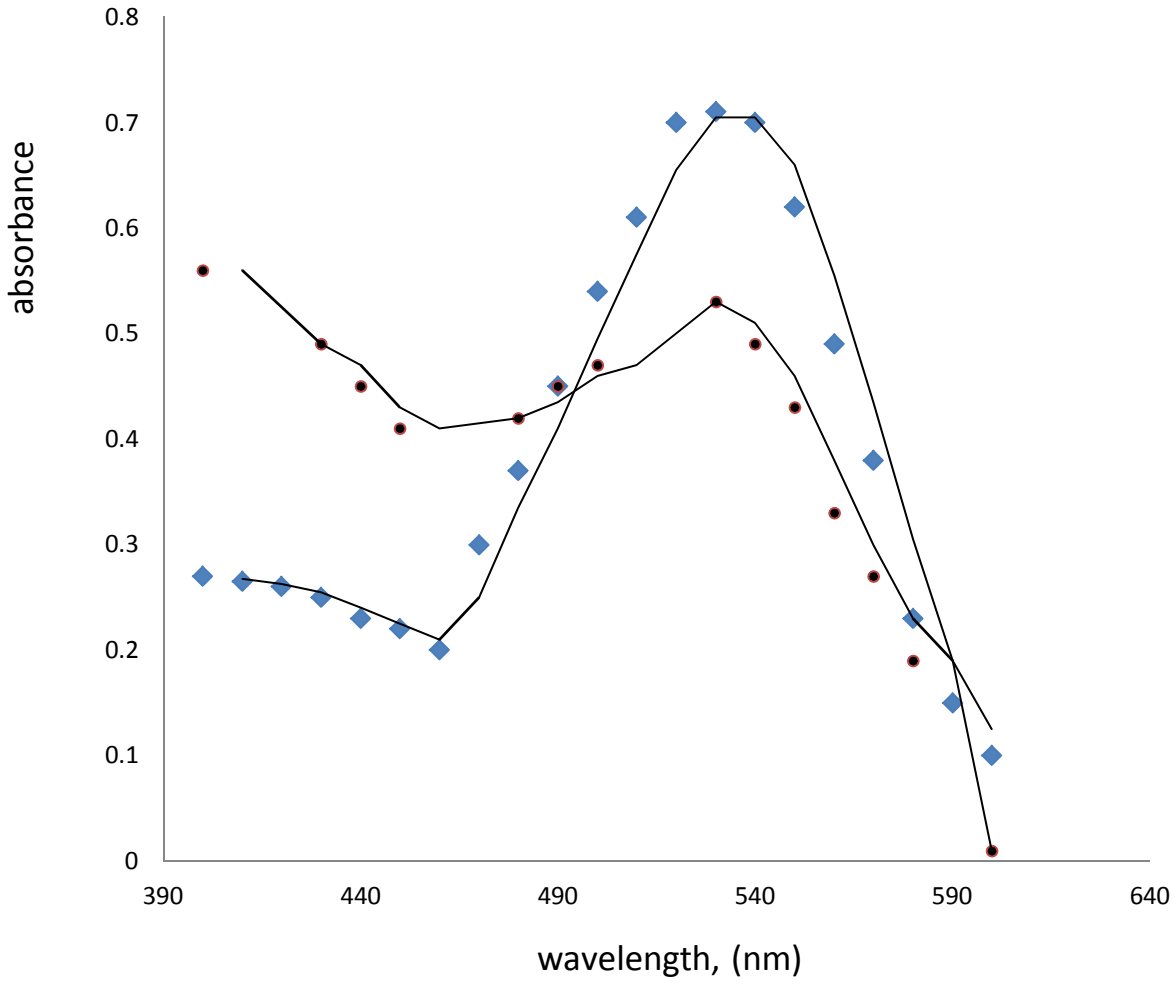


Figure: 4.25: Spectra of the redox reaction mixture of permanganate ion and caffeine after two minutes of reaction

MnO_4^-

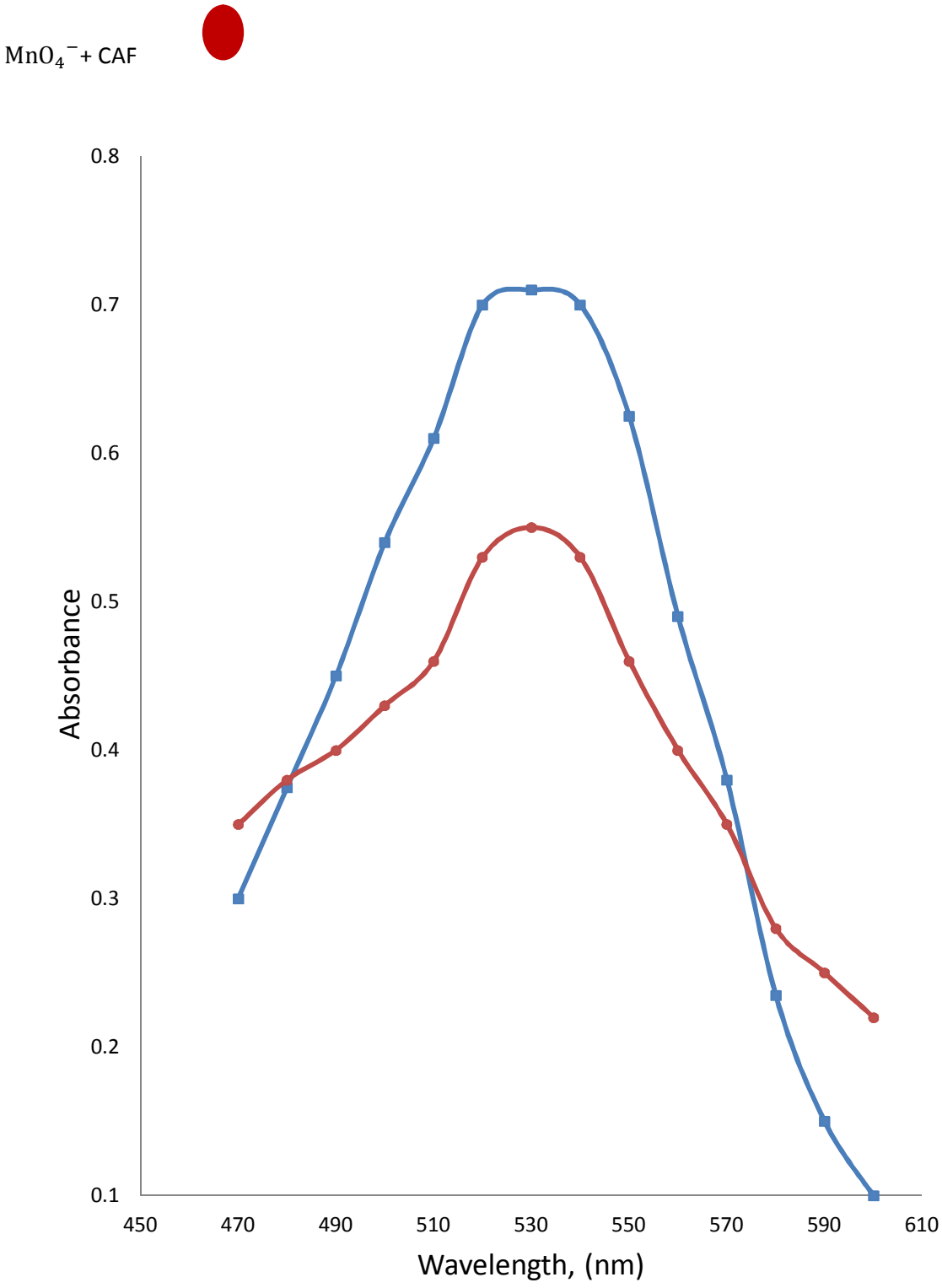


Figure 4.26: Spectra of the redox reaction mixture of permanganate ion and imidazole after two

minute of reaction



MnO_4^-



MnO_4^- + IDZ

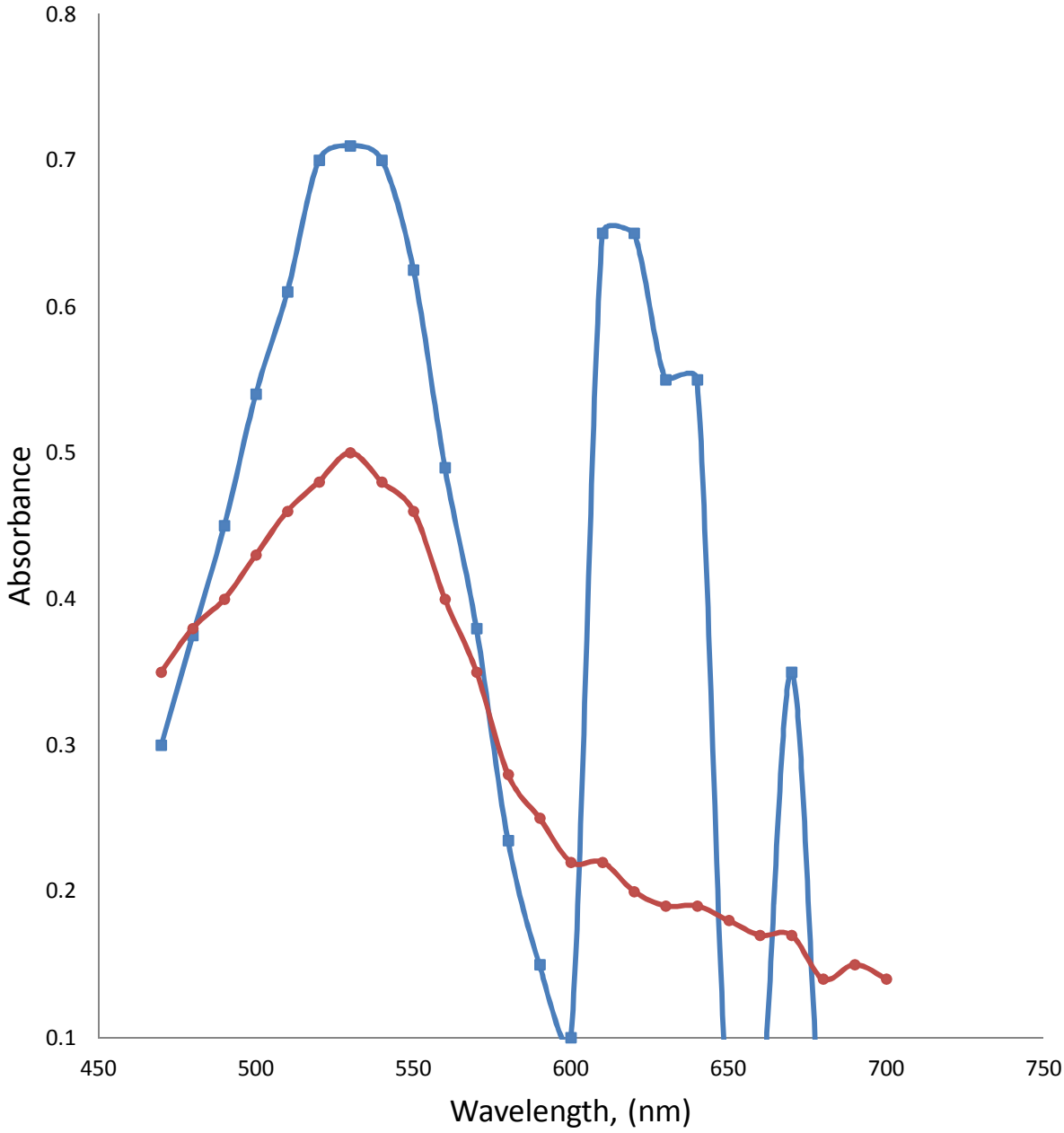


Figure 4.27: Spectra of the redox reaction mixture of permanganate ion and theobromine after two minute of reaction

ci

MnO_4^-

MnO_4^- + TB 

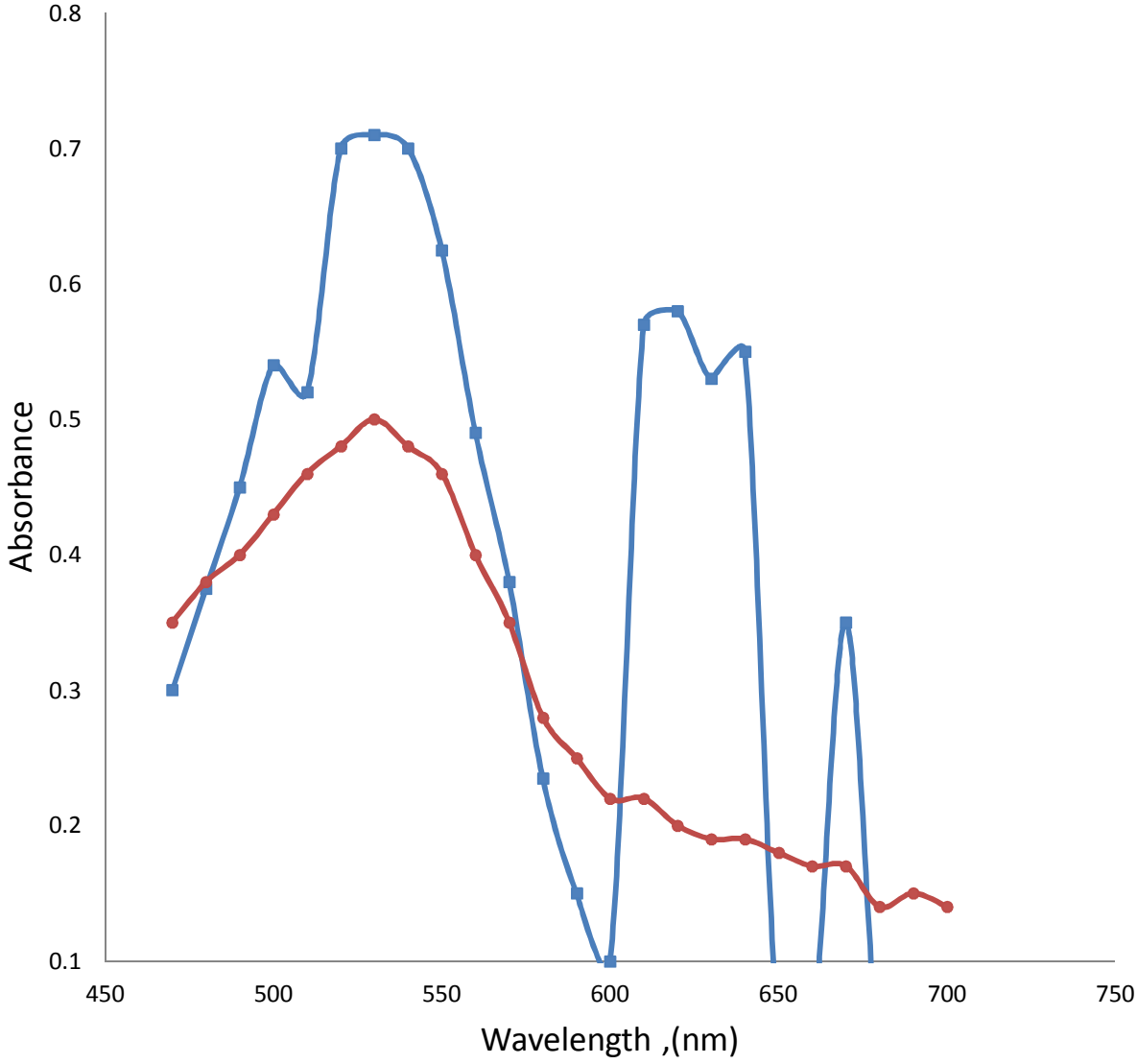


Figure 4.28: Spectra of the redox reaction mixture of permanganate ion and theophylline after two minute of reaction

MnO_4^-

MnO_4^- + TP

4.6.2 Michaelis – Menten Plot

Michaelis – Menten Plot of $^1/_{k_{obs}}$ Versus $^1/_{[CAF]}$ was plotted. The plots were linear passing through the origin. This suggests the absence of intermediate complex formation in the reactions. The Michaelis-Menten's plots are presented in Figures (4.29 – 4.32).

4.7 Test for free radicals

Addition of acrylonitrile to the partially oxidized reaction mixture for each of the systems was studied. It was observed that there was no gel formation or polymerization even when a large excess of methanol was added to the CAF–MnO_4^-, $IDZ - MnO_4^-$, $TB - MnO_4^-$ and $TP - MnO_4^-$ mixtures respectively. This suggests that probably free radicals were not formed in the course of the reactions.

4.8 Effect of added anions on the rate of the reaction

The effect of added ions (X= NO_3^- and $HCOO^-$) on the rates of the reactions was studied for each of the systems by keeping the concentrations of the other reactants constant while varying the concentration of the anions. It was observed that the presence of these anions mildly enhanced the rate of the reaction (Figures 4.33–4.39). Catalyses of the reactions by these ions indicate that the reaction might be operation via the outer-sphere mechanism. The values of the rate constants are presented in Tables (4.9-4.12).

4.9 Effect of added cation on the rate of the reaction

The effect of added cation on the rates of the reactions was investigated for [Z] = Mg^{2+}, and Ca^{2+} at (5.0-20.0) × 10^{-3} mol dm^{-3}. Addition of Mg^{2+} and Ca^{2+} mildly enhanced the rate of the reactions for all

the systems studied. Plots of cation dependent rate constant versus [Z] are shown in Figures (4.40-4.47). Results are presented in Tables (4.13-4.16).

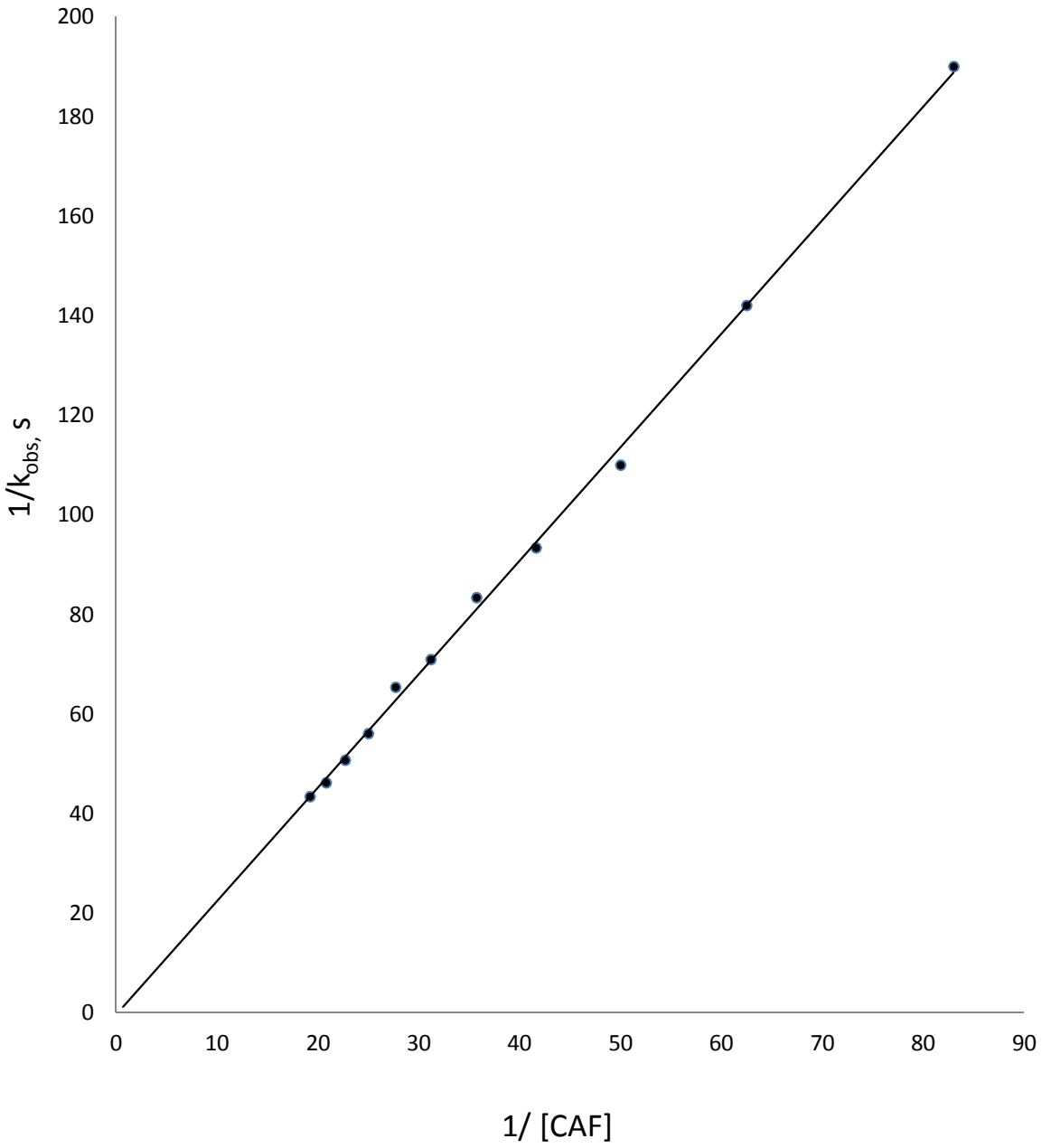


Figure 4.29: Michealis–Menten plot of 1/ k_1 versus 1/[CAF]at $[MnO_4^-]$ = 2.0×10^{-4} mol dm^{-3}, [CAF] = $(1.20 - 5.20) \times 10^{-2}$ mol dm^{-3},I = 0.5 mol dm^{-3} (Na_2SO_4) and T = 24.0 ± 0.1℃

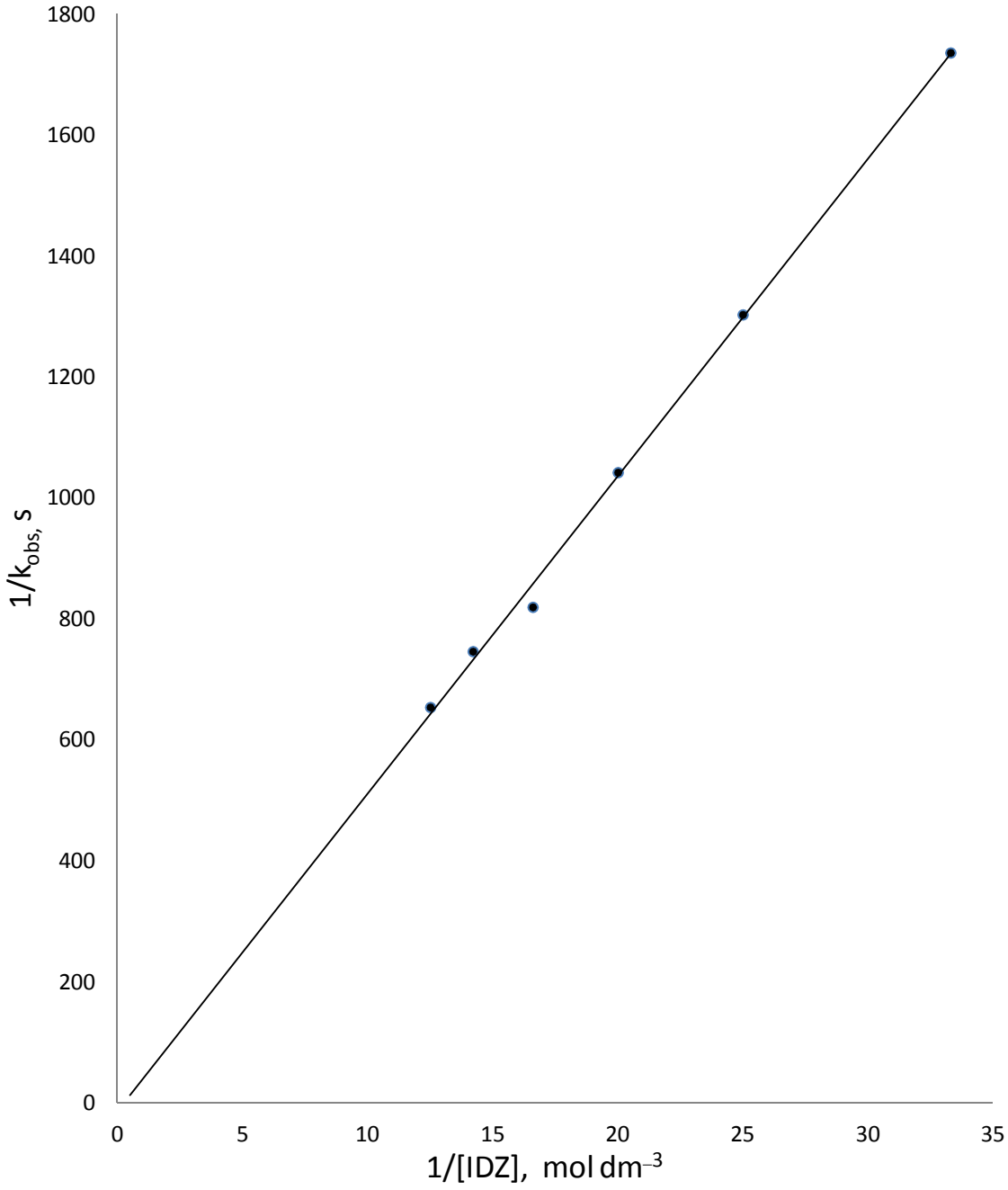

1800
1600
1400
1200
1000
800
600
400
200
0
1/k_obs, s
0
5
10
15
20
25
30
35
1/[IDZ], mol dm⁻³

Figure 4.30: Michealis– Menten plot of 1/ k_{obs} versus 1/ [IDZ] at $[MnO_4^-]$ = 2.0 × 10^{-4} mol dm^{-3}, [IDZ] = (3.0 – 8.0) × 10^{-2} mol dm^{-3}, I = 1.0 mol dm^{-3} (Na_2SO_4) and T = 24.0 ± 0.1℃

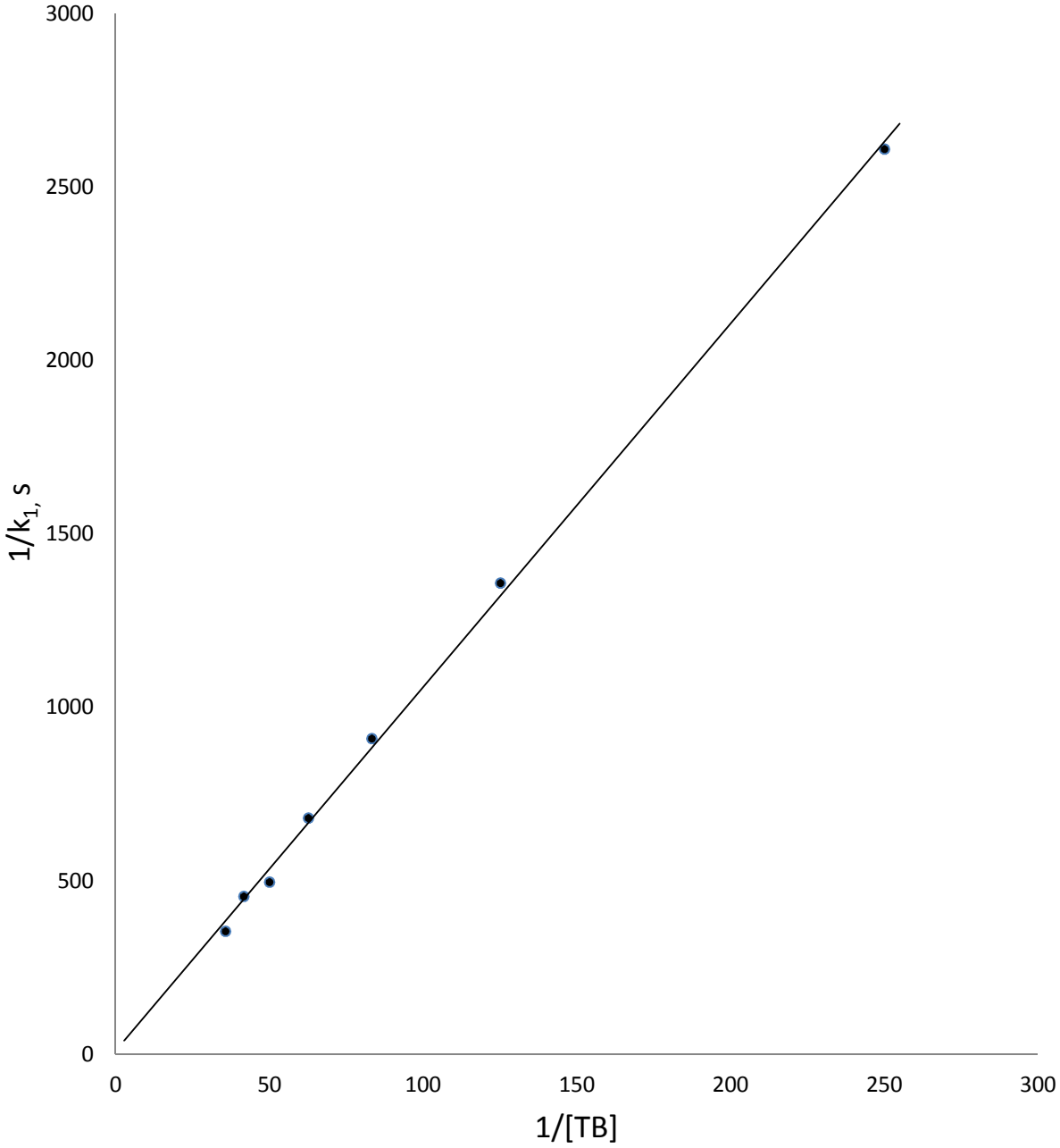


Figure 4.31: Michealis–Menten plot of 1/ k_{obs} versus 1/ [TB] at $[MnO_4^-]$ = 2.0 × 10^{-4} mol dm^{-3}, [TB] = 4.0 × 10^{-3} – 2.8 × 10^{-2} mol dm^{-3}, I = 1.0 mol dm^{-3} (Na_2SO_4) and T = 24 ± 0.1℃

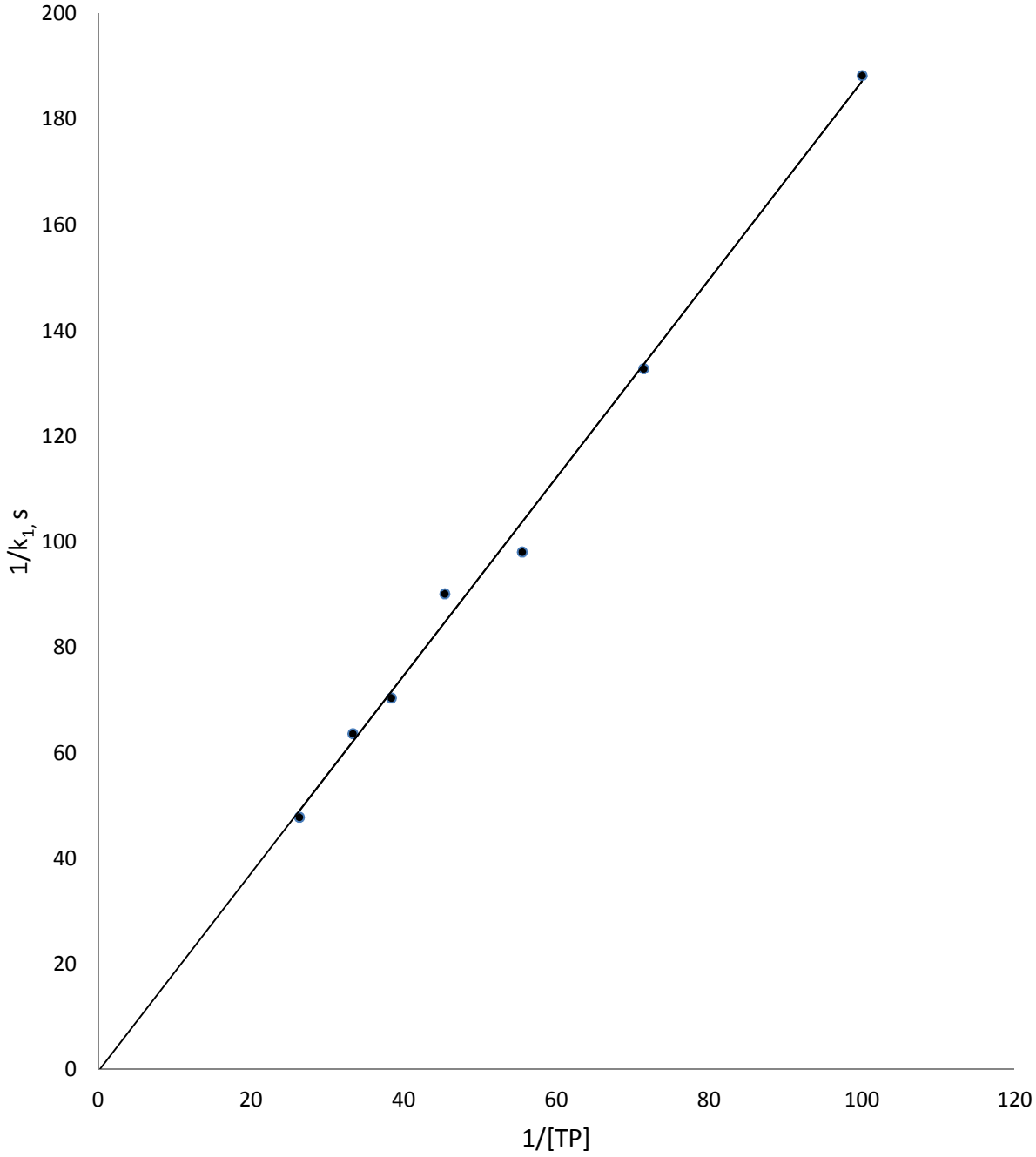


Figure 4.32: Michaelis–Menten plot of 1/ k_{obs} versus 1/ [TP] at$[MnO_4^-]$ = 2.0 × 10^{-4} mol dm^{-3}[TP] = (1.0 – 3.8) × 10^{-2} mol dm^{-3}, I = 0.5 mol dm^{-3} (Na_2SO_4) and T = 24 ± 0.1℃

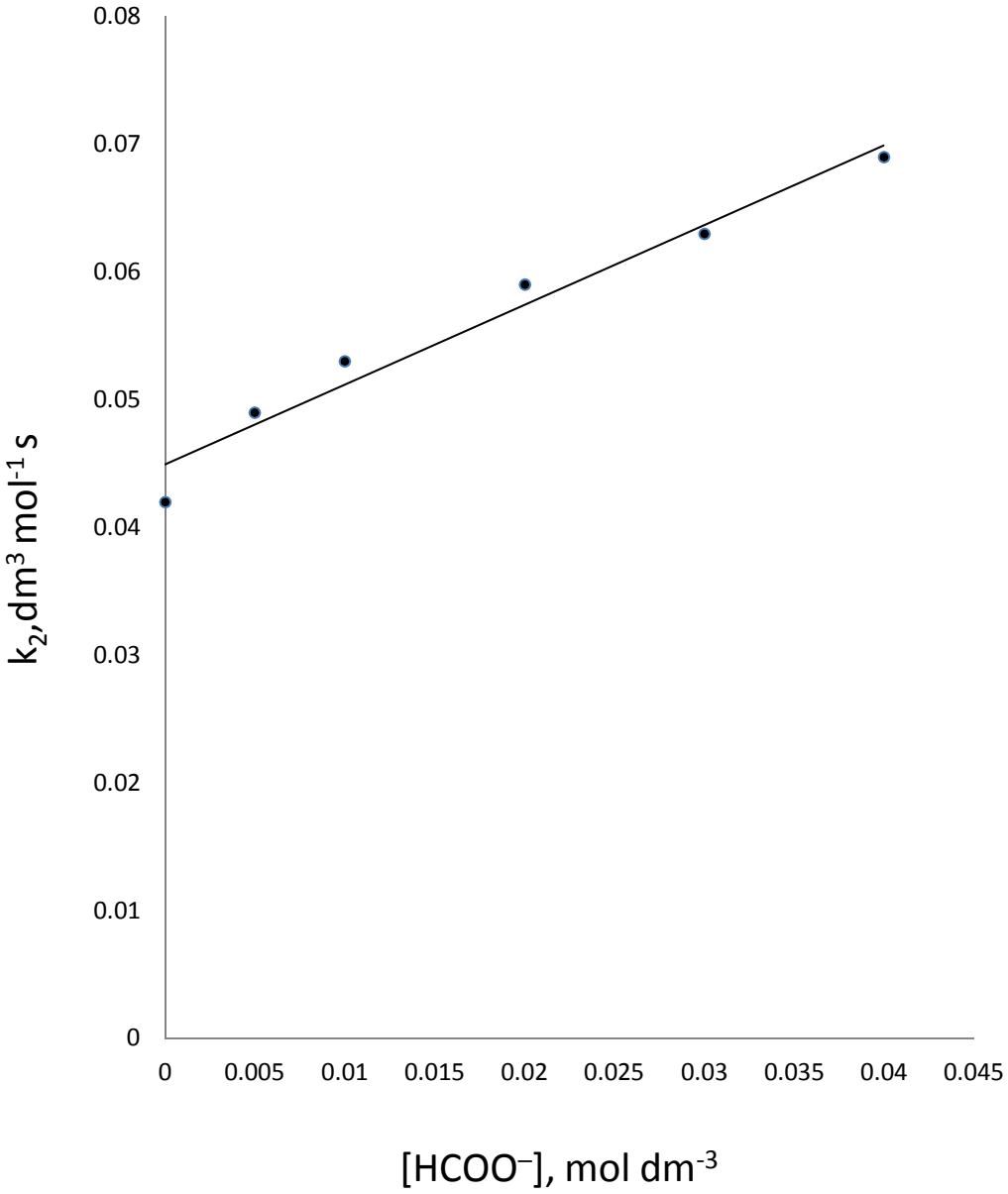


Figure 4.33: k_2 versus [$HCOO^-$] plot for the oxidation of CAF by MnO_4^- at [CAF] = 3.2×10^{-2} mol dm^{-3}, [MnO_4^-] = 2.0×10^{-4} mol dm^{-3}, [H^+] = 1.0×10^{-1} mol dm^{-3}, I = 0.5 mol dm^{-3} (Na_2SO_4) and T = 24.0 ± 0.1℃

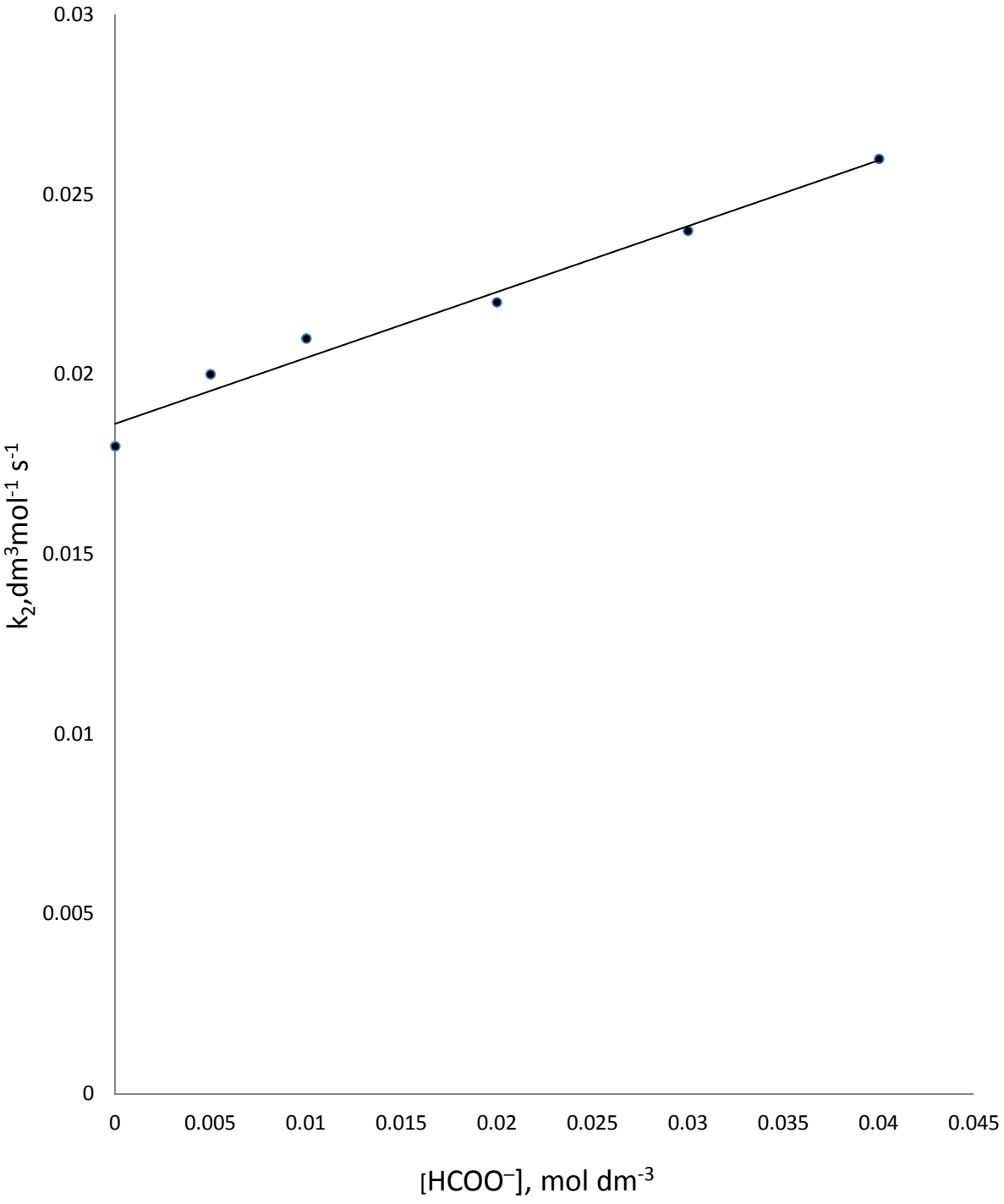


Figure 4.34: k_2 versus [$HCOO^-$] plot for the oxidation of IDZ by MnO_4^- at

[IDZ] = 7.0×10^{-2} mol dm^{-3}, $[H^+] = 3.2 \times 10^{-2}$ mol dm^{-3}, I = 1.0 mol dm^{-3} (Na_2SO_4) and T = 24 ± 0.1℃

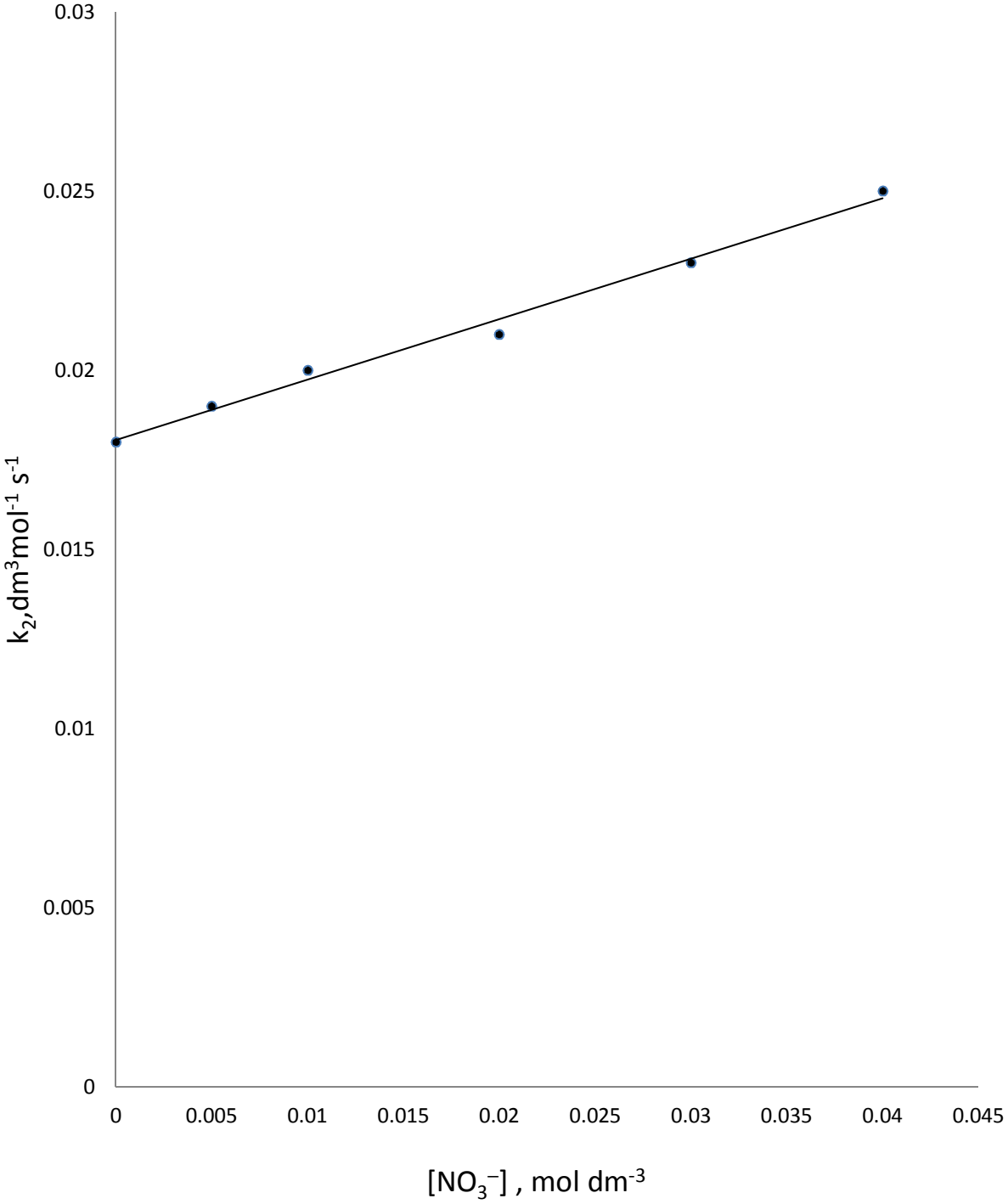


Figure 4.35: k_2 versus $[NO_3^-]$ plot for the oxidation of IDZ by MnO_4^- at [IDZ] = 7.0 × 10^{-2} mol dm^{-3}, $[MnO_4^-]$ = 2.0 × 10^{-4} mol dm^{-3}, $[H^+]$ = 3.2 ×10^{-1} mol dm^{-3}, I = 1.0 mol dm^{-3} (Na_2SO_4) and T = 24 ± 0.1℃

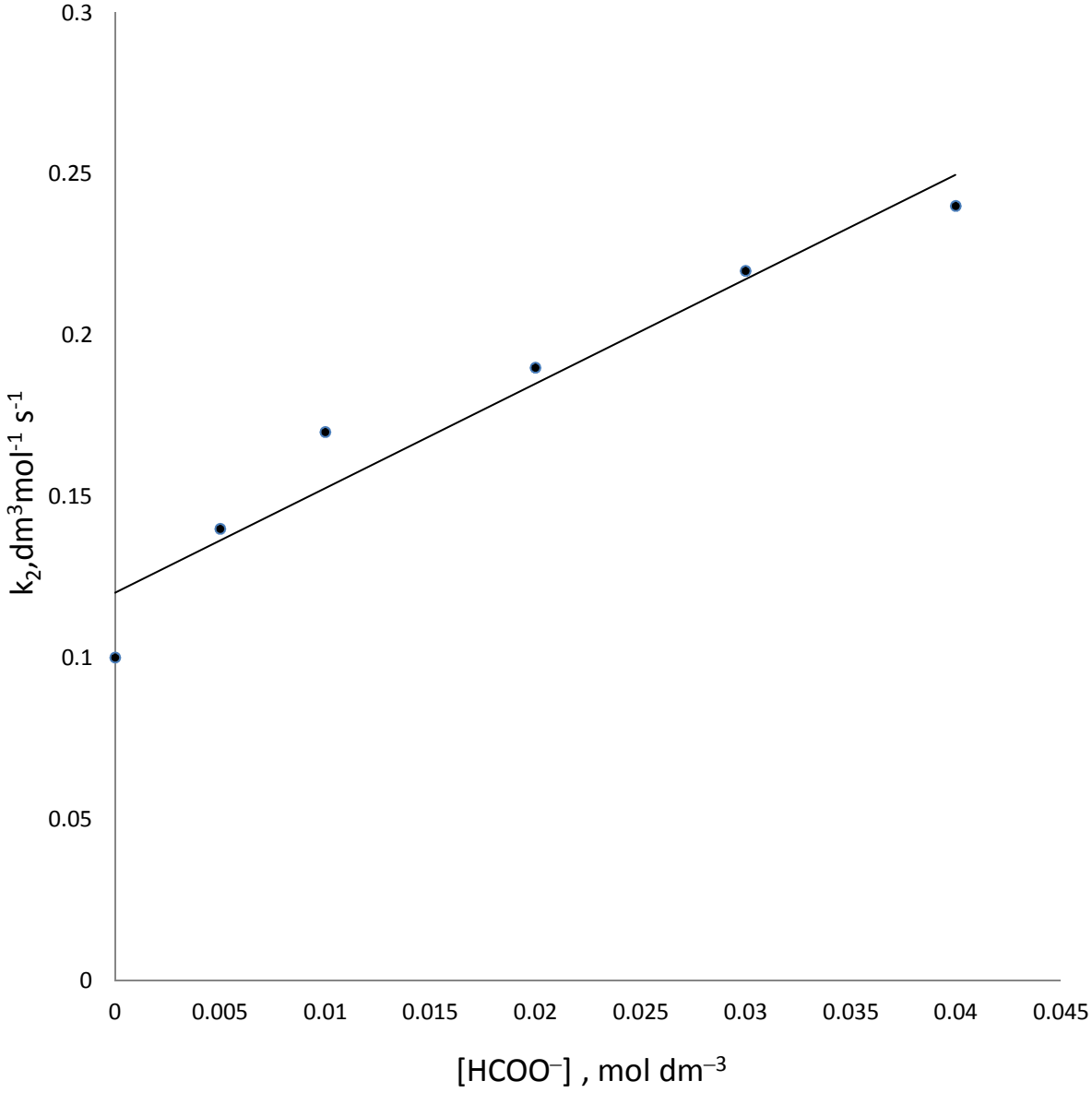


Figure 4.36: k_2 versus [$HCOO^-$] plot for the oxidation of TB by MnO_4^- at [TB] = 2.0×10^{-2} mol dm^{-3}, [MnO_4^-] = 2.0×10^{-4} mol dm^{-3}, [H^+] = 3.2×10^{-1} mol dm^{-3}, I = 1.0 mol dm^{-3} (Na_2SO_4) and T = 24 ± 0.1℃

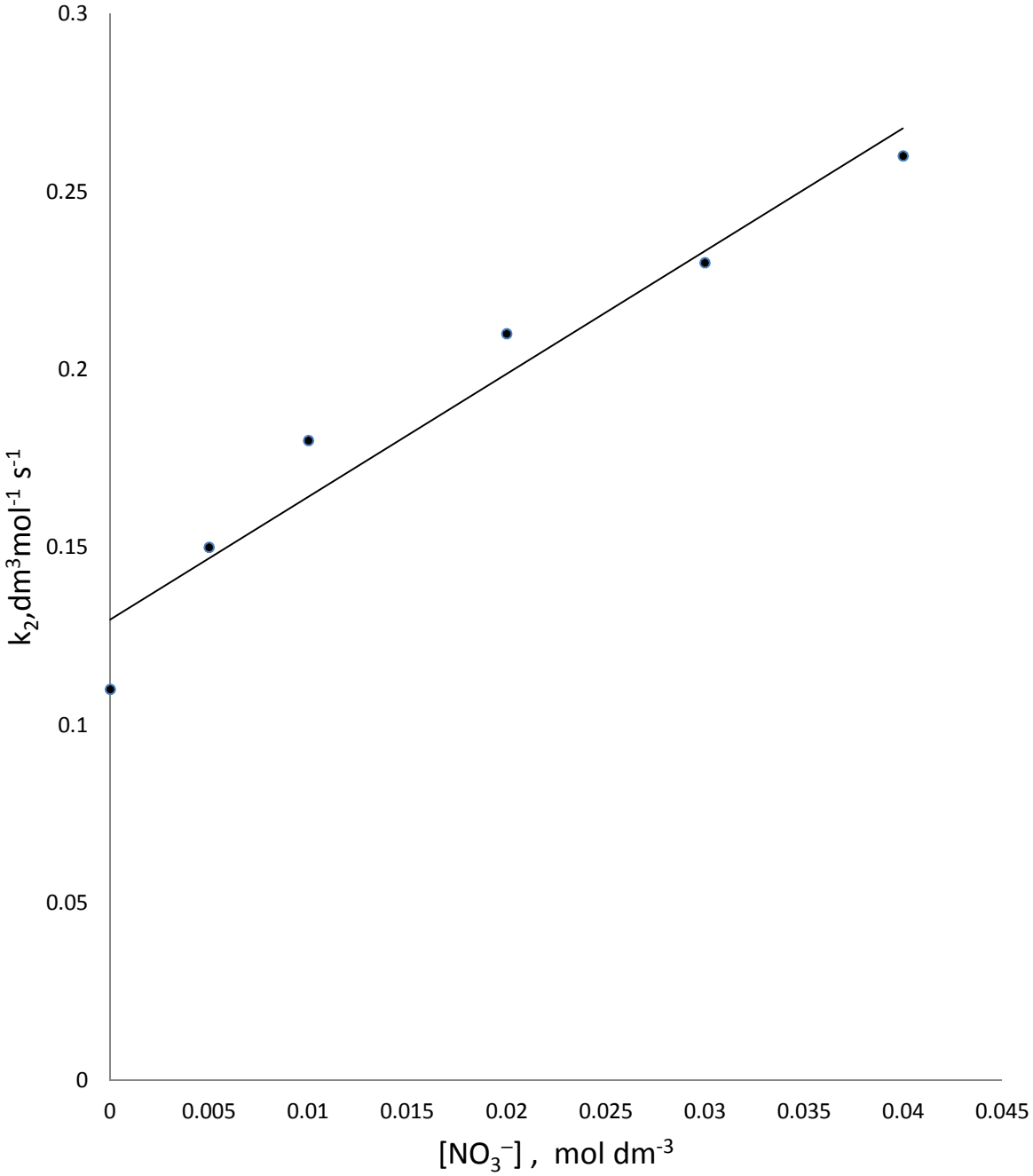


Figure 4.37: k_2 versus $[NO_3^-]$ plot for the oxidation of [TB] by $[MnO_4^-]$ at [TB] = 2.0×10^{-2} mol dm^{-3}, $[MnO_4^-] = 2.0 \times 10^{-4}$ mol dm^{-3}, $[H^+] = 3.2 \times 10^{-1}$ mol dm^{-3}, I = 1.0 mol dm^{-3} (Na_2SO_4) and T = 24.0 ± 0.1℃

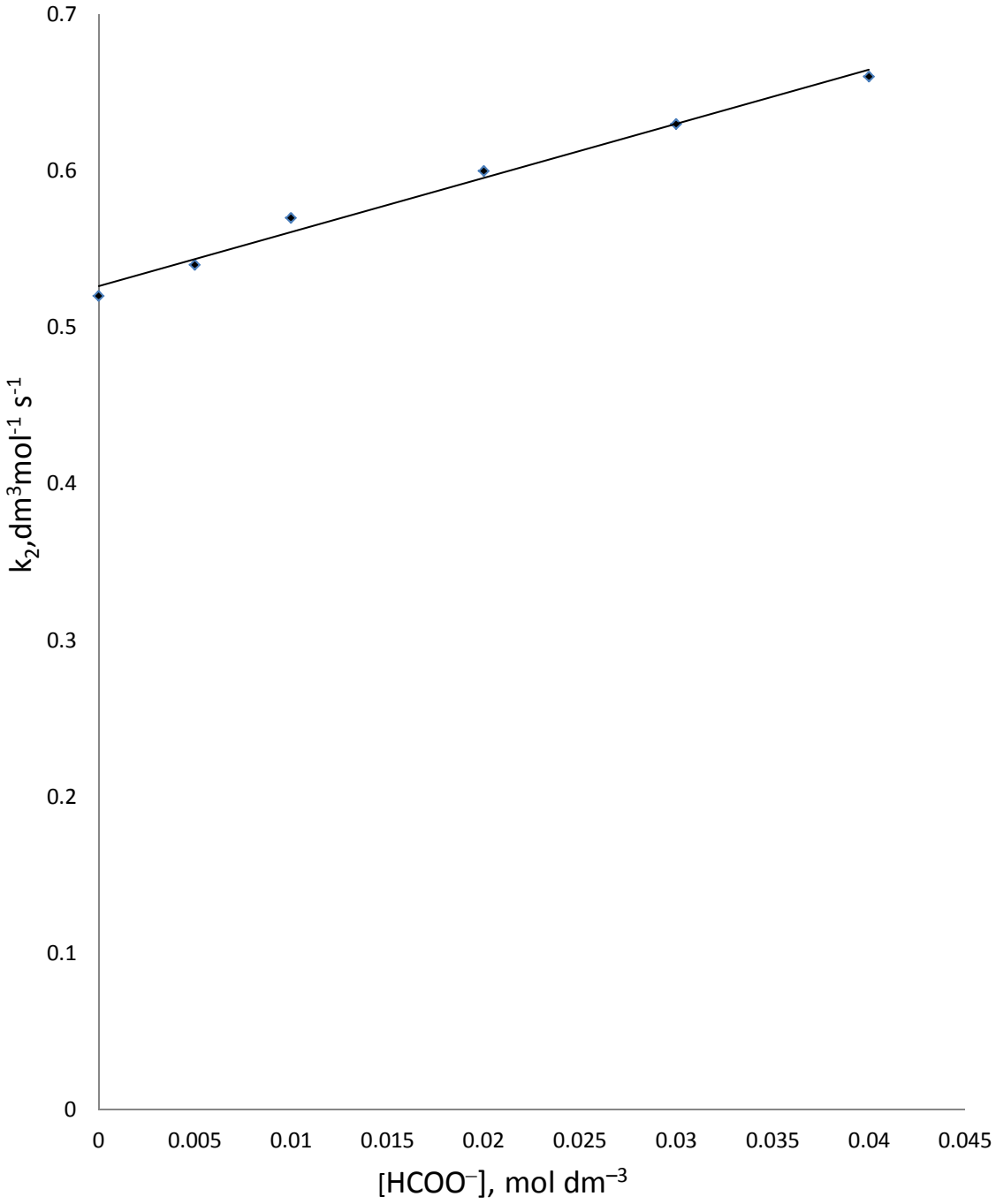


Figure 4.38: k_2 versus [$HCOO^-$] plot for the oxidation of TP by MnO_4^- at [TP] = 1.0 × 10^{-2} mol dm^{-3},[MnO_4^-] = 2.0 × 10^{-4} mol dm^{-3},[H^+] = 1.0 × 10^{-2} mol dm^{-3}, I = 0.5 mol dm^{-3} (Na_2SO_4) and T = 24 ± 0.1℃

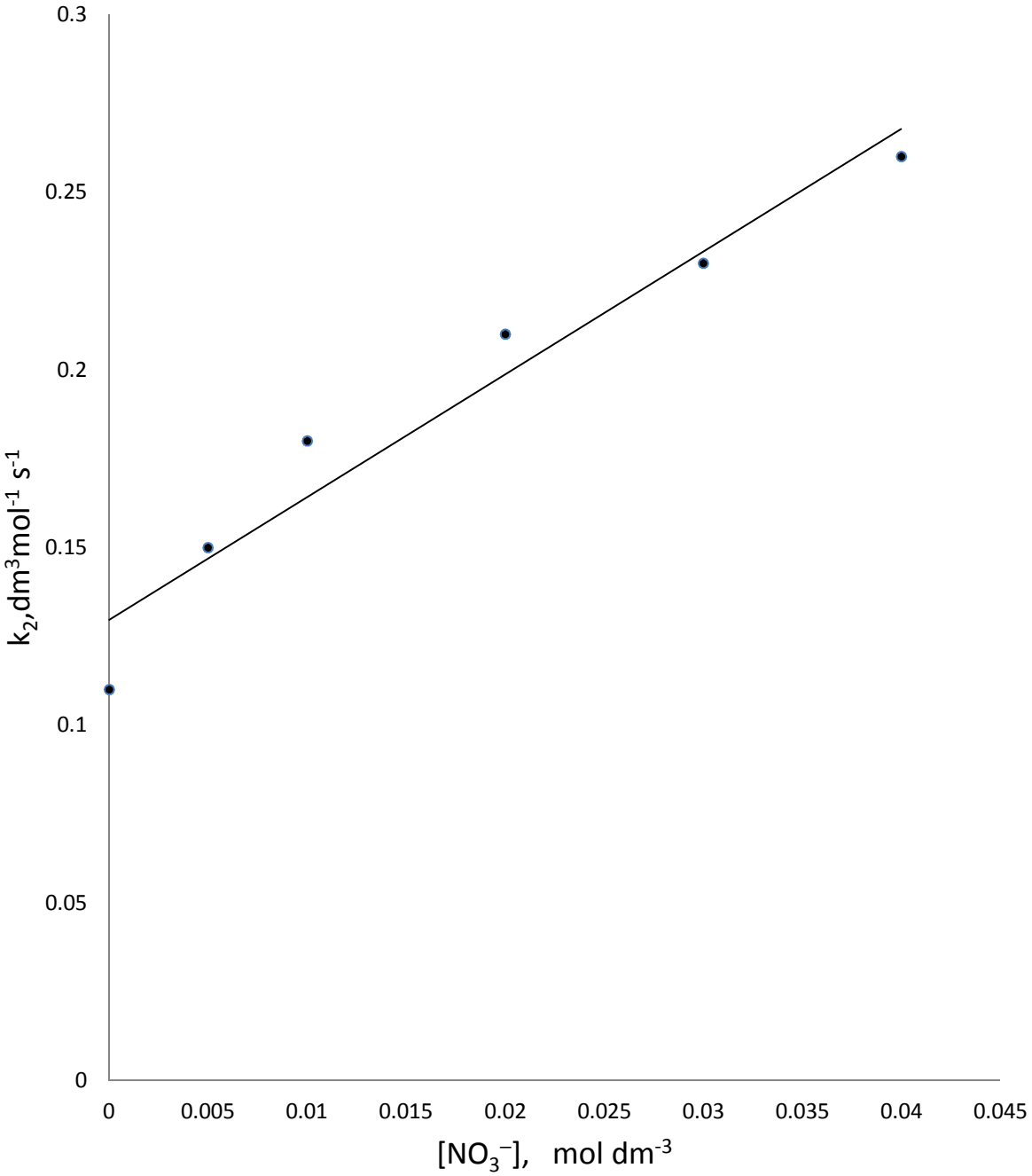


Figure 4.39: k_2 versus $[NO_3^-]$ plot for the oxidation of TP by MnO_4^- at [TP] = 1.0 × 10^{-2} mol dm^{-3}, $[MnO_4^-]$ = 2.0 × 10^{-4} mol dm^{-3}, $[H^+]$ = 1.0 × 10^{-1} mol dm^{-3}, I = 0.5 mol dm^{-3} (Na_2SO_4) and T = 24 ± 0.1℃

Table 4.9: The effect of added anions on the rate of oxidation of CAF by MnO_4^-, at [CAF] = 3.2 × 10^{-2} mol dm^{-3}, $[H^+]$ = 1.0 ×10^{-1} mol dm^{-3}, I= 0.5 mol dm^{-3} (Na_2SO_4) and $[MnO_4^-]$ = 2.0 × 10^{-4} mol dm^{-3}

X	10^3 [X], mol dm^{-3}	10^3 k_{obs}, s^{-1}	10^2 k_2, dm^3 $mol^{-1}s^{-1}$
$HCOO^-$	0.00	1.35	4.20
	5.00	1.59	4.90
	10.0	1.71	5.30
	20.0	1.90	5.90
	30.0	2.02	6.30
	40.0	2.23	6.90

Table 4.10: The effect of added anions on the rate of oxidation of IDZ by MnO_4^-, at [IDZ] = 1.0×10^{-2} mol dm^{-3}, $[H^+] = 3.2 \times 10^{-1}$ mol dm^{-3}, I = 1.0 mol dm^{-3} (Na_2SO_4) and $[MnO_4^-] = 2.0 \times 10^{-4}$ mol dm^{-3}

X	10^3 [X], mol dm^{-3}	$10^3 k_{obs}$, s^{-1}	k_2, $dm^3\ mol^{-1}s^{-1}$
$HCOO^-$	0.00	1.26	0.018
	5.00	1.38	0.020
	10.0	1.47	0.021
	20.0	1.58	0.022
	30.0	1.74	0.024
	40.0	1.84	0.026
NO_3^-	0.00	1.28	0.018
	5.00	1.34	0.019
	10.0	1.43	0.020
	20.0	1.53	0.022
	30.0	1.62	0.023
	40.0	I.79	0.025

Table 4.11: The effect of added anions on the rate of oxidation of TB by MnO_4^-, at [TB] = 2.0×10^{-2} mol dm^{-3}, $[H^+] = 3.2 \times 10^{-1}$ mol dm^{-3}, I= 1.0 mol dm^{-3} (Na_2SO_4) and $[MnO_4^-] = 2.0 \times 10^{-4}$ mol dm^{-3}

X	10^3 [X], mol dm^{-3}	$10^3 k_{obs}$, s^{-1}	k_2, $dm^3\ mol^{-1}s^{-1}$
$HCOO^-$	0.00	2.03	0.10
	5.00	3.26	0.14
	10.0	3.45	0.17
	20.0	3.83	0.19
	30.0	4.41	0.22
	40.0	4.98	0.24
NO_3^-	0.00	2.73	0.11
	5.00	3.64	0.15

10.0	4.03	0.18
20.0	4.41	0.21
30.0	4.60	0.23
40.0	5.37	0.26

Table 4.12: The effect of added anions on the rate of oxidation of TP by MnO_4^-, at [TP] = 1.0×10^{-2} mol dm^{-3}, [H^+] = 1.0×10^{-1} mol dm^{-3}, I= 0.5 mol dm^{-3} (Na_2SO_4) and [MnO_4^-] = 2.0×10^{-4} mol dm^{-3}

X	10^3 [X], mol dm^{-3}	10^3 k_{obs}, s^{-1}	$10k_2$, dm^3 $mol^{-1}s^{-1}$
$HCOO^-$	0.00	5.22	5.2
	5.00	5.40	5.4
	10.0	5.71	5.7
	20.0	6.04	6.0
	30.0	6.32	6.3
	40.0	6.64	6.6
NO_3^-	0.00	5.37	5.3
	5.00	5.52	5.5
	10.0	5.73	5.7
	20.0	6.00	6.0

30.0	6.20	6.2
40.0	6.40	6.4

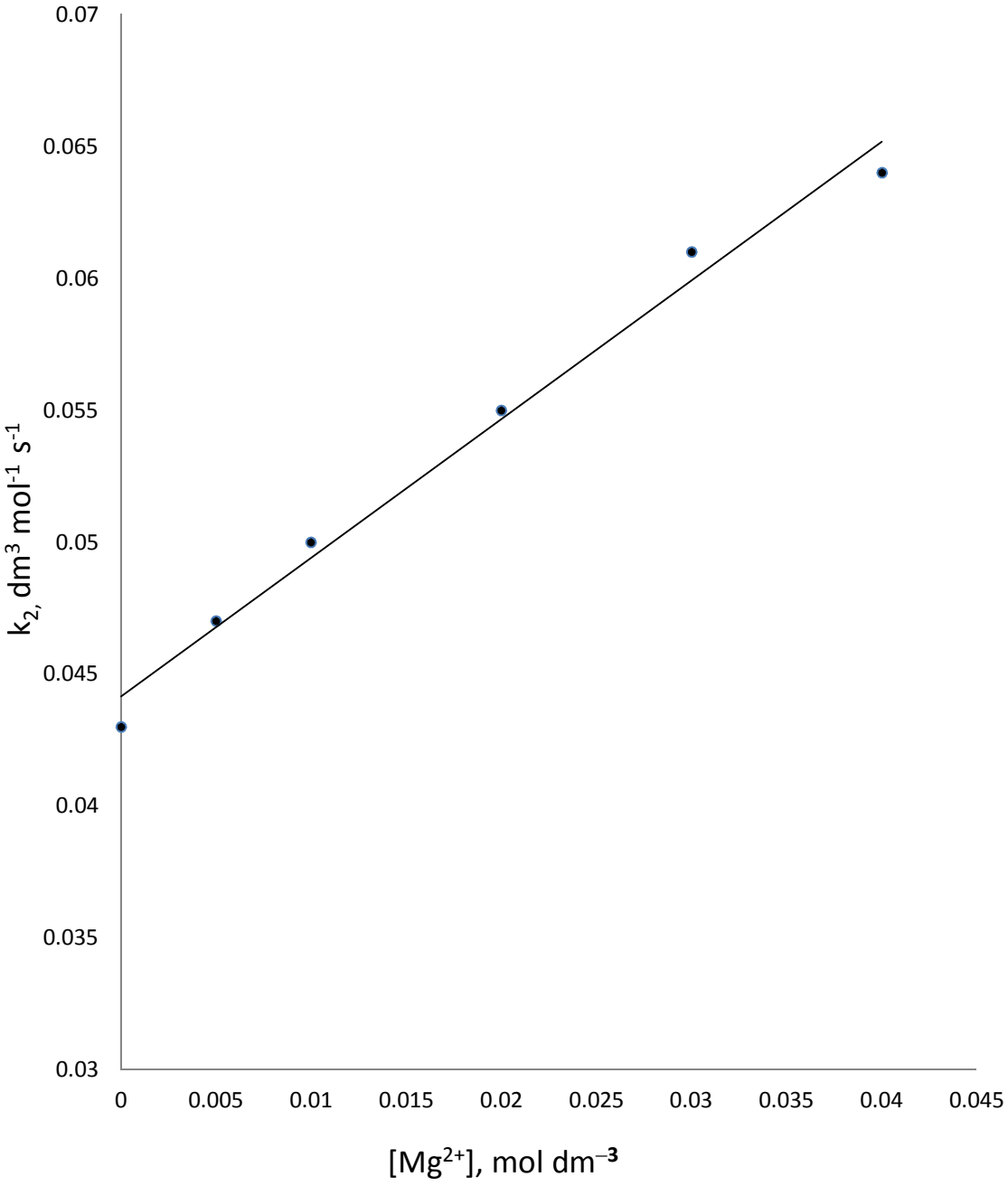

0.07
0.065
0.06
0.055
0.05
0.045
0.04
0.035
0.03
k_2, dm^3 mol^{-1} s^{-1}
0
0.005
0.01
0.015
0.02
0.025
0.03
0.035
0.04
0.045
$[Mg^{2+}]$, mol dm^{-3}

Figure 4.40: k_2 versus [Mg^{2+}] plot for the oxidation of CAF by MnO_4^- at [CAF] = 3.2×10^{-2} mol dm^{-3}, [MnO_4^-] = 2.0×10^{-4} mol dm^{-3}, [H^+] = 1.0×10^{-1} mol dm^{-3}, I = 0.5 mol dm^{-3} (Na_2SO_4) and T = 24.0± 0.1℃

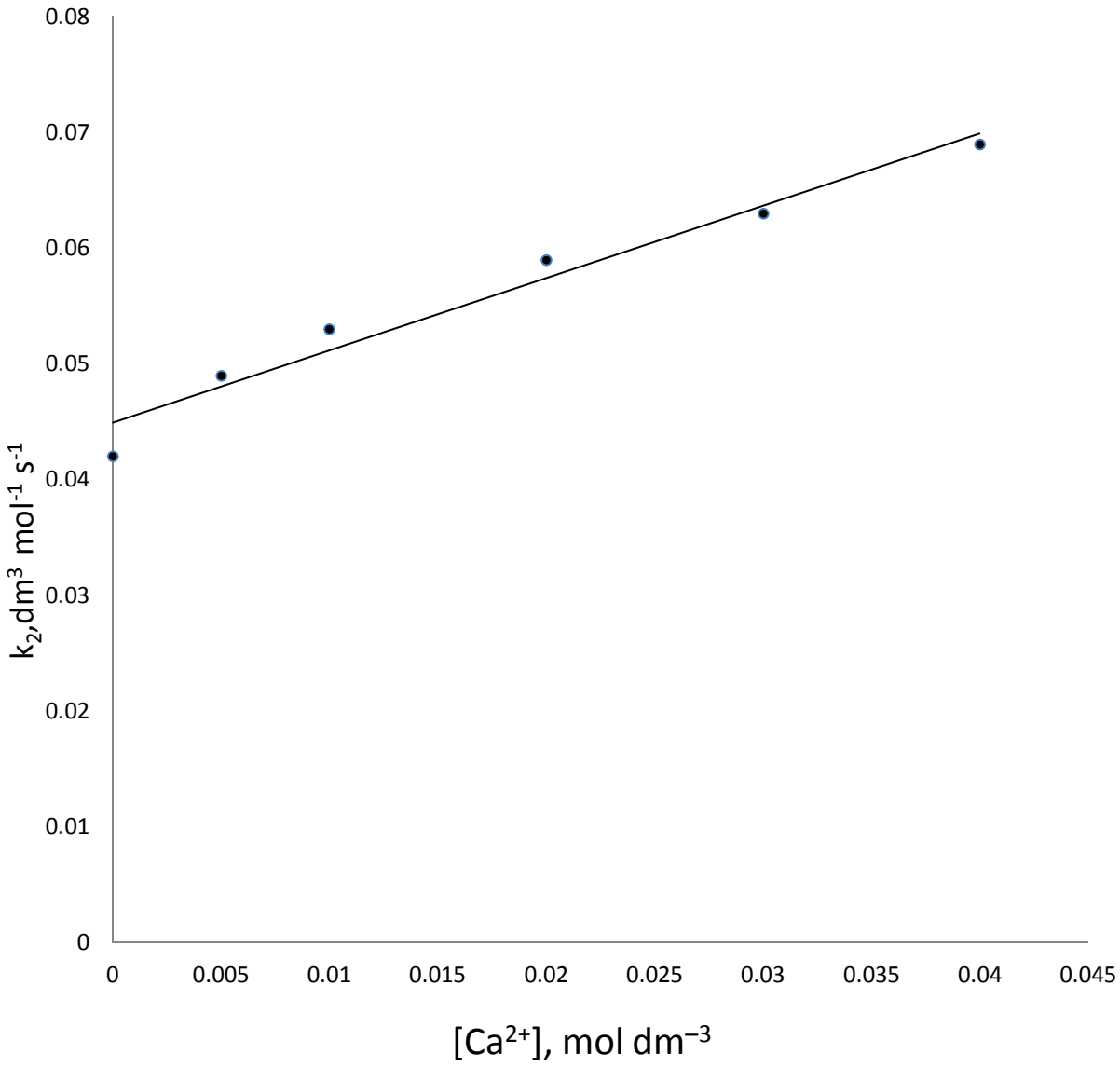


Figure 4.41: k_2 versus $[Ca^{2+}]$ plot for the oxidation of CAF by MnO_4^- at

$[CAF] = 3.2 \times 10^{-2}$ mol dm^{-3}, $[MnO_4^-] = 2.0 \times 10^{-4}$ mol dm^{-3},

$[H^+] = 1.0 \times 10^{-1}$ mol dm^{-3}, I = 0.5 mol dm^{-3} (Na_2SO_4) and T = 24.0 ± 0.1°C

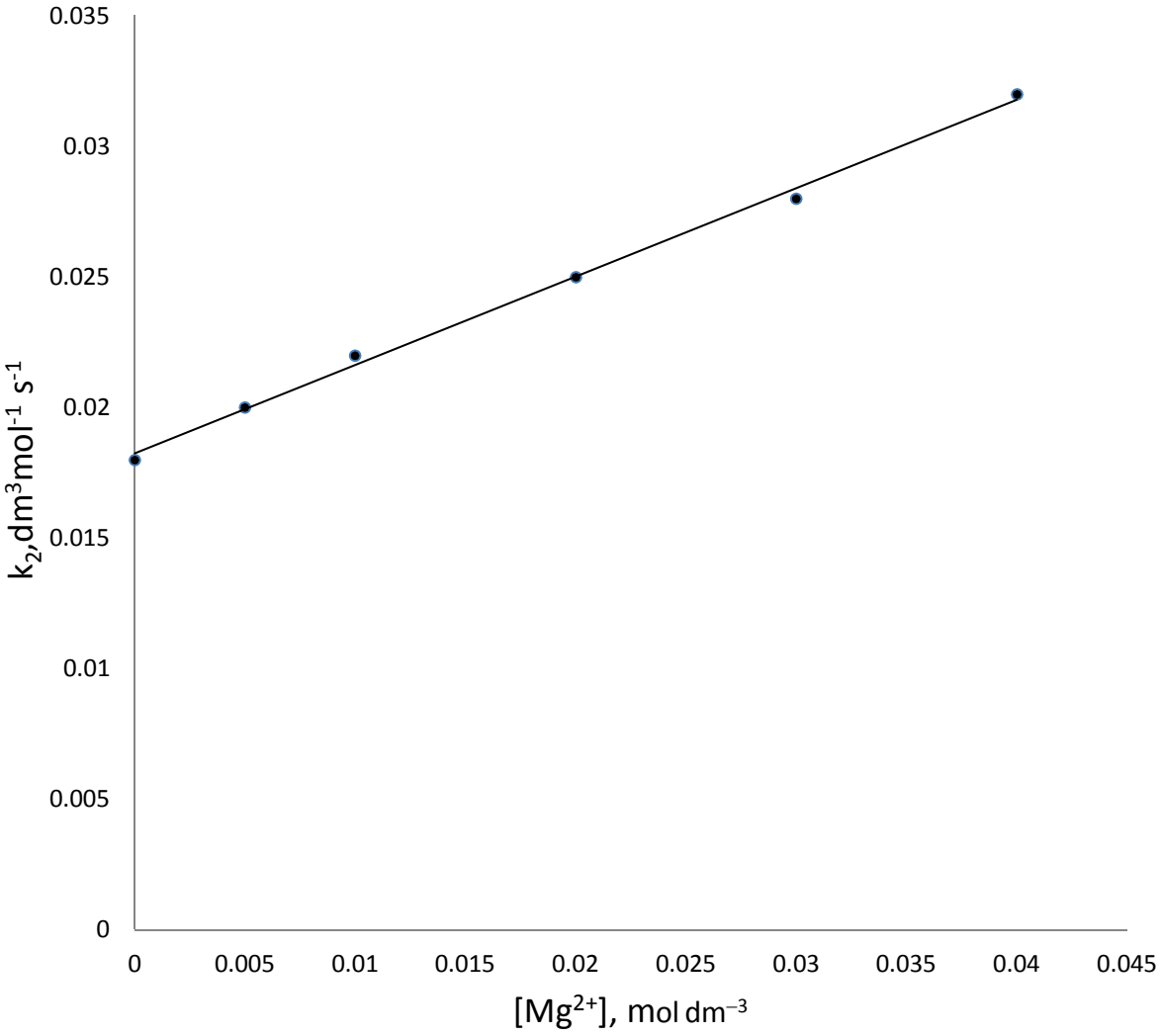


Figure 4.42: k_2 versus [Mg^{2+}] plot for the oxidation of IDZ by MnO_4^- at [IDZ] = 7.0×10^{-2} mol dm^{-3}, [MnO_4^-] = 2.0×10^{-4} mol dm^{-3},[H^+] = 3.2×10^{-2} mol dm^{-3}, I = 1.0 mol dm^{-3} (Na_2SO_4) and T = 24 ± 0.1℃

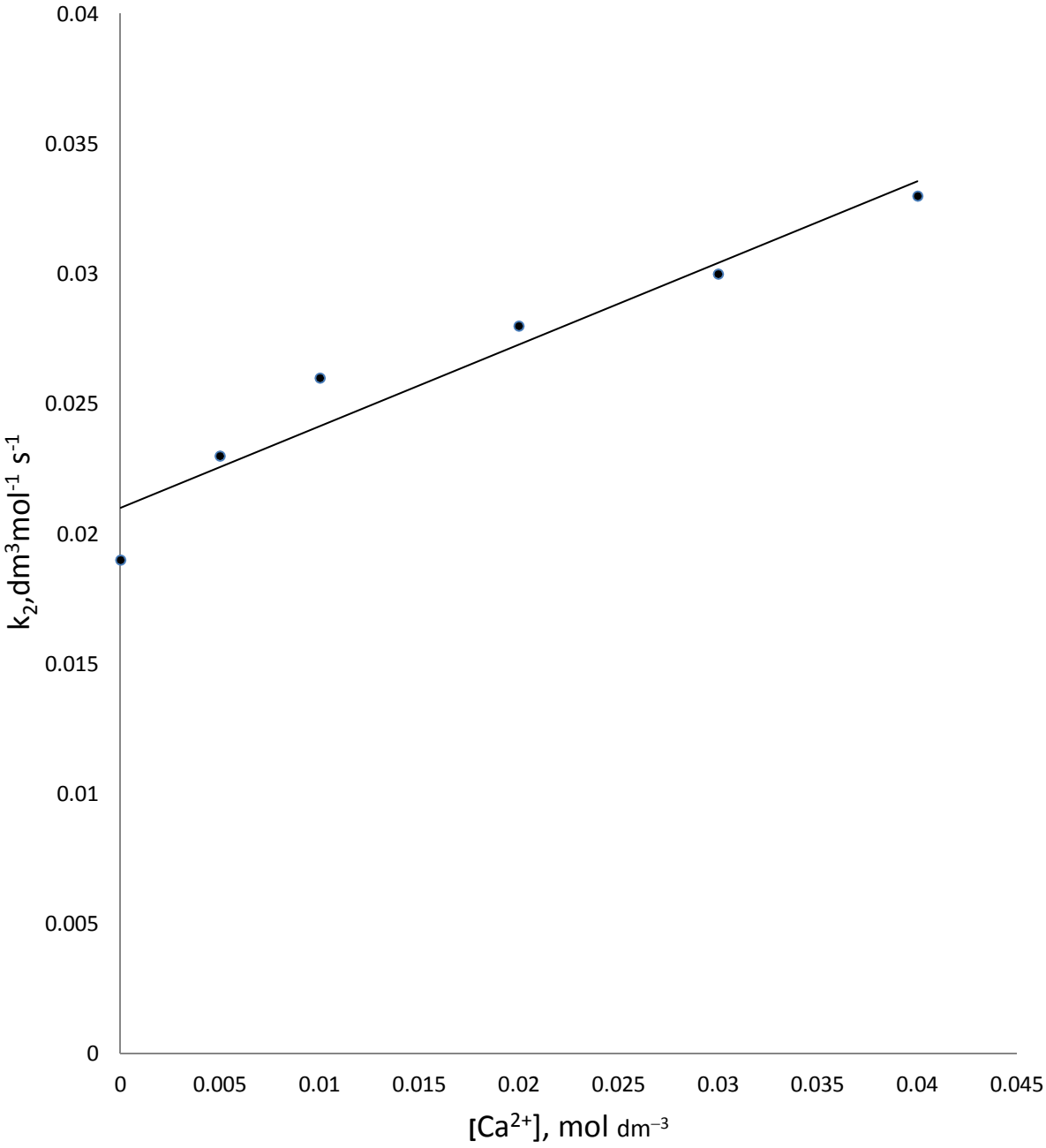

0.04
0.035
0.03
0.025
0.02
0.015
0.01
0.005
0
k2,dm3mol-1 s-1
0
0.005
0.01
0.015
0.02
0.025
0.03
0.035
0.04
0.045
[Ca2+], mol dm−3

Figure 4.43: k_2 versus [Ca^{2+}] plot for the oxidation of IDZ with MnO_4^- at [IDZ] = 7.0 × 10^{-2} mol dm^{-3}, [MnO_4^-] = 2.0 × 10^{-4} mol dm^{-3}, [H^+] = 3.2 × 10^{-1} mol dm^{-3}, I = 1.0 mol dm^{-3} (Na_2SO_4) and T = 24 ± 0.1℃

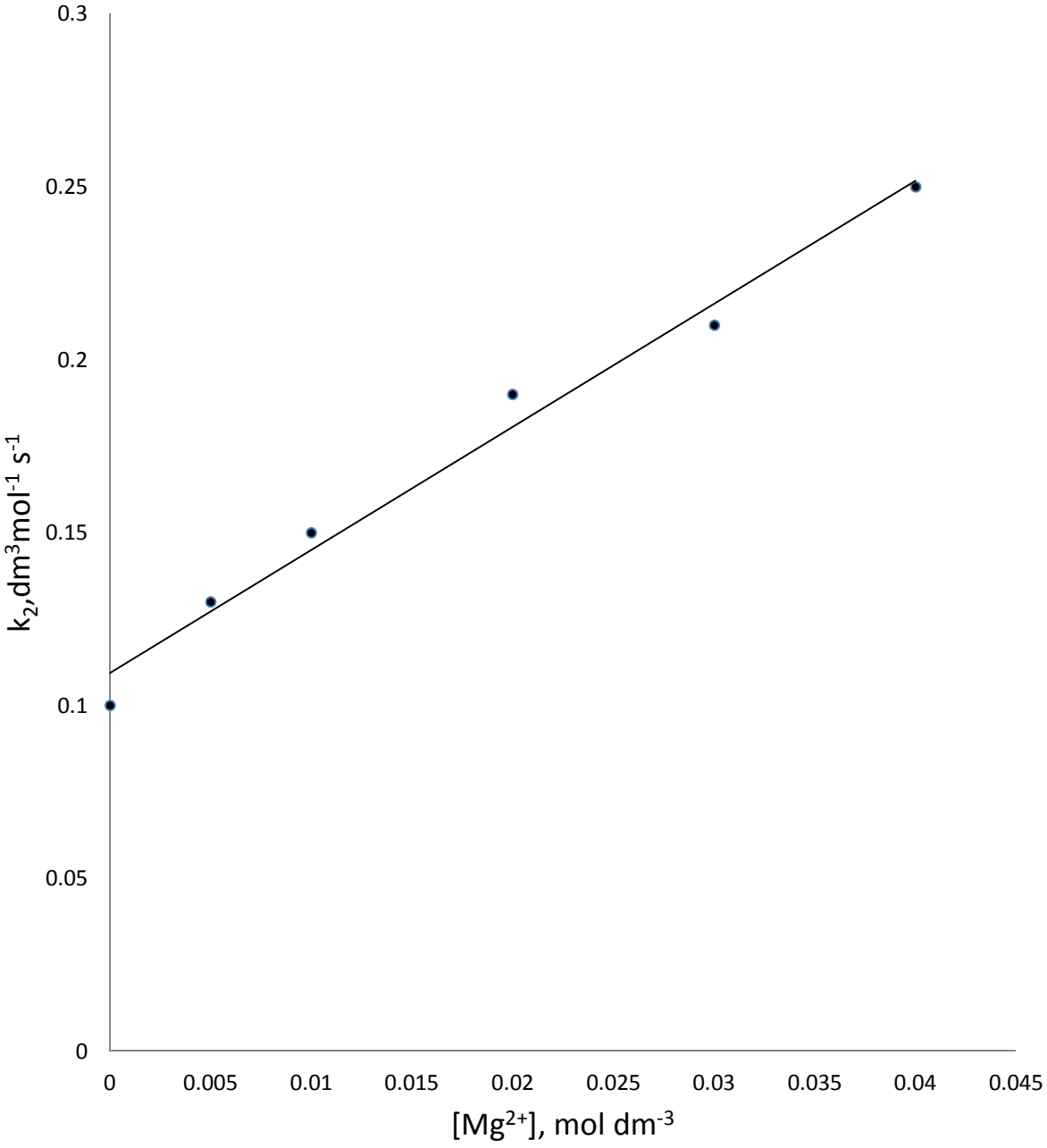


Figure 4.44: k_2 versus [Mg^{2+}] plot for the oxidation of [TB] by [MnO_4^-] at [TB] = 2.0×10^{-2} mol dm^{-3}, [MnO_4^-] = 2.0×10^{-4} mol dm^{-3}, [H^+] = 3.2×10^{-1} mol dm^{-3}, I = 1.0 mol dm^{-3} (Na_2SO_4) and T = 24 ± 0.1°C

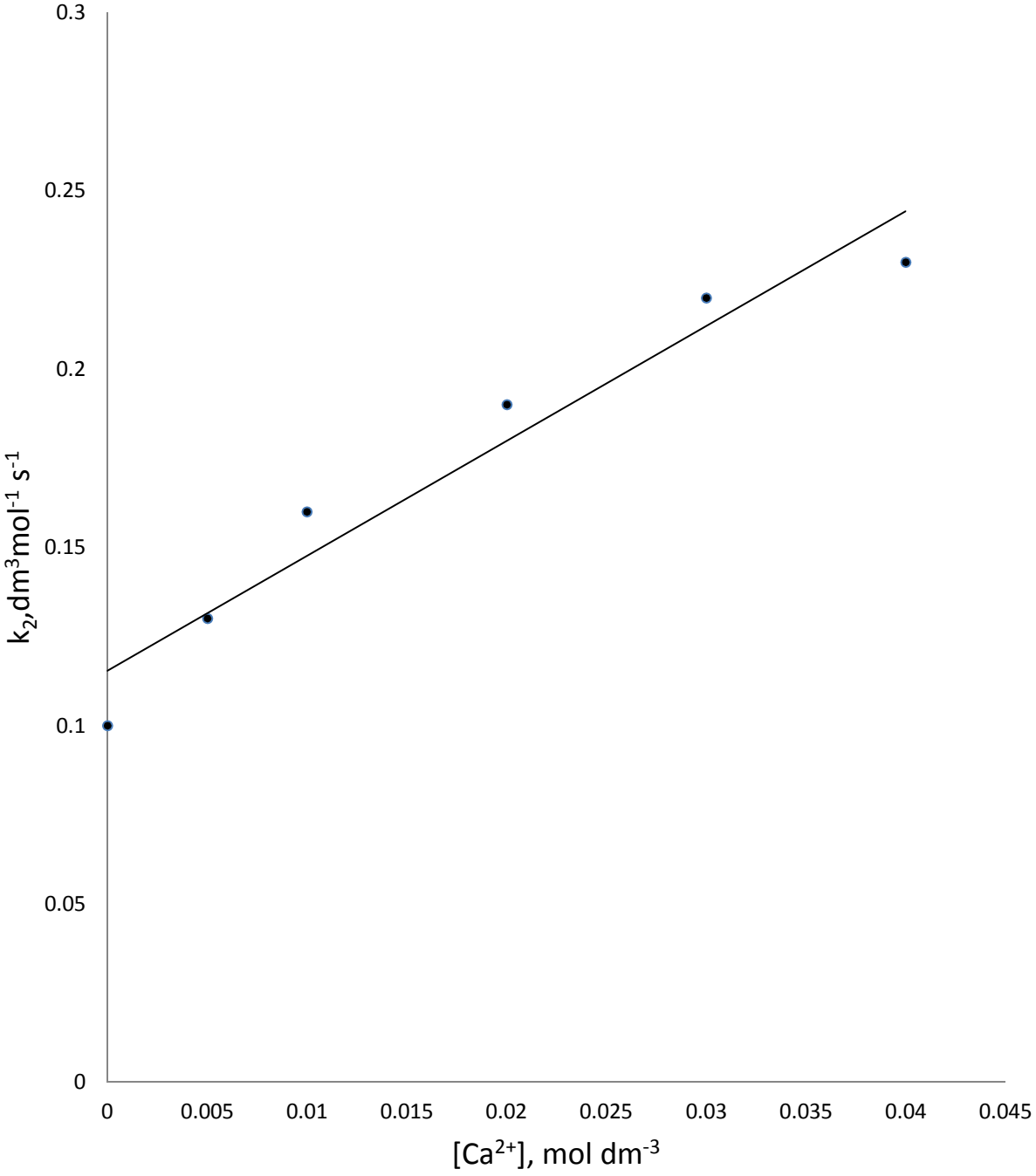


Figure 4.45: k_2 versus $[Ca^{2+}]$ plot for the oxidation of TB by MnO_4^- at [TB] = 2.0×10^{-2} mol dm^{-3}, $[MnO_4^-] = 2.0 \times 10^{-4}$ mol dm^{-3}, $[H^+] = 3.2 \times 10^{-1}$ mol dm^{-3}, I = 1.0 mol dm^{-3} (Na_2SO_4) and T = 24.0 ± 0.1°C

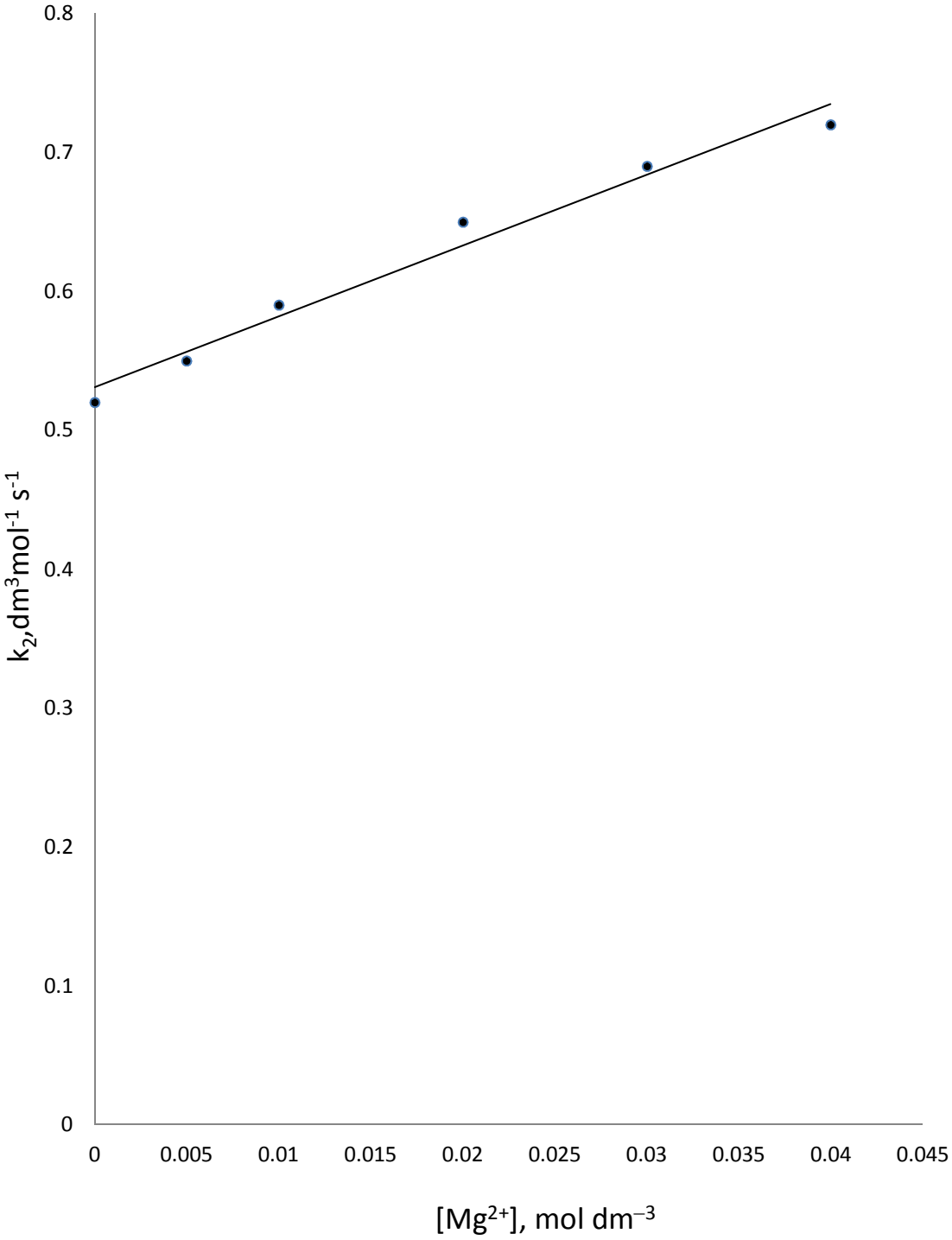


Figure 4.46: k_2 versus [Mg^{2+}] plot for the oxidation of TP by MnO_4^- at [TP] = 1.0×10^{-2} mol dm^{-3}, [MnO_4^-] = 2.0×10^{-4} mol dm^{-3}, [H^+] = 1.0×10^2 mol dm^{-3}, I = 0.5 mol dm^{-3} (Na_2SO_4) and T = 24.0 ± 0.1℃

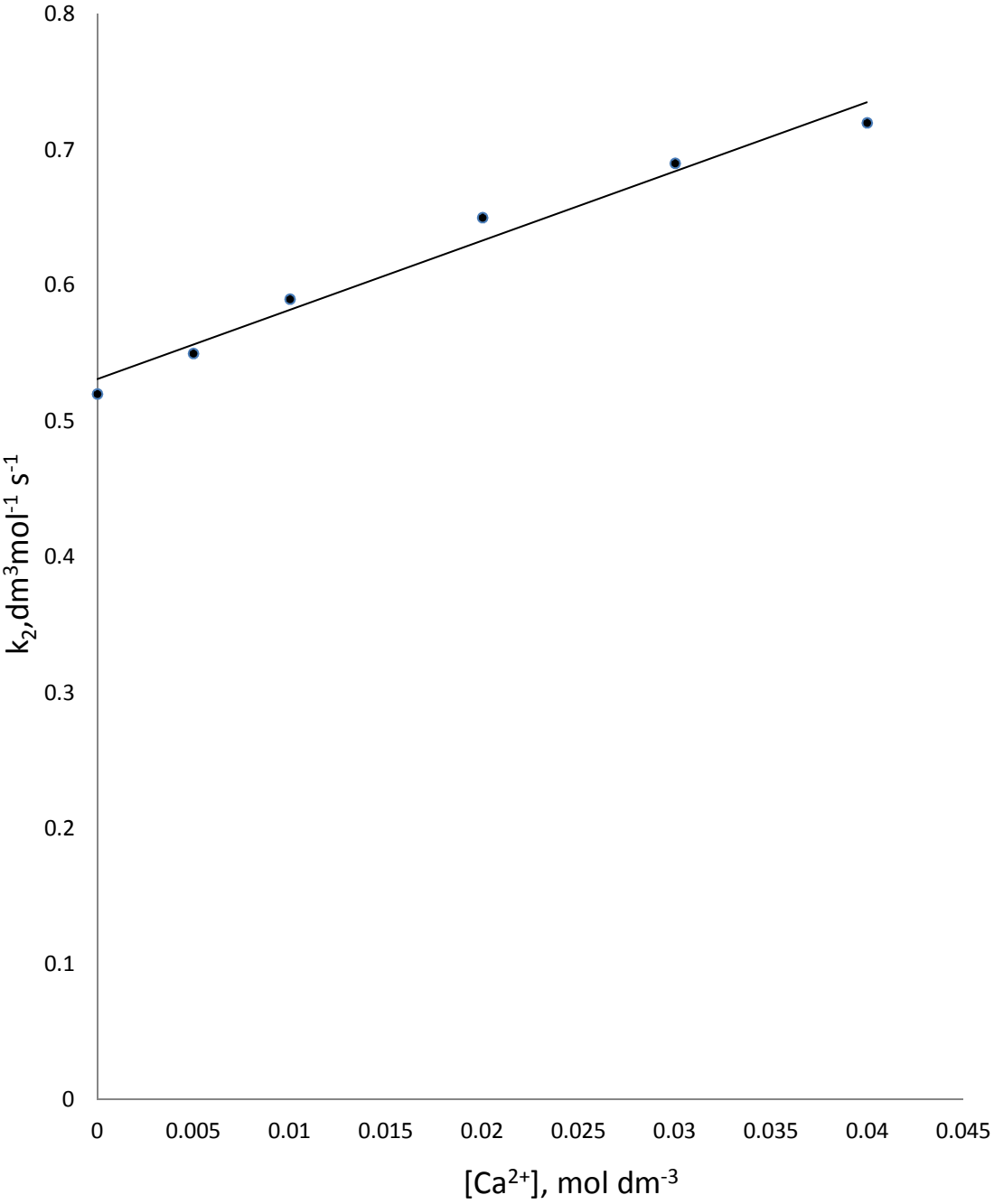


Figure 4.47: k_2 versus $[Ca^{2+}]$ plot for the oxidation of TP at MnO_4^- at [TP] = 1.0 × 10^{-2} mol dm^{-3}, $[MnO_4^-]$ = 2.0 × 10^{-4} mol dm^{-3}, $[H^+]$ = 1.0 × 10^{-2} mol dm^{-3}, I = 0.5 mol dm^{-3} (Na_2SO_4) and T = 24.0 ± 0.1℃

Table 4.13: Rate constants for the effect of cation for the oxidation of caffeine by MnO_4^- at [CAF] = 3.2 × 10^{-2} mol dm^{-3}, $[H^+]$ =1.0 ×10^{-1} mol dm^{-3} $[MnO_4^-]$ = 2.0 × 10^{-4} mol dm^{-3} and I = 0.5 mol dm^{-3} (Na_2SO_4)

Z	**10^3 [Z], mol dm^{-3}**	**10^3 k_{obs}, s^{-1}**	**k_2, dm^3 $mol^{-1}s^{-1}$**
Mg^{2+}	0.00	1.41	4.30
	5.00	1.53	4.70
	10.0	1.62	5.00
	20.0	1.78	5.50
	30.0	1.96	6.10
	40.0	2.07	6.40
Ca^{2+}	0.00	1.34	4.20
	5.00	1.57	4.90
	10.0	1.77	5.50
	20.0	1.90	5.90
	30.0	2.04	6.30
	40.0	2.10	6.50

Table 4.14: Rate constants for the effect of added cation for the oxidation of imidazole by MnO_4^- at [IDZ] = 1.0×10^{-2} mol dm^{-3}, $[H^+]$ = 3.2×10^{-2} mol dm^{-3}, $[MnO_4^-]$ = 2.0×10^{-4} mol dm^{-3}, and I = 0.5 mol dm^{-3} (Na_2SO_4)

.

Z	10^3 [Z], mol dm^{-3}	10^3 k_{obs}, s^{-1}	10^2k_2, dm^3 $mol^{-1}s^{-1}$
Mg^{2+}	0.00	1.30	1.8
	5.00	1.41	2.0
	10.0	1.53	2.2
	20.0	1.76	2.5
	30.0	1.99	2.8
	40.0	2.30	3.2
Ca^{2+}	0.00	1.35	1.9
	5.00	1.61	2.3
	10.0	1.84	2.6
	20.0	1.99	2.8
	30.0	2.14	3.0
	40.0	2.32	3.3

Table 4.15: Rate constants for the effect of cation for the oxidation of theobromine by MnO_4^- at [TB] = 2.0×10^{-2} mol dm^{-3}, [H^+] = 3.2×10^{-1} mol dm^{-3},[$[MnO_4^-]$ = 2.0×10^{-4} mol dm^{-3} and I = 0.5 mol dm^{-3} (Na_2SO_4)

Z	**10^3 [Z], mol dm^{-3}**	**10^3 k_{obs}, S^{-1}**	**$10k_2$, dm^3 mol^{-1}s^{-1}**
Mg^{2+}	0.00	2.26	1.0
	5.00	2.68	1.3
	10.0	3.07	1.5
	20.0	3.83	1.9
	30.0	4.20	2.1
	40.0	4.79	2.5
Ca^{2+}	0.00	2.11	1.0
	5.00	3.45	1.3
	10.0	3.64	1.6
	20.0	3.83	1.9
	30.0	4.03	2.2
	40.0	4.41	2.3

Table 4.16: Rate constants for the effect of added cation for the oxidation of theophylline by MnO_4^- at [TP] = 1.0×10^{-2} mol dm^{-3}, [H^+] = 1.0×10^{-2} mol dm^{-3}, [$[MnO_4^-]$] = 2.0×10^{-4} mol dm^{-3} and I = 0.5 mol dm^{-3} (Na_2SO_4)

Z	10^3 [Z], mol dm^{-3}	10^3 k_{obs}, s^{-1}	$10k_2$, dm^3 $mol^{-1}s^{-1}$
Mg^{2+}	0.00	5.26	5.2
	5.00	5.59	5.5
	10.0	5.92	5.9
	20.0	6.52	6.5
	30.0	6.90	6.9
	40.0	7.29	7.2
Ca^{2+}	0.00	5.37	5.3
	5.00	5.57	5.5
	10.0	5.83	5.8
	20.0	6.22	6.2
	30.0	6.72	6.7
	40.0	7.04	7.0

CHAPTER FIVE

5.0 Discussion

5.1 Oxidation of caffeine by permanganate ion

The results on stoichiometry show that one mole of the caffeine was consumed by one mole of the permanganate ion. The overall equation can be represented by equation (5.1)

$C_8H_{10}N_4O_2 + MnO_4^- + H^+ \longrightarrow Mn^{2+} + H_2O$ + Other products …5.1

Similar stoichiometries have been reported for the oxidation of malachite green by permanganate ion (Mohammed *et al*., 2009) and for the oxidation of nicotine by permanganate ion (Azafarany, 2010).

The product for CAF $-MnO_4^-$ reaction was analyzed for Mn(II) ion. The colourless product was reacted with potassium perchlorate and a purple coloration was observed suggesting the presence of Mn (II) ion. Potassium perchlorate oxidizes Mn (II) to purple Mn (VII) as can be represented by the equation below.

$2Mn^{2+} + 5KClO_4 + 3H_2O \longrightarrow 2MnO_4^- + 5KClO_3 + 6H^+$ …5.2

Colorless Purple

Pseudo-first order plot of log (A_t–A_∞) versus time were linear to more than 75%

The pseudo-first order rate constants k_{obs}, were determined from the slope of these plots and are reported in Table (1). Plot of logk_1 versus [CAF] showed that CAF–MnO_4^- reaction is first order in [CAF] as the graph was linear with a slope of 0.91± 0.1 (Figure 4.5).The order with respect to permanganate was found from the plot of logk_{obs}, versus [MnO_4^-] for the reaction gave first order in [MnO_4^-], a slope of 0.92 and correlation of 0.98 implying that the reaction is also first order in [MnO_4^-].Thus, the rate

equation for the reaction can be represented by equation (5.3) at I = 0.5 mo ldm^{-3}(Na_2SO_4) [H^+] =1.0 × 10^{-1} mol dm^{-3}.

$$-d[MnO_4^-]/dt=k_2[MnO_4^-][CAF] \quad \ldots 5.3$$

The rate of the reaction was enhanced by increase in [H^+]. The rate of the reaction showed two parallel pathways of reaction; involving the protonated and the unprotonated species both reacting to give a product as in other reactions of MnO_4^- (Iyun,1989). The Plot of logk_{obs} versus log [H^+] gave a slope of 1.26 indicating that the reaction is first order with respect to [H^+]. Plot of k_2 versus [H^+] was linear with positive intercept, as represented in Figure (4.13) so that the acid rate constant for the reaction can be represented by equation (5.4)

$$-d[MnO_4^-]/dt = (a+b[H^+])[CAF][MnO_4^-] \quad \ldots 5.4$$

where a= 0.26 dm^{3}mol^{-1}s^{-1} and b= 1.8 dm^{3}mol^{-1}s^{-1} .

It was observed that the rate of the reaction decreased with increase in ionic strength, suggesting a negative salt effect (Bronsted, 1922). Linear plot was obtained for logk_2 versus $I^{1/2}$ with R value of 0.975 (Figure 4.9). Result of the ionic strength effect is presented in Table (4.1). The rate constant increased as the dielectric constant of reaction medium increased thus, suggesting that outer-sphere mechanism is probably in operation.

Added anion (CH_3OO^-) and cation (Mg^{2+} and Ca^{2+}) led to the mild enhancement of the reactions. This is suggestive of outer-sphere mechanism. Acrylonitrile added to the partially oxidized reaction mixture of permanganate and caffeine did not polymerize or form gel even when a large excess of methanol was added to the CAF–MnO_4^-system this indicates that free radicals were not formed during the reaction.

Spectroscopic studies indicate that there was no clear shift from 530nm (Figure 4.25), the wavelength of maximum absorption of MnO_4^- studied. This indicates the absence of formation of intermediate complex during the course of the reaction. Michaelis–Menten plot of $1/k_{obs}$ versus $1/[CAF]$ was linear passing through the origin. This further suggests the absence of intermediate complex formation in the reaction.

On the basis of the above finding, a plausible mechanism is proposed;

$$MnO_4^- + H^+ \underset{}{\overset{K_1}{\rightleftharpoons}} HMnO_4 \qquad ..5.5$$

$$CAF + HMnO_4 \xrightarrow{k_2} Mn^{2+} + H_2O + \text{Other products (slow)} \qquad ...5.6$$

$$CAF + MnO_4^- \xrightarrow{k_3} Mn^{2+} + H_2O + \text{Other products (slow)} \qquad ....5.7$$

From the acid dependence studies, both the protonated form ($HMnO_4$) and the unprotonated form (MnO_4^-) of the oxidant is reacting at the rate determining step which means that a two –term rate law is expected. Therefore, equations (5.6) and (5.7) are the rate determining steps.

$$\text{Rate} = k_2[CAF][HMnO_4] + k_3[CAF][MnO_4^-] \qquad ...5.8$$

But, $[HMnO_4]=K_1[H^+][MnO_4^-]$

Substituting equation (5.5) into equation (5.8)

$$\text{Rate} = K_1 k_2 [CAF][MnO_4^-][H^+] + k_3[CAF][MnO_4^-] \qquad ...5.9$$

Rate = $(k_3+K_1 k_2 [H^+])$ [CAF][MnO_4^-] ….5.10

Equation (5.10) is analogous to equation (4.10) where k_3 = a= 0.26 $dm^3mol^{-1} s^{-1}$ and K_1k_2 = b= 1.8 $dm^3mol^{-1} s^{-1}$.

5.2 Oxidation of imidazole by permanganate ion

The results of the stoichiometric study showed that one mole of MnO_4^- was consumed by two moles of IDZ which is consistent with the stoichiometric equation of 1:2.

$2C_3H_4N_2 + MnO_4^- + H^+ \longrightarrow Mn^{2+} + H_2O$ + Other products …….5.11

Similar stoichiometry has been reported for the oxidation of L–ascorbic acid by permanganate ion (Babatunde, 2008).

The plots of ($logA_t$-A_∞) versus time were linear to more than 80% extent of reaction indicating that the reaction is first order dependent on $[MnO_4^-]$. Also, plot of $logk_{obs}$ versus log[IDZ] gave a slope of 0.92 suggesting that the reaction is also first order in [IDZ] . The reaction is second order overall. This trend has also been reported for the redox reactions of some oxyanions (Lohdip and Iyun, 1998). The rate equation for the reaction is;

$-d[MnO_4^-]/dt = k_2[MnO_4^-][IDZ]$ …5.12

The rate of the reaction increases with increase in $[H^+]$ as shown in Table (4.2).This observation correlates some earlier acid dependence studies involving permanganate and esters (Hussain, *et al;* 2010). Plot of $logk_{obs}$ versus $log[H^+]$ gave a slope of 1.03, indicating that the reaction is first order with

respect to $[H^+]$. Plot of k_2 versus $[H^+]$ was linear with positive intercept, as represented in Figure (4.14) the acid dependence for the reaction can be represented by equation (5.13).

$$-d[MnO_4^-]/dt = (a+b[H^+])[IDZ][MnO_4^-] \quad \ldots 5.13$$

The reaction thus occurs by an acid independent and first order acid dependent pathways

where a= 0.412 $dm^3mol^{-1}s^{-1}$ and b= 0.004 $dm^3mol^{-1}s^{-1}$.

The rate of the reaction increased with increase in ionic strength of the reaction medium, this suggests positive salt effect. This means that both species at the activated complex are of the same charges in the rate determine step (Benson, 1967). A linear plot was obtained for $\log k_2$ versus $I^{1/2}$ with R value of 0.987 (Figure 4.18).

The enhancement of the rate by added ions ($HCOO^-$, NO_3^-, Mg^{2+} and Ca^{2+}) suggests that the reaction most probably occurred by outer–sphere mechanism. Outer-sphere mechanism has also been proposed for the reaction between $MnO_4^-$and $[Fe(CN)]_6^{4-}$, $Ru(CN)_6^{-4}$ (Ajibade and Iyun, 1992).

The mechanism proposed below accommodates all the experimental finding for the reaction of IDZ with MnO_4^-. Reaction scheme;

$$H_2L + H^+ \underset{}{\overset{K}{\rightleftharpoons}} H_3L^+ \quad \ldots 5.14$$

$$H_2L + MnO_4^- \xrightarrow[\text{slow}]{k_1} L + MnO_3^- + H_2O \quad \ldots 5.15$$

$$H_3L^+ + MnO_4^- \xrightarrow[\text{slow}]{k_2} HMnO_3 + L + H_2O \quad \ldots 5.16$$

$MnO_3^- + H^+ \longrightarrow HMnO_3$ …5.17

fast

$2HMnO_3 + 2H_2L \rightarrow 2Mn^{2+} + 2L + 3H_2O$ …5.18

Equations (5.15) and (5.16) are the rate determining steps, therefore,

$Rate = k_1 [H_2L] [MnO_4^-] + k_2 [H_3L^+] [MnO_4^-]$ …5.19

From equation (5.14)

$[H_3L^+] = K [H_2L] [H^+]$ ….5.20

Substituting equation (5.20) into (5.19)

$Rate = k_1 [H_2L] [MnO_4^-] + Kk_2[H_2L] [MnO_4^-] [H^+]$ …5.21

$Rate = (k_1 + Kk_2 [H^+]) [H_2L] [MnO_4^-]$ …5.22 Equation (5.22) is is analogous to equation (4.10) where k_1 = a= 0.412 $dm^3mol^{-1}s^{-1}$ and Kk_2 = b= 0.004 $dm^3mol^{-1}s^{-1}$.

5.3 Oxidation of theobromine by permanganate ion

The Spectrophotometric titration showed that for every one mole of MnO_4^-, two moles of TB were oxidized as represented by the equation (5.23).

$2C_4H_8N_4O_2 + MnO_4^- + H^+ \longrightarrow Mn^{2+} + H_2O +$ Other products ……5.24.

Similar stoichiometry has been reported for the oxidation of DL–alanine by permanganate ion (Refat, 1999).

The linearity of the pseudo-first order plots of ($\log A_t - A_\infty$) versus time indicates that the reaction is first order dependence on MnO_4^-. Also, plot of log k_{obs} versus log [TB] gave a slope of 0.92 suggesting that the reaction is also first order in [TB]. Similar order has been reported in the redox reaction of permanganate ion with catechol (Iyun, 1990). The reaction is second order overall. The rate equation for the reaction is;

$-d[MnO_4^-]/dt = k_2[MnO_4^-][TB]$ ….5.25

The rate of the reaction increased with increase in $[H^+]$. Plot of $\log k_{obs}$ versus $\log[H^+]$ gave a slope of 1.31 dependent rate equations indicating that the reaction is first order with respect to $[H^+]$. Plot of k_2 versus $[H^+]$ was linear with positive intercept, as represented in Figure (4.15) the acid for the reaction can be represented by equation (5.26)

$-d[MnO_4^-]/dt = (a+b[H^+])[TB][MnO_4^-]$ ……5.26

The reaction thus occurs by an acid independent and first order acid dependent pathways where a= 0.041 $dm^3mol^{-1}s^{-1}$ and b= 0.028 $dm^3mol^{-1}s^{-1}$ .The increase in ionic strength of the medium resulted in increase in the rate of the reaction suggesting positive Bronsted-Debye salt effect. Linear plot was obtained for $\log k_2$ versus $I^{1/2}$ with R value of 0.951 (Figure 4.17).

The added anions (NO_3^- and $HCOO^-$) and cations (Mg^{2+} and Ca^{2+}) enhanced the rates of the reactions. An indication that the reaction might be operation via the outer-sphere mechanism.

The Michaelis–Menten plot $\frac{1}{k}$ versus $\frac{1}{[TB]}$ showed no intercept on the 1/k, axis, suggesting the absence of an intermediate complex formation. Spectrophotometric measurement showed no clear shift in the λ_{max} of from 530nm when reactants were mixed together and the electronic spectrum was recorded after 20 minutes of mixing. This further suggests the absence of intermediate complex formation.

The following reaction mechanism is therefore proposed to accommodate all the experimental observations.

$$MnO_4^+ + H^+ \underset{}{\overset{K}{\rightleftharpoons}} HMnO_4 \qquad \ldots 5.27$$

$$TB + HMnO_4 \xrightarrow{k_1} Mn^{2+} + H_2O + \text{Other products} \quad \text{(slow)} \qquad \ldots\ldots 5.28$$

$$TB + MnO_4^- \xrightarrow{k_2} Mn^{2+} + H_2O + \text{Other products} \quad \text{(slow)} \qquad \ldots. 5.29$$

Equations (5.28) and (5.29) are the rate determining steps. Therefore,

$$\text{Rate} = k_1 [TB] [HMnO_4] + k_2 [TB] [MnO_4^-] \qquad \ldots 5.30$$

$$\text{But, } [HMnO_4] = K [H^+] [MnO_4^-] \qquad \ldots 5.31$$

Substituting equation (5.31) into (5.30)

Rate = K k_2 [TB] [MnO_4^-] [H^+] + k_2 [TB] [MnO_4^-] …5.32

Rate = (k_2 + Kk_1[H^+]) [TB][MnO_4^-] …5.33

Equation (5.33) is analogous to equation (4.10) where k_2 = a= 0.041 dm^3 mol^{-1} s^{-1} and Kk_1 = b= 0.028 dm^3mol^{-1} s^{-1}.

5.4 Oxidation of theophylline by permanganate ion

The stoichiometric study indicates that one mole of theophylline was consumed by one mole of permanganate ion. The overall reaction is given by equation (5.34)

$C_4H_8N_4O_2$ + MnO_4^- + H^+ ⟶ Mn^{2+} + H_2O + Other products …5.34

Similar stoichiometry has been reported for the oxidation of malachite green by permanganate ion and for the oxidation of nicotine by permanganate. The product of the reaction was confirmed by chemical test. The Mn^{2+} in the product was tested with indole (Lohdip and Iyun, 1998) and a white precipitate was obtained indicating the presence of Mn^{2+}.

The kinetic results indicate that the reaction exhibits first order in both theophylline and permanganate ion as, pseudo–first order plots of log(A_t –A_∞) versus time were linear to more than 80% extent of reaction, under the experimental conditions. The pseudo–first order rate constant was determined at different initial concentrations of TP. Plot of log k_{obs} versus log [TP] at , I= 0.5 mol $dm^{-3}$and [H^+] =1.0 x 10^{-2} mol dm^{-3} gave a slope of 0.92 ± 0.02 . This suggests a first order dependence on [TP]. The values of second order rate constant k_2 (k_2=k_{obs}/[TP]) were fairly constant (Table 4.4.), suggesting that the reaction is also first order in [TP] and that the reaction is second order overall.

Therefore, the rate equation

$-d[MnO_4^-]/dt = k_2[MnO_4^-][TB]$ ...5.35

The results suggest that the rate of the reaction increased with increase in $[H^+]$ at [TP] = 1.0×10^{-2} mol dm^{-3}, $[MnO_4^-]$ = 2.0×10^{-4} mol dm^{-3}, $[H^+]$ = $2.0 \times 10^{-2} - 3.4 \times 10^{-1}$ mol dm^{-3} I = 0.5 mol dm^{-3} (Na_2SO_4) and T = 24 ± 0.1. A plot of k_2 versus $[H^+]$(Figure 4.15) was linear with a positive intercept and can be represented as;

$k_2 = a + b[H^+]$ ...5.36

where a = 2.0×10^{-4} mol dm^{-3} and b = 0.5 mol dm^{-3} . The rate of the reaction showed two parallel pathways of reaction; one involving the protonated and the other the unprotonated species both reacting to give a product .Therefore the rate equation of the reaction becomes

$-d[MnO_4^-]/dt = (a+b[H^+])[TP][MnO_4^-]$ .....5.37 The increase in ionic strength of the medium resulted in increase in the rate of the reaction suggesting Bronsted–Debye positive salt effect. Linear plot was obtained for $\log k_2$ versus $I^{1/2}$ with R value of 0.960 (Figure 4.20).The added ions NO_3^-, $HCOO^-$, Mg^{2+} and Ca^{2+} mildly enhanced the rate of the reaction. Catalysis of the reaction by these ions indicates that the reaction might be operating via the outer–sphere mechanism.

Spectrophotometric measurement showed no clear shift in the λ_{max} of from 530nm characteristic of MnO_4^- when reactants were mixed together and the electronic spectrum was recorded after 2 minutes of mixing. This further suggests the absence of intermediate complex formation.

The kinetic and stoichiometric data are consistent with the following reaction scheme.

K

$MnO_4^+ + H^+ \rightleftharpoons HMnO_4$ ...5.38

TP + $HMnO_4$ $\xrightarrow{k_1}$ $Mn^{2+} + H_2O$ + Other products (slow) …5.39

TP + MnO_4^- $\xrightarrow{k_2}$ $Mn^{2+} + H_2O$ + Other products (slow) 5.40

Equations (5.39) and (5.40) are the rate determining steps. Therefore,

Rate = k_1 [TP] [$HMnO_4$] + k_2 [TP] [MnO_4^-] …5.41

But, [$HMnO_4$] = K [H^+] [MnO_4^-]

Rate = K k_1 [TP] [MnO_4^-] [H^+] + k_2 [TP] [MnO_4^-] …5.42

Rate = (k_2 + Kk_1 [H^+]) [TP][MnO_4^-] …5.43

Equation (5.43) is is analogous to equation (4.10) where k_2 = a= 2.0×10^{-4} $dm^3\ mol^{-1}\ s^{-1}$ and Kk_1 = b= 0.5 $dm^3\ mol^{-1}\ s^{-1}$.

5.5 Summary and conclusion

The kinetic and mechanistic studies on the redox reactions of permanganate ion with caffeine, imidazole, theobromine and theophylline have been carried out in aqueous acidic medium. Na_2SO_4 was used to maintain the ionic strengths of the reaction medium. The stoichiometry of 1:1 (oxidant: reductant) was observed for CAF–permanganate and TP–permanganate systems, while stoichiometry of 1:2 was observed for IDZ–permanganate and TB–permanganate systems. A second order overall rate law was observed in all the systems studied. The rates of the reactions of CAF–permanganate, IDZ–

permanganate, and TB–permanganate and TP– permanganate showed first order dependence in both [oxidant] and [reductant] and also in $[H^+]$. Mn^{2+} was qualitatively identified as one of the products of the reactions. The reaction of CAF–permanganate was inhibited by change in ionic strength of the reaction medium while, IDZ–permanganate, TB–permanganate and TP–permanganate reactions were enhanced by these changes. In all the systems studied, change in dielectric constant increased the rate of the reactions, except for CAF–permanganate system. Free radical intermediates were not observed in all the reactions. Added anion ($HCOO^-$ and NO_3^-) and added cation (Mg^{2+} and Ca^{2+}) led to the enhancement of the reactions, suggesting outer–sphere mechanism. Michaelis-Menten plots of $^1/_{k_{obs}}$ versus $^1/_{[reductant]}$ were linear passing through the origin. This further suggests the absence of intermediate complex formation in the reactions. Therefore, both kinetic studies and spectroscopic evidences point towards the outer–sphere mechanism as a possible mechanistic path for the reactions of all the systems studied.

REFERENCES

Abe, Y., Takigami, M., Sugino, K., Taguchi, M., Kojima, T., Umemura, T., Tsunoda, K. (2003). Decomposition of phenolics Endocrine Disrupting chemicals by potassium permanganate and gamma ray irradiation. *Bulletin of Chemical Society of Japan, 76* (8): 1681-1685.

Adegite, A., Iyun, J.F. and Ojo, J.F. (1977). Kinetics and mechanism of electron-transfer reaction between uranium(III) and some ruthenium (II) ammines complexes. *Journal of Chemical Society, Dalton Transaction,* 115.

Adetoro.A., Iyun, J.F. and Idris, S.O. (2010). Bromate ion oxidation of pyrocatechol violet in aqueous hydrochloric acid. Kinetic and mechanism. *Journal of Applied Science Res*earch, 2(6): 177 – 184.

Ajibade, F. and Iyun, J.F. (1992). The kinetics and mechanism of oxidation of acetaldehyde by dichromate and permanganate ions in aqueous acidic medium. *Journal of Chemical. Society of Nigeria*, 15: 80.

Alan, R.K. (1984). *Comprehensive Heterocyclic Chemistry.* Elsevier. Vol. 5, 2. Pp. 469-498.

Al-Jallal, N. A. and Sulfab,Y. (1983). Kinetics of the oxidation of aquo(ethylenediamine) tetraacetatochromium(III) by periodate. *Transition Metal Chemistry*, 8:51-60.

Antonijevic, M.M. and Petrovic, M.B. (2008). Copper corrosion inhibition: Review. *International Journal of Electrochemical Science, 3:1-28.*

Azafarany, I. (2010). Kinetics and Mechanism of Oxidation of nicotine by permanganate ion in acid perchlorate solution. *International Journal of Chemistry.* 21, 2.

Babatunde, O.A. and Iyun, J.F. (2009). Kinetics and Mechanism of the Reaction of Di- μ -Oxo- Tetrakis (1,10-Phenanthroline)-Dimaganese(III, IV) perchlorate by sulphite ion in acidic solution. *European Journal of Scientific Research*, 26.3:406-416.

Bahrami, H. and Zahedi, M. (2004). Kinetics and mechanism of the oxidation of L– ά –amino–n–butyric acid in moderately concentrated sulfuric acid. *Canadian Journal of Chemistry*, 82: 430–436.

Basalo, F. and Pearson, G.R. (1967). *Mechanism of Inorganic Reactions*. A study of metal complex in solution. Wiley and Sons, New York, Pp. 454 – 525.

Bhatnagar, A., Sharma, P.K. and Kumar, N. (2011). A review on imidazoles. The chemistry and pharmacological potentials. *International Journal of Pharmaceutical Technical Research, 3 (1): 268-282.*

Burgess, J. (1978). *Metal ions in Solution*. Wiley and sons, New York, Chapter 3.

Caldin, E.F. (1964). *Fast reaction in Solution*. Blackwell Scientific, Oxford. England.

Campion, J. R., Deck, F.C., King Jnr. P. and Wahl, C.A. (1967). Kinetics of electron exchange between hexacyanoferrate (II) and (III) ion. *Journal of Inorganic Chemistry. 6: 672 – 681.*

Candling, J.P. and Halpern, J.(1965).Volume of Activation of some Electron Transfer Reactions. *Inorganic Chemistry 4; 1086 – 1089*.

Cherysleva, N.N., Abdullin, I.F. and Budnikov, G.K. (2000). Coulometric determination of purine alkaloid series with electrogeneted chlorine. *Journal of Analytical Chemistry,* 7: (56).

Connick, E.R., and Poulson, E.R. (1959). Effect of paramagentic ions on the nuclear magnetic resonance of O_{17} no water and the rate of elimination of water molecules from the first coordination sphere of cations. *Journal of Chemical Physics 30: 759.*

Davasagayam,T.P.A., and Kesavan, P.C. (1966). Oxidation of caffeine with hydrogen peroxide catalyzed by metalloporphyrins. *Indian Journal of Experimental Biology, 34: 291*.

Deck, C.F. and Wahl, A.C. (1954). Rate of the ferrocyanide-ferricyanide exchange reaction. *Journal of American Chemical Society*, 76: 4054.

Diebler, H. and Tauber, H. (1965). Kinetics of the reaction of halopentammine cobalt(III) complexes by iron(II) and vanadium(II). *Inorganic Chemistry 4: 1029.*

Eigen, M. and De Meyer L. (1963). In Friess, S.L.Lewis E.S. and Wiessberger, A*. Technique of Organic Chemistry*. Interscience*,* New York, Pp. 895.

Espenson, H.J. (1965). Kinetics and echanism of reaction of Fe(II) and acid pentaammines

Co(III) ion. *Inorganic Chemistry*, 4: 121-130.

Fay, D.P and Sutin, N. (1970). Kinetics and mechanism of the oxidation of iron(II) by thiocyanatopentammine cobalt(III) ions. Comparison with related systems. *Inorganic Chemistry*, 9(5): 1291.

Finnegan, W.G, Pitter, R.L and Hinsvark, B.A. (2002). Redox reactions in growing single ice crystals: A mechanistic interpretation of experimental results. *Journal of Colloid and Interface Science,* 242 (2): 373.

Green, M., Taylor, R.S. and Sykes, A.G. (1971). Kinetics of the reduction of μ-amidosulphato and amido selenato-bis (tetra-ammine) Cobalt(III) and sulphatopentaammine cobalt(III) complexes with vanadium(II). *Journal of American Chemical Society*, (A).509.

Gilla, M. A. K. Meena, M., Baghmar, I. K., Sharma and Vinta .S. (2011). Kinetics and mechanism of oxidation of some thioacids by imidazolium fluorochromate. *Journal of Chemical, Biological and Physical Science, 1 (1): 30 – 41.*

Gurdeep, R. C. (1996). *Organic Chemistry of Natural Products*. 4th edition. Himalaya Publishing House, London, Pp. 261-266.

Haim, A. (1983). Electron transfer reactions. The bridge activated complex progress *Inorganic Chemistry 30; 273 – 353*.

Haim, A. and Sutin, N. (1966). Inner-sphere mechanism for reduction of cobalt(III) complexes by iron (III). *Journal of American Chemical Society,88: 5343*.

Halpern, J., Legare, R. J. and Lumry, R. (1963). Measurements of the rate of electron transfer between Tris-(4,7-dimethyl-1,10-phenanthroline iron(III) and hexachloroiridate(IV) by T-jump method. *Journal of American Chemical Society*, 85:680.

Hassan, R.M. (1991). Kinetics and mechanism of oxidation of DL-alanine by acid perchlorate ion media solution*. Canadian Journal Chemistry, 69: 2018*

Hazen and Sawyer. (1992). *Disinfection Alternatives for Safe Drinking Water*. Van Nostrand, Holland, Pp. 435-452.

He, D., Guan, X.H., Ma, J. and Yu, M. (2009). Influence of different molecular weight fraction of humic acid on phenol oxidation by permanganate. *Journal of Enviromental Science and Technology,* 43 (21): 8332-8337.

Hiremath, G.A., Timmanagonder, P. L. and Nanidibenoor, ST. (1996). Kinetics of oxidation of thalium by permanganate in aqueous HCl. *Transition Metal Chemistry. 21*:560.

Hubbard, C.D., Gerhard, A. Van Eldik, R. (1991). Oxidation of dilydroxylaronmatic substrate by hexachloroiodate(IV): Mechanistic information from volume of activation. *Inorganic Chemistry 80: 5023 – 5030.*

Hunt, J.B. and Earley, J. E. (1960). The effect of some non-bridging ligands on the Cr(II) – Cr (III) oxidation. *Journal American Chemical Society, 82: 5312.*

Idris.S.O., Ahmed, A.M. and J. F Iyun. (2007). Mechanism of the bromate oxidation of 1,4-dihydroxybenzene in aqueous acidic medium. *African Journal of Natural Scienc*e, 29 – 34.

Insauti, M.J.; F. Meta-Perez and Alvarez-Mach (1995). Kinetic study of the oxidation of

L-phenylalanine by potassium permanganate in acidic medium. *International Journal of Chemical Kinetic, 27:507.*

Irwin, J.P. (1997). *All about asthma*. Stop suffering and start living. Insight books, New York, P100.

Iyun, J.F. (1982). Kinetics and mechanism of the oxidation reduction and substitution reaction of some metal ion complexes in acid solution. Ph.D thesis, Ahmadu Bello University, Zaria – Nigeria.

Iyun, J.F. **(**1989). Kinetics and Mechanism of the redox reaction of catechol by permanganate and bromate ions in an acid medium. Paper presented at the 14th Annual conference of *Chemical Society of Nigeria*.Warri.

Iyun, J.F. and Tinuoye, E. O. (1998). Chromium(VI) oxidation of L-Cystein. *Journal of Chemical Society of Nigeria.*56 – 59.

Jiang, J., Pang, S.Y. and Ma, J. (2009). Oxidation of triclosan by permanganate (Mn (VII)). importance of ligands and insitu formed manganese oxides. Enviromental science and technology. *Journal of Chemical Physics*. 36: 1277.

Kesarana, P.C. and Sarma, L. (1995). In Sub. *Cellular Biochemistry*, *Ascorbic acid Biochemistry and Biomedical Cell biology* . Plenum,New York, Vol. 25 Pp. 407.

Kumar, M. and Adinarayana, M. (2000). Oxidation of caffeine by phosphate radical anion in aqueous solution under anoxic conditions. *Journal of Chemical Science. 112*,: 551-557.

Larsen, D.W. and Wahl, A. C. (1965). Electron transfer rates for unsubstituted and dimethyl-substituted tris (1, 10-Phenanthroline)-Iron(II) and (III) ions from nuclear magnetic. resonance studies. *Journal of Chemical Physics, 43: 3765*.

Lippards, S.J. (1973). *Current research topics in Bioinorganic Chemistry*. John Wiley and Sons, New York, Pp 14.

Lohdip, Y.N. and Iyun, J.F. (1998). Kinetics of reduction of Di- μ- oxotetrakis (1, 10-phenanthroline) dimanganese(111, 1V) perchlorate by dimethronine in acid solution. *Bulletin of Chemical Society of Ethiopia,* 12: 113-119.

Malisoff, M.W. (1943). *Dictionary of Biochemistry and related subjects*. Philosophical library Pp. 311,530,573.

Marcus, R. A. (1956). Theory of oxidation reduction involving electron transfer (II). *Journal of Chemical Physics. 24: 966 -978.*

Mayer, T.J. and Taube, H. (1987).*Comprehensive Coordination Chemistry*: The synthesis, reaction, properties and application of coordination compounds. Pergamon Press, United Kingdom, Pp. 384.

Mohammed, Y. Iyun, J.F. and Idris, S.O. (2009). Kinetics approach to the mechanism of the redox reaction of malachite green and permanganate ion in aqueous acidic medium. *African Journal of Pure and Appllied Chemistry,* 31 (12): 269 – 274.

Nunes, C., Mahendrasingam, A., Uryanarayanan, R. (2006). Investigation of the multi-step dehydration reaction of theophylline monohydrate using 2-dimensional powder X-ray diffractiometry. *Pharmaceutical Research*, 23(10): 2393-2404.

Orhanvoic, M. and Earley, J.E. (1975). Kinetics of reduction of pentaammine chlorocobalt(II) and cis- and trans-bis(1,2 ethanediammine) dichlorocobalt(I) by titanium(III). *Inorganic Chemistry*, 14: 1478.

Pearson, G.R. and Buch, T. (1962). Electron paramagnetic relaxation in ionic solutions. *Journal of Chemical Physics*, 36: 1277.

Platzman, R. and Franck, J. (1954). Hydration configuration in electron processes involving ions in aqueous solution. *Chemical Abstract* 48: 133-648.

Purcell, K.F. and Kotz, J.C. (1977). *Inorganic Chemistry*. Saunders, Phildelphia. Pp. 659 – 693.

Rajayashree, P., Kumar, Y., and Singh, S.M. (2011). Electrochemical study of Zn^{2+} - theophylline complex. *International Journal of Chemical Technical Research*, 1(3): 43-50.

Refat, M. H., Ahmed. F., Gamal, A.A., Ishaq A. Z., Bassim H. A., Hideo, D. and Takagi, Y.I. (2011).Kinetics and mechanism of permanganate oxidation of iota-lambda-carrageenan polysachride as sulfated carbohydrate in acid perchlorate solution.Carbohydrate research.Reinhold, New York, Pp. 342.

Rosseinsky, D.R. (1972). Aqueous electron transfer reaction: Vanadium(IV) as a reductant compound with iron(II). *Chemical Review,* 72 – 215.

Rossenheim, L., Speciser, D. and Laim, A. (1974). Reduction of ethylenediamin tetraecetatoabalt(III) complexes by hexacyanoferrate(III). *Journal of Inorganic Chem*istry, 11: 1571 – 1575.

Sarathi Partha,T.V.N., Dharma, B R., Nageswara, G. R and Vani, P. (2011). Kinetics and mechanism of oxidation glycine by permanganate in alkaline medium. *Research Journal of Pharmaceutical, Biological and Chemical Science*, 2 (1): 149.

Sen, P.K., Saniyan, A. and Gupta, K.S. (1995). Evidence of protonation during oxidation of some alcohol by permanganate ions in perchloric acid medium and mechanism of the oxidation processes. *International Journal of Chemical Kin*etics, 27: 379.

Shargel, L. (2008). *Comprehensive pharmacy review.* 6th edition. Elsevier, New York. Pp. 930.

Shelini, K.K. and Nitin, P.S. (2010). Imidazole and its biological activities: A review. *Chemical Reseach*,3: 36-47.

Singh, D.K and Sah, A. (2006). Spectrophotometric determination of caffeine and theophylline in pure alkaloid and its application in pharmaceutical formulations .*Journal of Analalytical Biochem*istry 349 (2):176-180.

Stephen, H. Stocker. (2008). *General Organic and Biological Chemistry*. 5th edition Pp. 526.

Stranks, D.R. (1960). Mechanism of Some Electron Exchange Reactions. Dis. Faaday Society; Pp 31, 270.

Stewart,R (1965). *Oxidation in organic chemistry.* New York, and London.

Sukalyn, D., Sabita, P. and Bijayk, M. (2009). *Oxidation by permanganate: synthetic and mechanistic aspect. Tetrahedron*, 65: 707-739.

Sutin, N. (1968). Free Energy Barriers and Reactivity Pattern's in Oxidation-reduction Reactions. *Chemical Reseach,* (8); 225 – 231.

Sykes, A.G. (1966). *Kinetics of Inorganic Reactions*, Pergamon Press, London, Pp. 223-241.

Sykes, A.G. and Green M. (1970). The identification of one and two equivalent paths in the reaction of vanadium (II) with mercury(II). *Journal of Chemical Society,* (A), 3221.

Taube, H., Mayer, H. and Rich, R.L. (1953).Observation on the mechanism of electron transfer in solution. *Journal of American Chemical Society*. 76: 4118-4127.

Telo, P.J. and Viera, A.J. (1997). Mechanism of free radical oxidation of caffeine in aqueous solution. *Journal of Chemical Society, Perkin Trans*action, 2: 1755.

Trease, G.E. and Evans, M.C. (2008). *Textbook of Pharamcognosy.* Sounders. Elsevier, Pp. 353.

Vogel, A. I. (1978). Vogel's *textbook of Quantitative Inorganic Analysis*, 4th edition, Longman limited, England, Pp. 223.

Waldemer, R.H. and Tratnyek, P.G. (2006). Kinetics of contaminant degradation by permanganate. *Enviromental Science and Technology*. 40 (3): 1055-1061.

Wang, R.T. and Espenson, J.H. (1971). Kinetics and mechanism of reduction of cobalt(III) complexes by uramum(III) ion. *Journal of American Chemical So*ciety, 93 (2):380 – 386.

Weiss, J. (1954). The Theory of electron transfer processes in aqueous solutions. *Proceeding of Royal Chemical Society*. London A 222 : 128 – 134.

Wilkins, R.G. (1974). The *Study of Kinetics and Mechanism of Reactions of Metal Complexes.* Allyn and Bacon, Boston, pp. 181 – 290.

Wilkinson. (1980). *Chemical Kinetics and Reaction Mechanism*. van Nostrand Reinold . pp. 66-94

Yoshihara, K., Tominaga, K. and Nagasawa, Y. (1995). Effect of solvent dynamics and vibrational motions in electron transfer. *Bulletin of Chemical Society of Japan, 68(3): 696-712.*